DELINEATING THE ROLE OF AUTOPHAGY IN THE MOLECULAR PATHOGENESIS OF LUMPY SKIN DISEASE IN THE CELL CULTURE SYSTEM

Thesis

Submitted to the
DEEMED UNIVERSITY
Indian Veterinary Research Institute
Izatnagar - 243 122 (U.P.), India

Dr. Syam Sugunan
Roll No. M-6282

IN PARTIAL FULFILMENT OF THE REQUIREMENTS FOR THE DEGREE OF

Master of Veterinary Science
(Veterinary Pathology)

2023


Dedicated to...
My Beloved Guide,
Family, Teachers
&
Friends

ICAR- INDIAN VETERINARY RESEARCH INSTITUTE
Mukteswar, Nainital (Uttarakhand)- 263138
Tel: 0091-5942-286578(O), 286348(O), Fax: 0091-5942-286347,
E-mail: schand_vet@yahoo.co.in

Dr. Siddharth Gautam, MVSc., PhD.
I/C Pathology Lab

Dated: 17-11-2023

CERTIFICATE

This is to be certified that the research work embodied in this thesis entitled **"Delineating the role of autophagy in the molecular pathogenesis of the Lumpy skin disease in the cell culture system"** submitted by **Dr. Syam Sugunan, Roll no: M-6282**, for the award of **Master of Veterinary Science** Degree in **Veterinary Pathology** at Indian Veterinary Research Institute, Izatnagar, is the original work carried out by the candidate herself under my supervision and guidance.

It is further certified that **Dr. Syam Sugunan, Roll no: M-6282** has worked for more than 21 months in the Institute and has put in more than 150 days of attendance under me from the date of registration for the **Master of Veterinary Science** Degree in this Deemed University, as required under the relevant ordinance.

(Siddharth Gautam)
Chairman
Student's Advisory Committee

CERTIFICATE

We the undersigned members of Advisory Committee of **Dr. Syam Sugunan**, Roll no: **M-6282**, a candidate for the degree of **Master of Veterinary Science** with the major discipline in **Veterinary Pathology** agree that the thesis entitled "**Delineating the role of autophagy in the molecular pathogenesis of the lumpy skin disease in the cell culture system**" may be submitted in partial fulfilment of the requirement for the degree.

We have gone through the contents of the thesis and are fully satisfied with the work carried out by the candidate, which is being presented for the award of **Master of Veterinary Science** Degree of this Institute.

It is further certified that the candidate has completed all the prescribed requirements governing the award of **Master of Veterinary Science** Degree of the Deemed University, Indian Veterinary Research Institute, Izatnagar.

Signature of the External Examiner
Name Dr R. Singh
Date 08/12/2023

(Siddharth Gautam)
Chairperson,
Student's Advisor Committee
Date: 17/11/2023

Sr No.	Name & Designation	Signature
1.	**Dr. Vidya Singh** Senior Scientist Division of Pathology, IVRI, Izatnagar	
2.	**Dr. Asok Kumar** Scientist (SS) Division of Pathology, IVRI, Izatnagar	
3.	**Dr. Amit Kumar** Scientist (SS) Division of Virology, IVRI Mukteswar	
4.	**Dr. Karam Chand** Senior Scientist Division of Virology, IVRI, Mukteswar	
5.	**Dr. Chhabi Lal Patel** Senior Scientist Division of Virology, IVRI, Mukteswar	

ACKNOWLEDGEMENTS

I express my sincere gratitude and thanks to **Dr. Siddharth Gautam**, Scientist, Division of Virology, ICAR- IVRI Mukteswar, for his constant support, constructive criticism, meticulous supervision, and valuable suggestions throughout my research work. I consider it a proud privilege to have such a young, talented, multifaceted scientist as the chairman of my Advisory committee. I would not have been able to complete my research work in time without his constant inspiration and guidance and I am deeply indebted to him for the effort he has put in this regard.

I wish to record my deep sense of gratitude and sincere thanks to **Dr. R. V.S. Pawaiya** and **Dr. G. Saikumar**, the present and former Heads of the Division of Pathology, ICAR- IVRI Izatnagar for providing me with basic amenities and for their help in the completion of my work in the stipulated time.

I was honored to have most helping hands as members of my Student Advisory Committee **Dr. Vidya Singh** and **Dr. Asok Kumar** from the Division of Pathology, Izatnagar., **Dr. Amit Kumar, Dr. Karam Chand** and **Dr C. L. Patel** from the Division of Virology Mukteswar who have helped me in my research by extending their technical support and equipped me with facilities required for my study.

I would like to extend my scinere gratitude to all the Joint Directors of IVRI, JD (Academics), JD (Research) and JD (Extension) for the part they played in the successful completion of my thesis work.

I wish to thank my dearest faculties of our division, **Dr. Chandrakanta Jana**, **Dr. Pawan**, **Dr. Karikalan**, and **Dr. Saminathan** for their erudite guidance during the period of coursework at the Izatnagar campus. I also take this opportunity to extend my gratitude to **Dr. Vinodkumar**, Senior Scientist, Division of Epidemiology, for helping me with the statistical analysis for my thesis work, which helped in improving the authenticity of my results.

I am deeply indebted to the support showered on me by the scientists on the Mukteswar campus especially **Dr. B. Mondal**, **Dr. Madhusoodan**, **Dr. Deepika Bisht**, **Dr.**

Chandrasekhar, **Dr. Nitish Singh Kharayat**, **Dr. Amol**, **Dr. Aditya**, **Dr. Sagar**, **Dr. Amir**, **Dr. Ashutosh**, who made my stay and studies at the Mukteswar campus comfortable.

I could benefit from the knowledge of my seniors at the Mukteswar and Bareilly campuses, **Dr. Saicharan**, **Dr. Shilpa**, **Dr. Sumi**, **Dr. Waseem Mirzab**, **Dr. Megha Sharma**, **Dr. Faslu**, **Dr. Vinaykumar**, **Dr. Sreelekshmi**, **Dr. Vaibhav**, **Dr. Sonu,** and **Dr. Chris Einstein**. Their help throughout my research period augmented the completion of my work at the right time.

My colleagues **Dr. Arun Chatla** and **Dr. Athira Subhash** were a constant source of inspiration and help in my research pursuit. With their help and encouragement, I could manage my research work with much ease. I will always cherish the happy moments I spent with them during my coursework period in Bareilly.

My batchmates at Mukeswar were a constant source of support in my work and we shared and cared for our comfortable stay there. I sincerely thank **Dr. Abhishek**, **Dr.Aswin P. Kumar**, **Dr. Chering**, **Dr. Bhanupriya**, **Dr. Rupali**, **Dr. Apeksha**, **Dr. Aswini**, and **Dr. Babasaheb** for the part they have played. My special thanks to **Mr. Ankit Prasad** and **Mis. Sanjana Ginwal**, Young Professionals (Microbiology) for their technical support during my research.

I extend my love and gratitude towards my friends, **Dr. Amalin Mariya**, **Dr. Muhammad Sayyaf**, **Dr. Muhammed Aslam**, **Mr. Ashique Manzoor**, **Dr. Rushikesh Borse**, **Dr. Deepu Thomas**, **Dr. Binoy**, **Dr. Ajithlal**, **Dr. Aravind K. Unni**, **Dr. Mufeeda**, **Dr. Nijil**, **Dr. Sajin Muhammed**, **Dr. Anu Krishna**, **Dr. Basil Hyder**, **Dr. Sandeep N. C.**, **Dr. Vishnu**, **Dr. Amal Cheemadan**, **Dr. Vinayak**, **Dr. Anjana**, **Dr. Balaji**, **Dr. Neethu**, **Dr. Priyanka**, who were present virtually and being pillars of mental and emotional support without whose support, I would not have completed my work with ease.

I sincerely thank the staff of IVRI Mukteswar for their steadfast support and caring, especially **Puranji**, **Savitriji**, **Sobhaji** (Clinical Bacteriology Lab), **Rameshji**, **Rajpalji** (Bluetongue lab)., **Gireesh bhaiya**, **Ramesh bhaiya**, **Mukesh bhaiya** (Pox lab), **Patel bhaiya** and **Pritam bhaiya** (Engineering section), **Bhatji and team** (Canteen) who made my stay at IVRI Mukteswar comfortable.

Words are not enough to express my gratitude to my mother who stood by my side amidst all struggles and hardship. She has always been my source of inspiration in achieving every milestone in my life. I am thankful for her prayers and support throughout the work of this project.

I deeply acknowledge the mental support given by my elder sister **Miss. Shilpa** and all the relatives who have marked their footprints in my path towards the completion of my thesis work. I take this opportunity to thank myself for the patience, self-respect and confidence that I have invested during this research period.

Date: ***(Syam Sugunan)***

Place: *ICAR-IVRI, Mukteswar*

ABBREVIATIONS

%	:	Per cent
°C	:	Degree Celsius
APS	:	Ammonium persulfate
BEF	:	Bovine embryonic fibroblast
BEI	:	Binary ethyleneimine
BSA	:	Bovine serum albumin
cDNA	:	Complimentary Deoxyribose Nucleic Acid
CMA	:	Chaperone- mediated autophagy
CPE	:	Cytopathic Effect
DAB	:	Diaminobenzidine
DMEM	:	Dulbecco's Modified Eagle Medium
DMSO	:	Dimethyl sulfoxide
DNA	:	Deoxyribonucleic Acid
EDTA	:	Ethylenediamine tetra acetic acid
FBS	:	Fetal Bovine Serum
GTPV	:	Goatpox Virus
KSGP	:	Kenyan Sheep and Goatpox
LAMP	:	Lysosome- associated Membrane Protein
LC3	:	Microtubule- associated protein (light chain 3)
LSD	:	Lumpy skin disease
MDBK	:	Madin-Darby Bovine Kidney
MHC	:	Major Histocompatibility Complex
NBF	:	Neutral buffered formalin
NC	:	Negative Control
NFW	:	Nuclease free water
NTC	:	Non template control
PBS	:	Phosphate Buffered Saline
PC	:	Positive Control
PCR	:	Polymerase chain reaction
PVDF	:	Polyvinylidene difluoride

RNA	:	Ribonucleic Acid
SDS- PAGE	:	Sodium dodecyl sulfate- Polyacrylamide gel electrophoresis
SPPV	:	Sheeppox Virus
TBST	:	Tris- Buffered Saline Tween-20
TEMED	:	Tetramethylethylenediamine
WB	:	Western blotting
µg	:	Microgram
µL	:	Microlitre

LIST OF TABLES

LIST OF FIGURES

CONTENTS

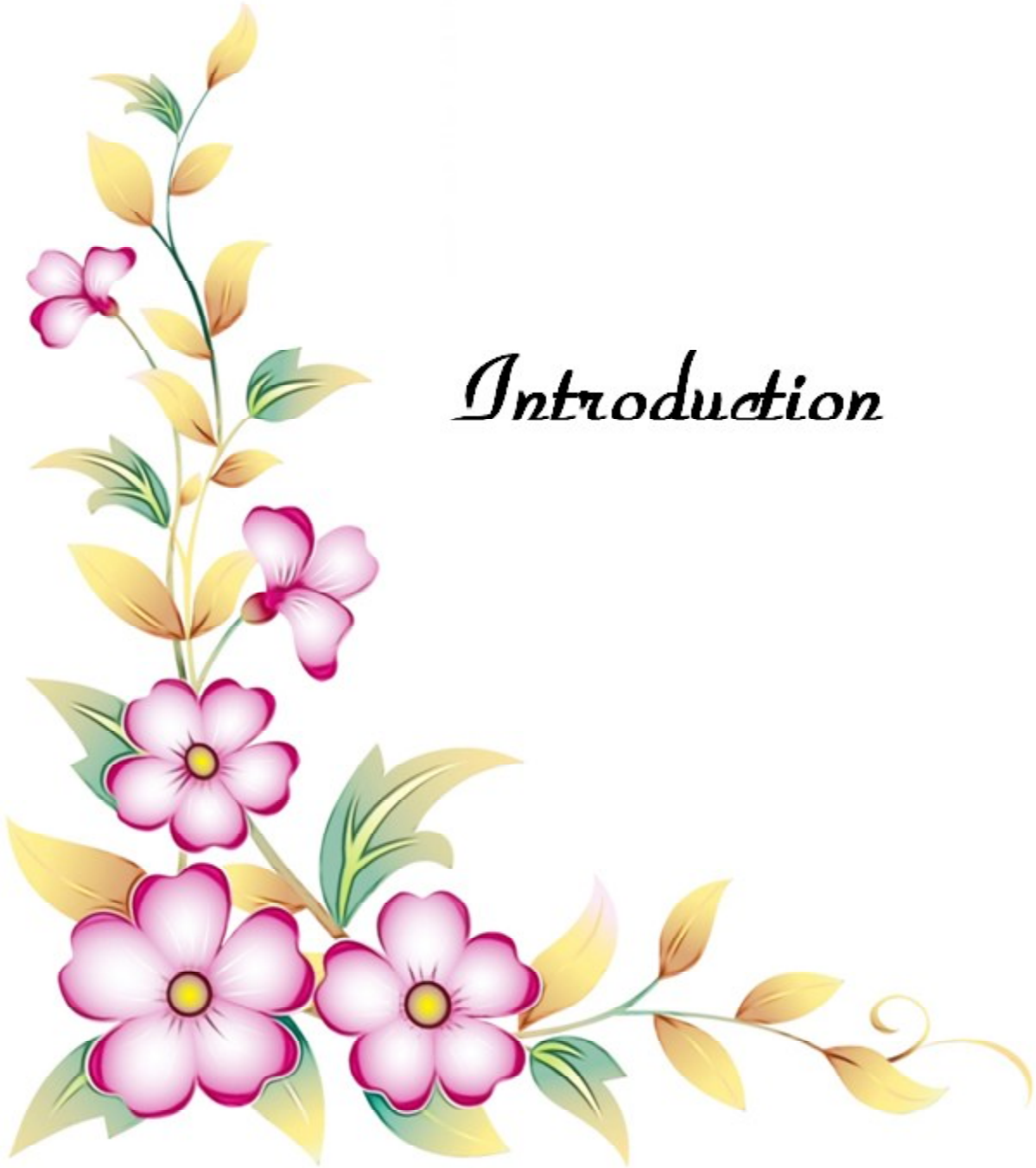

Introduction

1 INTRODUCTION

Animal husbandry is an intricate attribute of the human foodchain and livelihood. Cattle, being the most commonly domesticated livestock animal after poultry, cover a global population of 192.49 million (FAO, 2019) and serve as the bread and butter for the vast majority of small and medium-scale farmers. Any disease condition affecting the livestock is a great scourge for the economy, particularly those relying on agricultural outputs. Lumpy skin disease (LSD) is one of the most devastating infectious viral diseases of cattle and buffaloes and has affected almost eight million cattle in the African continent since its first occurrence in 1929 (Wainwright *et al*., 2013). More importantly, LSD has crossed international boundaries in recent years and has spread to Europe and Asian countries. Currently, LSD is the biggest threat to the cattle population in the majority of South-Asian countries, including India. Credited to its significant economic impact and potential to readily cross national and international borders (Tuppurainen and Oura, 2012), LSD is included in the list of notifiable diseases of cattle by the World Organization for Animal Health (OIE).

Lumpy Skin Disease virus (LSDV; Genus – *Capripoxvirus* and Family - *Poxviridae*), the etiological agent of LSD, produces a progressive and nodular infection in cattle and buffalo and is closely related antigenically to sheeppox and goatpox viruses. The major mode of LSDV transmission is the bite of an arthropod vector (Chihota *et al*., 2001; Lubinga *et al*., 2014), though direct transmission has been reported (Annandale *et al.*, 2014). Clinically, the disease is characterized by pyrexia, inappetence, salivation, lachrymation, enlarged lymph nodes, a considerable decline in milk production, weight loss, and an eruption of multiple, firm, circumscribed nodules mainly on the head, neck, perineum, genitalia, udder, and limbs

(Abutarbush *et al.*, 2017). Histologically, the LSDV replicates and produces characteristic intracytoplasmic inclusion bodies in keratinocytes, endothelium, pericytes, fibrocytes, and macrophages, and results in vasculitis, lymphangitis, thrombosis, and infarction (Coetzer and Tuppurainen, 2004). The clinical course and histological progression of LSD in cattle have been documented (Turan, 2017), however, the molecular aspects during LSD infection, in particular, the pathways involved in cell survival/death, remain largely unexplored.

One such evolutionary conserved and highly regulated cell survival/death pathway during viral infections is autophagy. Autophagy is a self-degradative process as well as a survival mechanism occurring at the cellular level in response to stress and plays a pivotal role in the removal of misfolded proteins, clearing damaged organelles, and eliminating intracellular pathogens (Cooper, 2018). As an integral part of the host's innate immune response, autophagy regulates the lysosome-mediated degradation of intracellular pathogens. Additionally, autophagy augments adaptive immune response by facilitating antigen presentation and antibody production (Deretic, 2009; Kudchodkar and Levine, 2009; Orvedahl *et al.*, 2010). Overall, autophagy plays a pivotal role in the outcome of viral infections by modulating the cellular immune response against a variety of viral insults.

To counter autophagy, viruses adopt multiple strategies, including either escaping/evading autophagy or utilizing it for their benefit (Kudchodkar and Levine, 2009). Autophagy plays an anti-viral role in the pathogenesis of herpes simplex virus-1 (HSV-1), vesicular stomatitis virus (VSV), respiratory syncytial virus (RSV), Rift Valley fever virus (RVFV), bovine viral diarrhea virus (BVDV) and foot and mouth disease virus (FMDV), whereas, the autophagic machinery is reported to enhance the replication of coronaviruses, coxsackie virus B3, poliovirus, hepatitis C virus (HCV), dengue fever virus, PPRV, canine distemper virus and Newcastle disease virus (Khandia *et al.*, 2019). However, the literature on the role of autophagy in the host-pathogen interaction of Poxviruses is limited. Autophagy induced by the Moscow strain of Ectromelia (mousepox) virus boosts viral proliferation and encourages cell necrosis, particularly in the spleen of vulnerable mouse strains (Martyniszyn *et al.*, 2013). Autophagy inhibition enhances the replication of the vaccinia virus, whereas it has no significant role in the replication of Orf viruses, even though infection of the host with the Orf virus has induced some autophagic

response (Mauthe *et al*., 2016; Lan *et al*., 2016). The impact of autophagy on the replication of Capripox viruses, particularly LSDV, and vice-versa remains largely unexplored. The knowledge gaps on the molecular events during LSDV infection, with special reference to autophagy, make it necessary to understand the autophagic machinery during the LSDV infection.

To this end, the current research proposal entitled **"Delineating the role of autophagy in the molecular pathogenesis of lumpy skin disease in the cell-culture system"** has been envisaged with the following objectives:

1. **To delineate the *in vitro* regulation of autophagy during the LSDV infection.**
2. **To investigate the cellular autophagic machinery in response to an inactivated LSDV.**

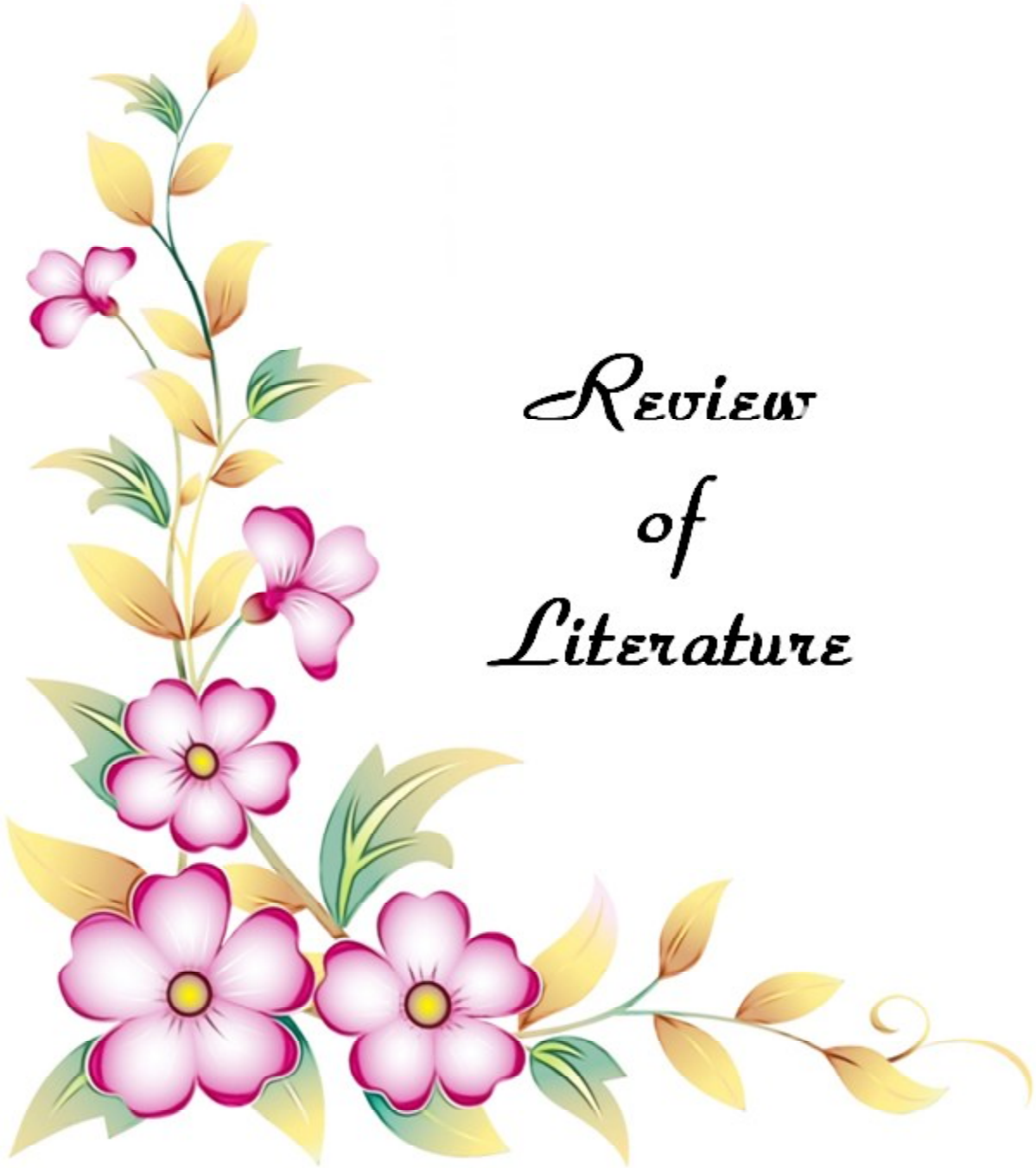

Review of Literature

2 REVIEW OF LITERATURE

2.1 Aetiology of LSD

The aetiological agent of Lumpy Skin Disease (LSD) is the LSDV belonging to the Poxviridae family, Chordopoxvirinae subfamily, and Capripox virus genus (Quinn *et al*., 2015). The genus includes three host-specific viral species, goatpox virus (GTPV), sheeppox virus (SPPV), and LSDV (King *et al*., 2012). LSDV is an enveloped virus with 151 kbp of linear and double-stranded DNA with a central coding region transcribing 156 putative genes encased by comparable 2.4 kbp terminal repeats (Bhanuprakash *et al*., 2006). LSDV has a dimension of about 300 × 270 nm and a complex symmetry. LSDV genome reveals 97% nucleotide homology with SPPV and GTPV (Tulman *et al*., 2002). Nevertheless, nine genes in the terminal region of the LSDV genome (including LSDV 132, Myxoma virus M003.2 and M004.1, Interleukin-1 receptor, vaccinia virus N2L, K7L, and F11L genes) are either disrupted or absent in SPPV and GTPV and are likely responsible for virulence and host range functions (Tulman *et al*., 2002).

2.2 History of LSD

The first clinical case of LSD occurred in Zambia in Africa in 1929 (Morris, 1930). Earlier, the clinical signs were mistaken for poisoning or hypersensitivity to insect bites, later infectious nature of the disease was recognized in subsequent outbreaks in Botswana, Zimbabwe, and the Republic of South Africa between 1943 and 1945. LSD occurred as a panzootic event in South Africa which vanished the lives of about eight million cattle and the disease continued until 1949 creating mass economic losses (Thomas and Mare 1945; Von

Backstrom, 1945; Diesel, 1949). The disease created havoc in Kenya, Sudan, West Africa, and Somalia in the years 1957, 1972, 1974, and 1983, respectively (Ali and Obeid, 1977; Davies, 1991a and 1991b). LSD outbreak occurred and re-emerged in Egypt due to the movement of infected cattle from affected African countries because of a lack of restrictions on cattle movement (Ali *et al*., 1990). Israel witnessed its first outbreak in 1989 which is believed to be due to the movement of infected *Stomoxys calcitrans* from Egypt (Yeruham *et al*., 1995). The disease further spread into the Middle East (2012), Europe (2015), Russia (2017), and the majority of Southeast Asian countries (2019), including India (Sudhakar *et al*., 2020).

2.3 Stability of LSDV

LSDV is extremely robust, may endure room temperatures for extended periods, and is preferably found in dried scabs. It is extremely defiant to inactivation. The virus can persist in dry scabs, hides, and nodules, respectively for at least 35, 18, and 33 days (Tuppurainen *et al*., 2015). LSDV is inactivated at 55°C for two hours and 65°C for 30 minutes. The virus is vulnerable to high acidic or alkaline pH and can be inactivated by using 2-4% sodium hypochlorite, 2% phenol, sodium dodecyl sulfate, iodine compounds (1:33), 0.5% quaternary ammonium compounds, etc (OIE, 2013). Reports suggest that the nodular lesions stored at -80 ºC for 9 years and infected tissue culture fluid held at 4 ºC for 6 months can still act as a source of LSDV (Mulatu and Feyisa, 2018).

2.4 Epidemiology of LSD

The morbidity and mortality rates of LSD outbreaks vary greatly depending on geographic region, climate, management practices, nutritional status, breed, immune status, population sizes, the spread of potential insect vectors, and virulence of the virus strain (Tuppurainen *et al*., 2017). Although 1% to 5% morbidity rates are thought to be more typical, the morbidity rates of LSD may range from 5% to 45%, while the mortality rate may reach up to 10% (Coetzer and Tuppurainen, 2004). An appreciably higher number of cases have been reported in epizootics from Southern, West, and East Africa and Sudan (Yeruham *et al*., 1995). Typically, it is connected to periods of intense precipitation, humid environments, and high

insect activity as a consequence. Other risk factors that may enhance the occurrence of the disease include the animal density, presence of arthropod vectors, unrestricted animal movements, and shared pasture and water troughs (Gari *et al*., 2010; Ince *et al*., 2016; Sevik and Dogan, 2017). Both sexes, all breeds, and ages of cattle are susceptible to the illness (Tuppurainen *et al*., 2011). There is a restricted vertebrate host range for LSD. The species that naturally contract the disease in the course of field outbreaks are cattle and buffalo. Clinical LSD instances in Asian water buffaloes, *Bubalus bubalis,* have been documented (Ali *et al*., 1990). One clinical case of Capripox infection, most likely caused by LSD, was reported in an Arabian oryx kept in a Saudi Arabian zoo (Greth *et al*., 1992). Experimental inoculation of wild animals, including the giraffe (*Giraffa camelopardalis*), Thomson's gazelle (*Gazella thomsonii*), and impala (*Aepyceros melampus*), led to the development of skin lesions characteristic of LSD (Tuppurainen *et al*., 2018). However, the role of wildlife in the prevalence and epidemiology of LSD remains unclear (Tuppurainen *et al*., 2017).

2.5 Economic Impact of LSD

In endemic areas, LSDV has resulted in significant economic losses. Due to high fever and subsequent mastitis, the illness may reduce milk yield by 10% to 85%. Damaged skins, a decrease in the growth rate of beef cattle, temporary or permanent infertility, miscarriage, treatment and immunization expenditures, and the death of afflicted animals further compound the economic impacts of the disease (Babiuk *et al*., 2008; Sajid *et al*., 2012; Sevik and Dogan, 2017). A study in Turkey encompassing 393 herds revealed a total loss of 822 940.7 GBP (Sevik and Dogan, 2017). For native zebu and Holstein Friesian, the projected financial damages in Ethiopia were 6.43 USD and 58 USD per head, respectively (Gari *et al*., 2010). Estimates of the disease's overall productivity losses in commercial cattle farms range from 45% to 65% (Tuppurainen and Oura, 2012). The budget for supportive antibiotic therapy for an epidemic in Jordan was determined to be 27.9 British pounds per client (Abutarbush *et al*., 2015). Given the culling rates and the number of bulls at risk, a risk analysis for LSD on an Ethiopian bull market indicated a financial loss of US$ 6,67,785.6 (Abutarbush *et al*., 2016). Estimated quarantine costs in the USA were 145,000 dollars, which included labor, feed, and diagnostic costs, costs associated with dismissing test positives, and other unsettling costs

(Agianniotaki *et al*., 2017). Israel spent roughly US$ 750,000 to manage the initial LSD outbreak by culling all suspected animals in the area and carrying out the ring vaccination (Casal *et al*., 2018; Rossiter and Hammadi, 2009).

High morbidity and mortality in the recent outbreaks of LSD in India had a huge impact on the economy of the livestock sector. Over 97,000 cattle succumbed to death across India in a span of three months (July to September 2022) involving 15 states with major epidemics in Gujarat and Rajasthan. Gujarat reported a decrease in milk collection in August 2022 by around 100,000 liters per day in some areas. Also, milk collection in Rajasthan dropped by almost 20% in August 2022, and in subsequent months; it had fallen by 500,000–600,000 liters per day. Rajasthan's milk collection had dropped to zero in several areas (https://en.m.wikipedia.org/wiki/Lumpy_skin_disease_outbreak_in_India).

2.6 Transmission of LSDV

Cattle, water buffalo, and wild ruminants can all be infected with lumpy skin disease. It appears that the virus does not affect sheep and goats (El-Nahas *et al*., 2011; Lamien *et al*., 2011). Arthropods, particularly blood-sucking insects (Chihota *et al*., 2001, 2003), feed and water contaminated with secretions of diseased animals, and direct transmission through nasal secretions, semen, and saliva are all means of LSDV transmission (Annandale *et al*., 2014; Irons *et al*., 2005; Tuppurainen *et al*., 2017). Reports suggest that the relation between animal density and infective rates is unapparent, highlighting the insignificance of direct virus transmission, at least in early stages as compared to the significant indirect transmission through the bite of arthropods (Carn and Kitching, 1995; Magori-Cohen *et al*., 2012). LSD outbreaks tend to occur during the summer when arthropod activity is at its peak, further signifying the importance of different types of blood-sucking vectors in the propagation of LSDV (Kahana-Sutin *et al*., 2017; Sprygin *et al*., 2018). Hard ticks are probably involved in LSDV transmission (Lubinga *et al*., 2015; Tuppurainen *et al*., 2011, 2013), and the tick components, including the hemocytes, salivary glands, and midgut, were reported to contain the LSDV and LSDV antigens (Lubinga *et al*., 2013, 2014). Furthermore, molecular evidence also suggests that ticks mechanically and transstadially transmit the LSDV (Tuppurainen and Oura, 2012). However, ticks serve as reservoir hosts as the quick emergence of widespread epidemics

could not be explained by their strong attachment to the host (Kahana *et al*., 2017). The only dipteran capable of fully transmitting the virus to vulnerable cattle is *Aedes aegypti* (Chihota *et al*., 2001). The virus could not be transmitted by mosquitoes like *Culicoides nubeculosus, Culex quinquefasciatus*, or *Anopheles stephensi* (Chihota *et al*., 2003). Despite the presence of *Stomoxys calcitrans* in LSD outbreaks and its ability to spread the Capripox virus to sheep and goats, LSDV has not been successfully transferred to susceptible animals (Baldacchino *et al*., 2013; Yeruham *et al.,* 1995). Furthermore, LSDV has been detected in *Culicoides punctatus* (Sevik and Dogan, 2017) and, the likelihood of LSDV transmission has been positively linked with the ratio of biting insects to the host population (Gubbins *et al*., 2008). The appearance of significant skin lesions in the aborted calves suggests an intra-uterine infection (Weiss, 1968; Irons *et al.,* 2005). Additionally, the heifers inseminated with LSDV spiked semen showed positivity for LSDV, indicating pathogenic potential of LSDV transmission through artificial insemination (Annandale *et al*., 2014).

2.7 Pathogenesis of LSDV

Limited investigations have been done on the pathogenesis of LSD in cattle (El-Kenawy and El-Íoloth, 2010). Following LSDV infection, the virus replicates in macrophages, fibroblasts, pericytes, endothelial cells, and keratinocytes. This is followed by viremia, pyrexia, and LSDV localized to the skin leading to the formation of hard nodular eruptions (Constable *et al*., 2016). Vasculitis and lymphangitis are common sequelae and are caused by LSDV replication in the endothelial and perivascular cells of the blood vessels and lymphatics in the affected areas. Severe infections may lead to thrombosis and infarction (Coetzer and Tuppurainen, 2004). After experimental intradermal inoculation of the LSDV, localized swelling in the form of 1-3 cm nodules at the inoculation site; viremia and release of virus in oral and nasal discharges; enlargement of regional lymph nodes and generalized skin nodular eruptions, and virus load in semen were detected 4 to 7, 6 to 18, 7 to 19 and 42-days post-infection, respectively (Coetzer and Tuppurainen, 2004). Young, underweight, and animals in the milking stage with compromised immune function are more prone to LSDV infection (Babiuk *et al*., 2008), whereas recovered animals have demonstrated lifetime immunity. Acquired immunity through maternal antibodies may persist and can protect calves for up to 6 months (Tuppurainen *et al*., 2005). Diseased

animals generally recover from the virus and do not act as LSDV carriers (Tuppurainen *et al*., 2017). In the majority of cases, animals that survive clinical disease establish a lifelong cell-mediated immunity.

2.8 Clinical presentation in LSD

The incubation period of LSD ranges from 1-4 weeks, after which fever and depression occur which may last for 4-14 days (Turan, 2017). Depending upon the number of skin nodules, the frequency of complications, the dose of the inoculum, the host's vulnerability, and the density of insect populations, LSD can exhibit mild and severe forms. Accordingly, the clinical signs of mildly afflicted cattle include the development of a few nodules within two days of the commencement of the fever (1 to 5 cm in diameter), depression, anorexia, excessive salivation, ocular and nasal discharge, agalactia, and emaciation. The nodular lesions may be painful and hyperaemic (Salib and Osman, 2011). On the other hand, serious lethargy, anorexia, and numerous similar- sized nodules are seen throughout the animal's body in severe cases, which may last for 7–12 days (Weiss, 1968). The nodules are hard, regular, and circumscribed and may coalesce to become larger, irregular nodules. They are round and about 0.5-5 cm in diameter and are seen as circumscribed areas of upright hair over slightly elevated skin regions. Frequently, a narrow ring of hemorrhage that affects the epidermis, dermis, nearby subcutis, and muscle separates the nodules from the surrounding normal skin, and exudation of serum from the skin is evident. Nodules may disappear, but they might also remain as hard lumps, transform into a moist, necrotic slough, or become ulcerated. Lesions devoid of skin could persist for long and (Constable *et al*., 2016) the sloughing away of skin lesions generates a cavity on the skin resulting in the "sit fast" lesion, an "inverted conical zone" of necrosis (Abutarbush *et al*., 2017). Excessive nasal discharge, salivation, emaciation, and other typical signs are manifested due to the necrotic plaques and nodular lesions in the conjunctiva, mucosal surfaces, and skin. Lesions in the udder may lead to secondary mastitis and reduced milk yield. Abortion in infected cows and pox- like lesions in the aborted calves support intra-uterine LSDV transmission. In infected bulls, orchitis is seen occasionally. Lymphadenopathy is a characteristic feature of LSD in which there will be 2-3 times enlargement of prescapular and prefemoral lymph nodes. Permanent sterility in both sexes may occur upon lesions in the

reproductive tracts (Constable *et al*., 2016). Deep ulcerative skin lesions, keratitis (unilateral or bilateral), and edematous inflammatory swellings of the brisket, face, and one or more limbs are also present in infected cows and can severely impair movement.

2.9 Haematological and biochemical findings in LSD infection

Neamat-Allah (2015) demonstrated that experimentally infected animals revealed a significant decrease in RBC, Hb, and PCV with an overall picture of macrocytic hypochromic anemia. Leucogram of LSDV-infected animals exhibited leucopenia and lymphopenia; agranulocytic leukocytosis probably due to secondary acute bacterial infections, particularly pyogenic bacterial infections (Neamat-Allah, 2015). In natural infections, LSD has also been linked to inflammatory thrombocytopenia, hyperfibrinogenemia, reduced creatinine concentration, hyperchloremia, and hyperkalemia (Abutarbush, 2015). Studies by Neamat-Allah (2015) and Abutarbush (2015) revealed a considerable drop in serum total protein and albumin, but a dramatic rise in globulin, particularly gamma globulins in LSD-infected cows. Studies conducted by Sevik and colleagues (2016) on the serum biochemical evaluation of calves infected with LSD revealed that aspartate aminotransferase and alkaline phosphatase levels rise along with concentrations of globulin protein and creatinine. Conclusively, the serum and biochemical alterations of LSDV are a result of hepatic and renal failures, a severe inflammatory process, anorexia, and diminished muscle mass.

2.10 Clinical Pathology

Skin nodules are often uniform in size, firmly rounded, and elevated, however, some may fuse into enormous irregular and circumscribed plaques. Skin nodules have a reddish-gray surface along with edema in the sub-cutis layer. The entire alimentary and respiratory tracts can develop characteristic circular necrotic lesions (Al-Salihi and Hassan, 2015; Tuppurainen *et al*., 2017). In addition to local cellulitis, regional lymph nodes proliferate (up to ten times their normal size), become edematous, congested, and have pyaemic foci (Salib and Osman, 2011). In extreme cases, pleuritis and mediastinal lymph node enlargement can be observed. The musculature and fascia of the leg are also invaded with the LSD nodular lesions, which are grey-white and bordered by red inflammatory tissue. The necrotic lesions progress

to ulcers that heal gradually by granulation. Bacterial pneumonia is the most common complication; tracheal stenosis and respiratory distress occur due to nodular involvement in mucous membranes and subcutaneous tissue (El-Neweshy *et al*., 2013).

Histopathological findings in LSD are characteristic and serve as a foundation for diagnosis. In addition to ballooning and cell layer degeneration, the pathognomonic eosinophilic intracytoplasmic inclusion bodies can be seen under a microscope in the keratinocytes, macrophages, endothelial cells, and pericytes from skin nodules. Eosinophils, lymphocytes, and macrophages invade the damaged tissue. Additionally, histological analysis reveals extensive vasculitis due to the viral tropism for endothelial cells (Gari *et al*., 2011; Body *et al*., 2012). Severe coagulative necrosis in subcutaneous muscle may be seen if there is a muscular injury during LSD. The different types of epithelial components, sebaceous glands, and follicular epithelium may have specific intracytoplasmic inclusions. Inclusion bodies are primarily eosinophilic purple and have a visible halo around them which is likely a processing artifact (Burdin, 1959; Ali *et al*., 1990; El-Neweshy *et al*., 2012).

2.11 Diagnosis of LSD

Diagnosis of LSD relies on the history, typical clinical signs, and lesions, combined with laboratory detection of virus or viral antigens/genome. Clinically suspected cases are confirmed usually by the detection of the LSDV genome through PCR (traditional real-time) (Bowden *et al*., 2008; Balinsky *et al*., 2008; Tuppurainen *et al*., 2005; Orlova *et al*., 2006; Zheng *et al*., 2007). Additionally, different species of *Capripoxviruses viz.* LSDV, sheep, and goatpox viruses could be differentiated using a real-time PCR method (Lamien *et al*., 2011). Loop-mediated Isothermal Amplification (LAMP) assay is also available for the identification of Capripox viruses with high sensitivity (Bowden *et al.,* 2008; Balinsky *et al*., 2008). Restriction Fragment Length Polymorphism (RFLP) is employed to distinguish virulent LSDV from the vaccine strain (Menasherow *et al*., 2014). In addition, LSDV has been detected using electron microscopy, virus isolation, virus neutralization, and serological methods (OIE 2018), though molecular methods are considered more accurate, efficient, and quick (Stubbs *et al*., 2012).

The only currently validated test among serological methods is the viral neutralization test, which is slow and expensive and has a high specificity but a low sensitivity (Beard, 2016). Agar gel immunodiffusion (AGID) though employed as a diagnostic tool, has the drawback of cross-reaction with bovine papular stomatitis and pseudocowpox viruses. Utilizing the produced structural P32 protein, an ELISA technique for the detection of antibodies against the Capripox virus has been devised (Carn *et al*., 1994; Heine *et al.,* 1999). Although the test is costly and challenging to perform, Western blot analysis offers a sensitive and specific approach for the identification of antibodies to Capripox virus structural proteins (OIE, 2018). Immunohistochemistry could also be used for the *in-situ* demonstration of LSDV antigens in tissue samples (Babiuk *et al*., 2008).

2.12 Prophylaxis and control of LSD

The best prophylaxis approach for LSD is immunization with homologous (Neethling strain) or heterologous live attenuated vaccine (Sheep/Goat pox vaccine) (Abera *et al*., 2015; OIE 2021). Different strains of LSDV and sheepox/goatpox virus have been used in different geographical regions of the world (Abutarbush, 2017). The Gorgan GTP vaccine could successfully protect cattle against LSDV, while the Neethling and KSGP O-180 vaccines were less effective against LSD in Ethiopia, suggesting the necessity of additional molecular characterization of LSD vaccines (Gari *et al*., 2015). Due to the safety concerns of a live attenuated LSDV vaccine in an LSD-free nation, where sheep/goat are protected against respective pox viruses by the sheep pox/goat pox vaccines, it is advised to use the same vaccine during LSD outbreaks (Tuppurainen and Oura, 2012).

For control and eradication, strict measures including quarantine and culling of infected animals, regular decontamination of animal facilities, proper waste disposal, and pest control are required along with enforcement of stern trade regulations (Constable *et al*., 2016). Since arthropods are likely the most important means of LSDV transmission, controlling LSD through quarantine and movement restrictions alone may prove insufficient to contain disease spread. However, using insecticides in conjunction with repellents helps in the prevention of the spread of LSD (Constable *et al*., 2016).

2.13 Autophagy – an innate immune response

Autophagy is a fundamental catabolic process that plays a vital role in cellular homeostasis and is necessary to preserve normal cellular activity during nutrient deficiency/ excess during physiological and pathological stress (Cooper, 2018). Organelles and proteins are degraded by the lysosomal system in a non-selective (bulk) or selective manner as a result of this basic cellular "self-eating," process (Yang *et al.,* 2011). In selective autophagy, cargo is recognized by particular receptors to allow for their precise identification, sequestration, and degradation by the autophagosome. In non-specific autophagy, however, all materials are digested by the lysosome in a non-specific manner (Kissová *et al.,* 2007; Zaffagnini and Martens, 2016). To degrade and recycle sequestered contents, autophagy (macroautophagy) involves the creation of double-membrane vesicles (autophagosomes), which later combine with lysosomes inside which the degradation occurs (Yang *et al*., 2011). To maintain the homeostasis of body systems and regulate healthy living processes, it combats carcinogenic, infectious, degenerative, and toxic agents; hence, its dysfunction is known to cause a variety of human disorders (Mizushima, 2007; Yang, 2010; Lee, 2018; Lee *et al*., 2018). However, the main focus is given on cancer (Yun and Lee, 2018; Daskalaki, 2018), microbial infection (Pleet *et al*., 2018; Sharma *et al*., 2018; Majdoul *et al*., 2017), and degenerative disorders (Fujikake *et al*., 2018; Metaxakis *et al*., 2018). Numerous cellular regulators, such as transcription factors and genes, control the physiological processes of autophagy. If these regulators are upset for genetic or functional reasons or as a result of overexertion, they may have an impact on homeostatic processing (Lee, 2018; Füllgrabe *et al*., 2016; Hsu and Shi, 2017). Thus errors in autophagy can influence the pathogenesis of certain diseases (Hsu and Shi, 2017).

2.14 Types of autophagy

Macroautophagy, microautophagy, and chaperone-mediated autophagy (CMA) are the three different forms of autophagy (Mizushima *et al*., 2008). Macroautophagy, or simply "autophagy," is the primary pathway that engulfs significant amounts of cytoplasm and cellular contents (such as damaged organelles, aggregated proteins, and intracellular microbes) into a

double-membraned vacuole called the autophagosome. The autophagosome then fuses with lysosomes to form an autolysosome, which degrades the autolysosomal contents (Kunz *et al*., 2004; Li *et al*., 2012; Ueno and Komatsu, 2017). Small amounts of the cytosolic substrate are immediately engulfed and digested by lysosomes during the process known as microautophagy without the formation of autophagosomes (Nagar, 2017; Paolini *et al*., 2018). A pentapeptide sequence similar to KFERQ in the heat shock cognate protein (HSC70; 71-kDa, also known as HSPA8), which is involved in CMA, is activated by physiological stressors such as prolonged fasting (Campbell *et al*., 2018; Majeski and Dice, 2004). The CMA pathway interacts with lysosome-associated membrane protein type 2A (LAMP-2A) to transport target proteins over lysosomal membranes and into the lysosomal lumen (Kunz *et al*., 2004). Consequently, as CMA does not require vesicular trafficking, it differs from microautophagy and macroautophagy (Campbell *et al*., 2018). Irrespective of the type, autophagy functions as a cleaning mechanism by expelling or degrading unnecessary substances from the body (such as proteins, microbes, and organelles), while retaining substances (such as biochemicals, and metabolites, and organelles) essential for survival, function, and development (Su *et al*., 2015; Hsu and Shi, 2017).

2.15 Mechanism of autophagy

Activated by a variety of triggers, such as nutrient deprivation (Su *et al*., 2015; Joy *et al*., 2018), oxidative stress (Li *et al*., 2016; Tang *et al*., 2015), pathogenic infection (Fu *et al*., 2014; Ahmad *et al*., 2018) and ER stress (Lee *et al*., 2015), autophagy is an evolutionarily conserved mechanism. Nutrient deprivation and stress can inhibit mTOR to start autophagy with a minimum of four complexes, the unc-51-like kinase (ULK) complex, made of ULK-1, Atg13, Atg101, and FAK-family interacting protein (FIP200); the PI3K complex, consisting of Atg14, vacuolar protein sorting (VPS)15, VPS34, Beclin 1, and Beclin 1-regulated autophagy protein 1 (AMBRA1) transmembrane protein complexes, including Atg9 and WIPI; and two ubiquitin-like protein conjugation systems (Atg12 and LC3) (Mizushima and Komatsu., 2011; Mercer *et al*., 2018).

The ULK complex assembles to begin autophagy, which phosphorylates AMBRA1 and activates the PI3K complex (Yu *et al.,* 2010; Mercer *et al.,* 2018). While PI3K and

Beclin 1 mediate membrane nucleation, Class III PI3K is known to take part in a variety of membrane trafficking activities. The Atg5-Atg12-Atg16 complex is drawn to the pre-autophagosomal structure (PAS), where it interacts with the phagophore's outer membrane to stop the early union of vesicles and lysosomes (Kaur and Debnath, 2015). The engagement of the second ubiquitin-like system promotes when phosphatidylethanolamine (PE) and Atg8/ microtubule-associated protein 1 light chain 3 (LC3) are bound to the phagosome (LAPosome), which has a high affinity for lysosome (Herb *et al*., 2020). For the extension and completeness of the autophagic membrane, Atg3, Atg4, and Atg7 convert LC3 into LC3-II, a molecular marker for autophagosomes which is present on both its inner and outer surfaces (Glick *et al.,* 2010). The Atg5-Atg12-Atg16 complex separates from the autophagosome during autophagosomal closure. Atg9 is essential for the creation of intraluminal vesicles and is confined inside the autolysosomes for acidification (Bader *et al.,* 2015). Additionally, Atg9 is moved to the region where autophagosomes are formed and a membrane is released for elongation of the limiting membrane, referred to as phagophore (Mari *et al.,* 2010). Later, the fusion of the autophagosome with the lysosome forms the autolysosome regulated by lysosomal membrane proteins as well as cytoskeletal proteins (Mizushima *et al.,* 2007). The maturation of the autophagosome is under the control of the LAMP-1/2 protein. Hydrolytic enzymes inside the autolysosome break down the accumulated cargo and the internal autophagosome membrane, and then the broken-down byproducts, including amino acids, are released which must be recycled, into the cytosol.

Detection of autophagy can be done either by directly observing the presence and fate of autophagy-related structures or by quantitatively measuring the autophagic degradation of various substrates.The presence of autophagosomes can be detected through a transmission electron microscope. Analysis of autophagic structures at an instantaneous point in time may be misinterpreted, and thus, there is a need to determine the autophagic flux, which is the amount of autophagic degradation occurring in the complete autophagic process (Klionsky *et al*., 2016). A plethora of autophagic- related factors, such as ULK-1,WIPI-1& 2, LAMP-1, ATG 5, STX-17, microtubule- associated protein light chain (LC3), etc have been used as a marker for autophagy, however, except for LC3, majority of these factors are involved in

other metabolic pathways and are not involved exclusively in autophagic degradation. LC3 is indispensable for the induction and progression of autophagy and is considered a specific marker of autophagic induction (Itakura *et al*., 2012). However, not only the induction of autophagy, but also the inhibition of lysosomal degradation can increase the concentration of cytoplasmic LC3, therefore the amount of the degraded substrate in a lysosome-dependent manner needs to be delineated for an accurate estimation of autophagy, i.e. the autophagic flux (Mizushima *et al*., 2010). Another widely used marker for measuring the autophagic flux is p62 (SQSTM-1). The p62 acts as a carrier and translocates the cargo/autophagic substrates to the autophagosome, and is degraded along with other substrates in the autolysosomes. Under an experimental setup, autophagy can be induced by either starvation or by the use of drugs/chemicals (Rapamycin, tunicamycin, trehalose, etc.). Similarly, autophagy can be reversed by supplying nutrients and can be chemically inhibited using bafilomycin A1, E64d, pepstatin A, 3-methyladenine, clarithromycin, chloroquine, etc (Mizushima and Yoshimori, 2007).

2.16 Role of autophagy in viral pathogenesis

Cells utilize autophagy for mounting antiviral immune response as it plays a crucial part in cellular defense against virus invasion (Orvedahl *et al*., 2010; Deretic, 2009; Kudchodkar and Levine, 2009). During an infection, autophagy aids in the removal of viral pathogens, regulates immune responses, and prevents harmful hyperactivation and inflammatory processes via diverse molecular mechanisms (Paul and Münz, 2016). As an illustration, autophagy enhances the presentation of endogenous viral antigens in the cell's MHC class I molecules in herpes simplex virus type 1 (HSV-1) infection. Autophagosome input is continually accepted by MHC class II molecules, enabling MHC class II molecules to deliver antigens (Nimmerjahn *et al*., 2003; Schmid *et al*., 2007). Vesicular stomatitis virus (VSV) resistance in Drosophila is mostly mediated by autophagy, which can transport viral antigens to TLRs for expression (Shelly *et al*., 2009; Nakamoto *et al*., 2012). Additionally, it has been demonstrated that SIRT1, an NAD (+)-dependent deacetylase, modifies the stimulation of dendritic cells and autophagy during induced immune responses against the respiratory syncytial virus (RSV), thereby directing an efficient anti-viral immune response (Owczarczyk *et al*., 2015). Rift Valley fever virus (RVFV) multiplication is regulated by TLR signaling in flies and mammals (Moy *et al*., 2014).

Salicylamide and its derivatives stimulate autophagy contrary to the Flaviviridae pestivirus cytopathic bovine viral diarrhea virus (cp-BVDV) (Needs *et al.,* 2016). By destroying Atg5-Atg12 using the viral protein 3Cpro, Foot-and-Mouth Disease Virus (FMDV) disease overcomes autophagy and NF-8B anti-viral activities, indicating that Atg5-Atg12 favourably controls anti-viral NF-8B and IRF3 pathways to restrict FMDV propagation (Fan *et al*., 2018).

When the cellular autophagic machinery is disrupted, pathogens can obtain resources for growth and reproduction (Shintani and Klionsky, 2004). Coronaviruses (Reggiori *et al*., 2010), coxsackie virus B3 (Wong *et al*., 2008), poliovirus (Taylor and Kirkeggard, 2007, hepatitis C virus (HCV) (Egger *et al*., 2002; Sir *et al*., 2008; Ke *et al*., 2011) and dengue fever virus (Lee *et al*., 2008) are all known to induce and involve autophagy for enhanced replication. Autophagy also plays a significant role in viral replication and pathogenesis (Li *et al*., 2017). When infected with influenza, autophagy-deficient cells are more likely to die, while altering cellular autophagy with chemotherapeutic drugs or RNA interference can prevent the build-up of viral proteins (Rossman and Lamb, 2009; Zhou *et al*., 2009). To increase viral replication, paramyxo viruses like Newcastle disease virus (NDV) have been found to induce autophagy in U251 glioma cells (Meng *et al*., 2012). Various strategies are used by the human immunodeficiency virus (HIV) to control autophagy and accelerate its replication (Zhou and Spector, 2008; Kyei *et al*., 2009). Coronavirus multiplication and the formation of their replicative structures depend heavily on autophagy. Through the use of an intermediate omegasome, the nonstructural proteins (nsp6) of the coronavirus drive the development of autophagosomes and omegasomes from the ER (Maier and Britton, 2012; Cottam *et al*., 2011). Rapamycin, an autophagy activator, was demonstrated to promote viral replication of FMDV, but 3-methyladenine or small-interfering RNAs inhibited the autophagosomal pathway to reduce viral replication (O'Donnell *et al*., 2011). It has been shown that restricting autophagic vacuoles promotes the maturation of the infectious bursal disease virus (Wang *et al*., 2017). By raising ATP, necessary to boost the metabolism of the infected cells and the amino acid pools for the biosynthesis of viral proteins, autophagy may favor adenoviral infection. Atg12-Atg5 complex is highly upregulated in the advanced phases of adenoviral infection as an indication of increased autophagy (Jiang *et al*., 2008).

2.17 Autophagic modulation by poxviruses

A limited number of studies have been carried out to ascertain the role of autophagy in the pathogenesis of pox viral infections; though the screening of autophagy-related proteins in the Vaccinia virus proved that autophagy inhibition enhanced its replication (Mauthe *et al*., 2016). Infection with the vaccinia virus revokes starvation-induced formation of autophagosomes and results in no degradation (Smith *et al*., 2002)**.** Autophagy induced by the Moscow strain of Ectromelia (mousepox) virus will boost viral proliferation and encourage cell necrosis, particularly in the spleen of vulnerable mouse strains (Martyniszyn *et al*., 2013). Infection of the host with the Orf virus has induced some autophagic response though not significant to influence its replication (Mauthe *et al*., 2016; Lan *et al*., 2016). The role of autophagy in the host-pathogen interaction of capripox viruses, particularly LSDV, remains largely unexplored. To this end, the present study is designed to assess the regulation of autophagic machinery in cells during LSDV infection.

2.18 Activation of autophagy by LSDV in BEF cells

A recent study conducted by the scientists of the Chinese Academy of Agricultural Sciences in Bovine embryonic fibroblast (BEF) cells reveals that infection of the cells with LSDV induces autophagy, which was confirmed by the detection of autophagy-specific protein Microtubule- associated protein light chain (LC3) through Western blotting and the presence of LC3 puncta through immunofluorescence.

Expression of LC3 was analyzed in LSDV- infected and uninfected BEF cells and the ratio of LC3 to LC3 was determined for 5- time intervals (0, 12, 24, 48, and 96 hpi) through Western blotting and immunofluorescence. They found that the ratio was unchanged at 0, 12, 24, and 48 hpi while being increased at 96 hpi suggesting that the virus may induce autophagy in BEF cells. For the visualization of autophagy and confirmation of the results obtained through Western blotting, LC3 puncta/spots were identified through immunofluorescence in which more than 20 LC3 spots were identified in BEF cells in 96 hpi, while no remarkable spots were observed either at initial periods or in mock- infected cells, which throws into light that LSDV infection could initiate autophagy in BEF cells (Tan *et al*., 2023).

Materials and Methods

3 MATERIALS AND METHODS

3.1 MATERIALS

3.1.1 Biologicals

3.1.1.1 Cell line

The Madin-Darby Bovine Kidney (MDBK) cell lines maintained at the Division of Virology, ICAR-IVRI, Mukteshwar, were used for the study. The cells were propagated in Leibovitz's L-15 medium (HIMEDIA, AL011), supplemented with Fetal Bovine Serum (FBS) (2-20%) and antibiotic-antimycotic solution in a humidified incubator at 37 °C.

3.1.1.2 Virus

Lumpy skin disease virus (LSDV-WB/IND/19), maintained in the Pox laboratory at the Division of Virology, ICAR-IVRI Mukteshwar, was employed for the study. The virus isolated in Lamb Testicular cells and was passaged once in Vero cells. The virus was adapted in MDBK cells for 7 passages, and the virus titer was determined using the Tissue Culture Infective Dose ($TCID_{50}$) method in MDBK cells.

3.1.1.3 Antibodies

1. Anti-LC3 Polyclonal Ab (Rabbit; Novus, Cat: NB100-2220)
2. Anti-Beta actin monoclonal Ab (Mouse; Invitrogen, Cat: AM4302)
3. Anti-Capripoxvirus polyclonal sera in rabbits (in-house produced)
4. Goat Anti-Rabbit IgG (Life Technologies, Cat: A16104)
5. Goat Anti-Mouse IgG (Life Technologies, Cat: A16072)

3.1.2 Instruments

1. Class II Type B2 Biological Safety Cabinet, LB2-4A2 (Esco Micro Pvt.Ltd., Singapore)
2. Weighing Balance (Citizon, India)
3. Inverted binocular microscope CX41RF (Olympus Optical Co. Ltd., Japan)
4. Sonicator (Sonics and Materials Inc., Newton, USA)
5. Icemaker (Ice-Matic, India)
6. Freezers (-80°C, -20 °C) (VetFrost, Denmark)
7. Refrigerator (4-8 °C) (LG, India)
8. Centrifuge (Eppendorf, Hamburg, Germany)
9. Vertical SDS-PAGE Apparatus (Bench Top)
10. Semi-Dry Blotting Apparatus (Hoefer Inc., Massachusetts, USA)
11. Circulating Water Bath (Julabo, Seelbach, Germany)
12. Haemocytometer (Cosmo scientific Traders, New Delhi)
13. pH Meter (Eutech Instruments, Singapore)
14. Incubator (Sanyo, Osaka, Japan)
15. Rocking platform/Shaker (Memmert, Pune, India)
16. Thermocycler (TaKaRa, Japan)
17. Nanodrop Spectrophotometer ND 1000 (Fotodyne Inc., Walnut Ridge, USA)
18. Dry bath (Model: LI-DB-120, GeNei, India)
19. Spinix Vortex Shaker (Tarsons, India)
20. Refrigerated Microcentrifuge (Eppendorf, Hamburg, Germany)
21. Real-Time Thermal Cycler (StepOne Plus, Applied Biosystems)
22. Inverted Fluorescent Microscope (Model: NAO30, Leica, Wetzlar, Germany)

3.1.3 Plastic and glassware

1. Serological pipettes (Axygen Scientific Inc., Union City, USA, and Cole-Parmer India Pvt Ltd., Mumbai, India).
2. Cell culture flasks - 25 cc and 75 cc capacities (Cole-Parmer India Pvt Ltd., Mumbai, India).
3. Multiwell cell culture plates - 6 and 96 wells (TPP, Zollstrasse, Switzerland).

4. Micropipettes and pipette tips of various volumes (Axygen Scientific Inc., USA, and Eppendorf, Hamburg, Germany).
5. Petri dish (90×15 mm, polystyrene Petri dish, Genetix Biotech, New Delhi, India).
6. Centrifuge tubes - 15 mL and 50 mL (SPL Life Sciences, Pocheon-si, Korea, Genaxy Scientific Pvt Ltd., New Delhi, India).

3.1.4 Reagents and chemicals

A. Cell culture reagents

1. Fetal bovine serum (Gibco, Billings, MT, USA)
2. Leibovitz's L15 medium (HIMEDIA, Mumbai, India)
3. 0.25%Trypsin EDTA (HIMEDIA, Mumbai, India)
4. Phosphate buffered saline (HIMEDIA, Mumbai, India)
5. Tissue culture grade sterile water (HIMEDIA, Mumbai, India)
6. Antibiotic-antimycotic Solution (100X) (HIMEDIA, Cat:A002)

B. SDS-PAGE and Western Blotting reagents

1. Protease phosphatase inhibitor(HIMEDIA, Mumbai, India)
2. 10X TBST (HIMEDIA, Mumbai, India)
3. 10X Tris-Glycine transfer buffer (Bio-Rad, U. S. A.)
4. 10X TRIS-glycine-SDS gel running buffer (HIMEDIA, Mumbai, India)
5. 5X Laemmli buffer (HIMEDIA, Mumbai, India)
6. Protein ladder (Gene to Protein, Cat: MWM010)
7. Distilled water (HIMEDIA, Mumbai, India)
8. Dimethyl sulfoxide (DMSO; PIERE, USA)
9. Disodium hydrogen orthophosphate (CDH, New Delhi)
10. 37-40% Formaldehyde (Merck, Darmstadt, Germany)
11. Sodium phosphate monobasic (PIERE, USA)
12. 40% Acrylamide-Bisarcylamide 29:1 (AMRESCO)
13. Ammonium persulphate (APS) (Sisco, Delhi)
14. N, N, N',N'-Tetra methyl ethylene diamine (TEMED; MP Biomedicals, Mumbai, India)
15. N- butanol (British drug house, England)

16. Tris base (HIMEDIA, Mumbai, India)
17. Glycine (MERCK, Darmstadt, Germany)
18. Sodium dodecyl sulfate (SDS) (HIMEDIA, Mumbai, India)
19. Absolute methanol (MERCK, Darmstadt, Germany)
20. Diaminobenzidine (DAB) powder (Biobasic)
21. Imidazole (HIMEDIA, Mumbai, India)
22. Cobalt Chloride (Sigma Aldrich, USA)
23. 3% Hydrogen peroxide (Life Sciences)
24. Beta mercaptoethanol (Biogene, USA)
25. Polyvinylidene difluoride (PVDF) membrane (BIO-RAD, Cat:1620177)

C. Immunofluorescence reagents

1. 2.5 % Normal Horse Serum (Vector Laboratories, California, USA)
2. Alexa Fluor 594 tagged anti-rabbit ready to use secondary Ab (Vector Laboratories, California, USA)
3. DAPI nuclear stain (Vector Laboratories, California, USA)
4. Tween-20 (Calbiochem, Cat: 655205)

D. Virus inactivation

1. Bromoethyl amine (Sigma Aldrich, USA)
2. Sodium hydroxide (Sigma Aldrich, USA)
3. Sodium thiosulfate (Merck, Darmstadt, Germany)

E. Miscellaneous reagents

1. Rapamycin (Selleck Chem, Cat: S1039)
2. Bafilomycin A1 (Enzo Life Sciences, Cat: 501031771)

3.1.5 Kits used

1. DNA isolation kit (Invitrogen, Cat No: K1820-02)
2. RNA purification kit **(**PROMEGA, Cat:Z3105)
3. cDNA synthesis kit (PROMEGA, Cat: A5000)
4. Real-time PCR kit (Puregene, Cat: QPS-201)
5. Autofluorescence quenching kit (Vector Laboratories, California, USA)

3.2 METHODS

3.2.1 Maintenance and propagation of MDBK cells

MDBK cells (passage level-102) maintained at the Division of Virology, ICAR-IVRI Mukteshwar was used for the study.

The cells were revived as follows**:**

- ✧ The cell vial was removed from liquid Nitrogen cryocan and immediately thawed in a 37 ºC water bath until some amount of ice crystals remained at the edges.
- ✧ The cell vial was transferred to the biosafety cabinet and disinfected using 70% alcohol. The cell suspension was transferred dropwise into a 15ml centrifuge tube containing 10 ml of Leibovitz's L-15 medium with 20% FBS and centrifuged at 1500 rpm for 15 minutes.
- ✧ The supernatant was removed and the cells were resuspended in 5 ml complete media (Leibovitz's L-15 media containing FBS) and centrifuged at 1200 rpm for 5 minutes.
- ✧ The supernatant was discarded and MDBK cells were resuspended in L-15 media containing 10% FBS and transferred to a 25cc culture flask and kept in an incubator (37 ºC) to stimulate growth.
- ✧ Routinely observed for the cell growth and morphology, media pH and change of the media was carried out accordingly.
- ✧ Routine subculture was done using 0.25%Trypsin EDTA when the monolayer attained 80-90% confluency in 1:4 split ratios.

3.2.2 Adaptation of LSDV in MDBK cells

LSDV virus has limited permissibility in cell lines. The virus was adapted in the MDBK cells using the following protocol:

- ✧ MDBK cells with 80-90% confluency were inoculated with LSDV passaged once in Vero cells (P1).
- ✧ Routine media change was done according to the requirement and cells were observed regularly for CPE.
- ✧ In the absence of apparent CPE, blind passages were given and the infected cells were harvested by 3 consecutive freeze-thaw cycles.

- ✧ Subsequent infection was given in the MDBK cells with the recovered virus until characteristic CPE (cell rounding, clustering, vacuolation, granulation, and presence of refractile cells) was observed.
- ✧ Sequential passaging was done up to P7, and the virus was harvested and stored at -20 °C in small aliquots.

3.2.3 Virus titration

The titration of LSDV was performed in MDBK cells as follows:

- ✧ The titration of the LSDV was performed on MDBK cells in a 96-well cell culture plate with serial ten-fold dilution (10^{-1} to 10^{-6}) and cells mock infected with complete media served as Control.
- ✧ MDBK cells in a 25-cc flask were subcultured using 0.25%Trypsin EDTA and the cell suspension was prepared in the complete growth medium. The cell concentration was estimated and 3×10^{4} cells were added to each well.
- ✧ A hundred microlitres of serially diluted LSDV was transferred to respective wells of the 96-well cell culture plate and 100 µl of media was added to the Control wells. Each dilution was tested in six replicates.
- ✧ The 96-well plate was incubated at 37 °C and plates were regularly observed for CPE.
- ✧ The final reading was taken on the 7^{th} day post-infection and the 50% endpoint dilution ($TCID_{50}$) was calculated using the Reed-Muench formula (Reed and Muench, 1938).

3.2.4 Induction of autophagy and autophagic flux in the MDBK cells

For induction of autophagy in the *in-vitro* system, starvation of cells and chemical inducers has been used at different concentrations (Cheng *et al*., 2019). In MDBK cells specifically, rapamycin at varying concentrations have been used (Fu *et al*., 2014; Zhou *et al.,* 2017; Cheng *et al.*, 2019). Based on the available literature, autophagy in the MDBK cells in the present study was induced as follows:

- ✧ MDBK cells (P_{108}) maintained in Leibovitz's L-15 medium were sub-cultured after attaining 80-90% confluency and seeded into 6- well (6×10^{5} cells/well) and 96-well

(7.3×10^4 cells/well) cell culture plates for assessment of autophagy induction through Western blotting and immunofluorescence, respectively.

- ✧ Cells were divided into 3 groups: i) treatment with autophagy inducer Rapamycin (250 nm) for 48 hours, ii) starved for 2 hours by replacing media with PBS, and iii) Negative control cells overlaid with complete medium.
- ✧ After the specified duration, cells in the 6-well cell culture plates were collected in cell lysis buffer in the presence of a protease inhibitor cocktail and further subjected to Western blotting (briefed in section 3.2.6) for the detection of the LC3B II protein. The cells in the 96-well culture plate were fixed with 10% NBF for 15 minutes and subjected to immunofluorescence assay (briefed in section 3.2.7) for the *in-situ* detection of the LC3B autophagy marker.
- ✧ The experiment was repeated twice and rapamycin (250 nM) was selected for inducing autophagy (Positive control) in the present study accounting for more uniform and consistent results (as assessed by Western blotting and IFT).

3.2.5 Inhibition of lysosomal degradation by bafilomycin A1

The accumulation of LC3 II in cells is subjected to a balance between its production and lysosomal degradation, and thus, LC3B II concentrations in the presence and absence of a lysosomal inhibitor is a prerequisite for meaningful interpretation. The inhibition of autophagic flux/lysosomal turnover was done as follows:

- ✧ MDBK cells (P_{112}) after attaining the desired confluency were seeded into 6-well and 96-well cell culture plates with a cell density of 1.5×10^6 cells/well in the 6-well and 8.4×10^4 cells/well in the 96-well culture plates.
- ✧ The cells were divided into 3 groups: i) treatment with autophagy inducer Rapamycin (250 nm) for 48 hours, ii) starved for 2 hours by replacing media with PBS, and iii) Negative control cells overlaid with complete medium.
- ✧ The cells of each group were treated with the lysosomal inhibitor Bafilomycin A1 at a concentration of 100 nM for 2 hours prior to the sample collection/fixation.
- ✧ After the stipulated time periods, cells were processed for immunofluorescence and Western blotting.

3.2.6 Detection of autophagy marker LC3B II in cells lysate

Western blot assay was optimized to detect the presence of LC3B II in cell lystaes. Briefly, the following protocol for Western blot assay was used:

- ✧ *Sample preparation:* The cells were resuspended in 40 µl of nuclease and protease free water supplemented with protease-phosphatase inhibitor cocktail (Cell Signaling Technology, Massachusetts, USA) followed by sonication (0.5 second sonication at 20% amplitude for 3 cycles with 9 seconds gap between cycles).
- ✧ *Separation of protein bands*: The protein bands were separated by running the lysate samples through 15% SDS-PAGE.
- ✧ *Membrane transfer:* The separated protein bands were transferred to a PVDF membrane (0.45 µm pore size) using Tris-Glycine buffer employing a semi-dry transfer method with the current density of 1.2 mA/cm^2 for 45 minutes.
- ✧ *Membrane blocking:* The blocking was done by commercially available WB blocking solution (TaKaRa) for overnight at 4 °C.
- ✧ *Primary antibody:* The membranes were incubated with primary antibody at 37 °C for 1 h with gentle shaking at following dilutions:
  Anti-LC3B in rabbit – 1:1000 dilution (Novus Biologicals)
  Anti-β-actin in mouse (endogenous control) – 1:20,000 dilution (Invitrogen)
- ✧ *Secondary antibody*: Following washing step, membranes were incubated in secondary antibodies at 37 °C for 1 h with gentle shaking at following dilutions:
  Anti-mouse HRPO conjugate – 1:5000 dilution (Life Technologies)
  Anti-rabbit HRPO conjugate – 1:5000 dilution (Life Technologies)
- ✧ *Immunodetection*: The chromogenic immunodetection was done using modified DAB containing Imidazole and cobalt chloride as described previously (Pukac *et al*., 1997).

3.2.7 *In-situ* detection of autophagy markers using immunofluorsence technique

In the autophagic assay for *in-situ* detection of LC3B in MDBK cells, immunofluorescence assay (IFT) was employed. The cells were fixed at each time point in all the groups and were processed for IFT as follows:

- ✧ MDBK cells showing 70-80% confluency were trypsinized and were seeded in 96-well plate at a seeding density of 6×10^4 cells/well.
- ✧ The cells were treated with either rapamycin (250 nM), or were starved for 2 h or mock-treated with complete media.
- ✧ After completion of each time point, the cells were fixed with 4% paraformaldehyde for 15 min at room temperature.
- ✧ The cells were washed twice with TBST (0.1% T-20).
- ✧ Protein blocking was done using 2.5% normal horse serum (Vector Laboratories, Burlingame CA USA) for 15 min at room temperature.
- ✧ The cells were incubated with primary antibody (Anti-LC3B, Novus Biologicals) at 1:100 dilution and kept at 37°C and room temperature for 1 hour each.
- ✧ Following washing, cells were incubated with duel fluorescence labelling reagent containing a cocktail of DyLight 488 conjugated anti-mouse and DyLight 594 conjugated anti-rabbit secondary antibodies (Vector Laboratories, Burlingame CA USA) for 45 min at room temperature.
- ✧ The cells were washed four times with PBST, 5 min each.
- ✧ Autofluorescence was quenched by Autofluorescence quenching reagents for 5 minutes (Vector Laboratories, Burlingame, CA, USA).
- ✧ The nuclei were counterstained with DAPI (Vector Laboratories, Burlingame CA USA) for 30 min at room temperature.
- ✧ The cells were examined under a fluorescent microscope (Leica, Wetzlar, Germany) at low and high magnification under TRITC/Rhodamine filter and the cells showing distinct bright red fluorescence were considered positive for LC3B.

3.2.8 *In-vitro* infection of MDBK cells with LSDV

After optimizing various reagent concentrations and parameters for Western blotting and immunofluorescence, the *in-vitro* experiment was performed to compare autophagic and autophagic flux in differently treated cells. The *in-vitro* experiment was repeated in triplicates, and the samples were collected and processed from each experiment.

3.2.8.1 Infection with live LSDV

LSDV adapted in MDBK cells (P_7) at a MOI of 0.005 was used for giving infection in the present study. The *in-vitro* infection was carried as follows:

- ✧ MDBK cells were trypsinized and seeded in a 6-well plate with 1.5 x 10^6 cells per well. The cells were divided into three groups: i) Negative control (mock-infected with media containing carrier DMSO 1:20,000 diluted), ii) Positive control (Rapamycin treated @ 250 nM), and iii) LSDV-infected where cells were infected with live LSDV (LSDV-WB/IND/19).
- ✧ For infection, the virus was allowed to adsorb for 1.5 h at 37 °C with intermittent tilting of cell culture plates.
- ✧ Following virus adsorption, the cells were washed twice with fresh media and overlaid with complete media containing 2% FBS. This time point was considered as 0 h time point. Simultaneously at 0 h, cells were mock-infected or treated with rapamycin.
- ✧ At predetermined time points of 6 h, 12 h, 24 h, 48 h, 72 h, and 96 h samples were collected for further processing.
- ✧ Additionally, for the autophagic flux study, each group was further divided into two groups: i) without Bafilomycin A1 and ii) with Bafilomycin A1 (BafA1). Cells were treated with lysosomal inhibitor BafA1 @ 100 nM for 2 h prior to sample collection for complete blockage of lysosomal turnover.

3.2.8.2 Collection and preservation of cells

At the completion of each predetermined time point, the samples were collected and preserved for further analysis as follows:

- ✧ The media was discarded and the cells were washed twice with sterile ice-cold PBS. The cells were scrapped in 500 µl ice-cold PBS, transferred to a 2 ml tube., and centrifuged at 10000 rpm at 4 ºC for 10 minutes.
- ✧ The supernatant was discarded and the cell pellet was resuspended in 200 µl ice-cold PBS. The cell suspension was further aliquoted into 5 tubes containing 40µl each and centrifuged at high speed.
- ✧ The supernatant was aspirated and the cell pellet was labelled for representative samples.

- ✧ For the Western blot assay, the cell pellet was stored in dried form directly at -20 ºC, whereas for relative quantification of autophagy-related genes, the cells were vortexed in 200 µl RNA lysis buffer (Promega) and stored at -20 ºC.
- ✧ The same experiment was repeated in 96-well plates and the cells were fixed for 15 min with 10% NBF at the end of each time point. The formalin-fixed cells were stored at 4 ºC until further processed for IFT.

3.2.9 Relative quantification of autophagy-related genes

To explore the expression of various autophagy-related genes (ATGs) during LSDV infection, the expression of ATG3, ATG5, ATG14 and LAMP2 genes were estimated relative to the housekeeping gene beta-actin using SYBR-green chemistry-based two-step RT-qPCR.

3.2.9.1 RNA isolation

Isolation and purification of RNA from collected cell pellets were done using a commercially available total RNA extraction kit (SV total RNA isolation kit, Promega, Cat no.- Z3105) as per the kit's recommendations. Briefly, the following protocol was used:

- ✧ 350µl RNA dilution buffer was added to the 200 µl of the cells lysed in RNA lysis buffer. The solution was mixed by inverting the tubes 3-4 times, and placed in a heating block at 70 ºC for 3 minutes.
- ✧ Following centrifugation at 12000 ×g for 10 minutes, the cleared lysate was transferred to a fresh centrifuge tube.
- ✧ 200 µl of 95% ethanol was added to the lysate and mixed by pipetting 3-4 times.
- ✧ The solution was transferred to a fresh spin column assembly and centrifuged at 12000×g for 1 minute.
- ✧ 600 µl of RNA wash solution was added to the spin columns and centrifuged at 12000×g for 1 minute.
- ✧ 50 µl of freshly prepared DNase incubation mix was added directly to the membrane and incubated for 15 minutes at 20-25 ºC.
- ✧ 200 µl of DNase stop solution was added to the spin columns and centrifuged at 12000×g for 1 minute.

- ✧ The columns were washed with RNA wash buffer twice and dried by centrifugation at maximum speed for 2 minutes.
- ✧ The spin column was transferred to a fresh centrifuge tube and 75 µl NFW was added directly to the membrane.
- ✧ The assembly was centrifuged at maximum speed, the spin column was discarded and the purified RNA was stored at -20 ºC until further used.

3.2.9.2 cDNA SYNTHESIS FROM THE PURIFIED RNA

cDNA was synthesized from the purified RNA using a commercially available kit (Promega, Cat. No- A5000) as per the manufacturer's instructions. The protocol used is as follows:

- ✧ The RNA mix was prepared by mixing the following components:

Experimental RNA	3µl
Oligonucleotide primer	1µl
Random primer	1µl

- ✧ Each tube of the RNA mix was closed tightly and heated to 70 ºC for 5 minutes and immediately chilled in ice for 5 minutes.
- ✧ The tubes were centrifuged briefly and stored in ice until a reverse transcription (RT) mix was added.
- ✧ RT mix was prepared by combining the following components in a sterile microcentrifuge tube on ice:

Sr. No.	Component	Volume (µl)
1.	5X reaction buffer	4
2.	$MgCl_2$	2.5
3.	Nucleotide mix	1
4.	RT enzyme	1
5.	RNase inhibitor	0.5
6.	NFW	6
	Total	15

- ✧ The RNA mix was added to the RT mix on ice to make a total volume of 20 µl.
- ✧ Annealing was done at 25ºC and 5 minutes.
- ✧ The tubes were incubated at 42ºC for 1 hour, followed by thermal inactivation of RT enzyme at 70 ºC for 15 minutes.
- ✧ The synthesized cDNA was stored at -20 ºC until real-time PCR was done.

3.2.9.3 Real-time PCR for the detection of autophagy-related genes

The expression levels of specific autophagy-related genes (ATG5, LAMP2, ATG3, and ATG14) regulating the cellular autophagic responses were assayed by quantitative real-time PCR using Thunderbird SYBR Green qPCR mix (Puregene, Cat: QPS-201) in StepOnePlus real-time thermal cycler (Applied Biosystems, CA, USA). The primers used in the RT-qPCR are detailed in the table 1. Each sample was run in duplicate. The fold change in the expression levels of each gene was calculated by the $2^{-\Delta\Delta Ct}$ method (Livak and Schmittgen, 2001) and normalized against the housekeeping β-Actin gene.

All reactions were set in a 20 µl reaction mix in 0.2 ml thin-walled PCR tubes (Axygen, Central Ave Union City, CA USA) as follows:

Components	**Volume (µl)**
2x PCR master mix	10.0
Forward primer (10 pmol/µl)	0.25
Reverse primer (10 pmol/µl)	0.25
Rox dye	0.40
Template	2.0
Nuclease-free water	7.1
Total:	**20.0 µl**

The details of optimized thermal cycling conditions used for the amplification of ATG genes are as follows:

Table 1: Details of primers used for the amplification of ATG genes using YBR-green chemistry-based real-time PCR

S. No.	Name	Primer	Sequence	Length (bp)	Optimal Annealing	Product length	Reference
1	ATG5	Forward	AGCATCATCCCGCAACCAAC	20	63ºC	191	Liu *et al*., 2021
		Reverse	GACCAGCCCTAGTGCCCTTA				
2	ATG3	Forward	GAGCAACGGCAGCCTTTAAC	20	60ºC	102	Fu *et al*., 2014
		Reverse	TGGTGGGAGATGAGGGTGAT				
3	ATG14	Forward	CCAGAGCGGCGATTTCGTCTACT	23	60ºC	342	Roy *et al*., 2021
		Reverse	CCAAGTTTGCGATTATGCCTCTG				
4	LAMP2	Forward	CCGTGTCTGGAGCATTTCAG	20	60ºC	110	Xu *et al*., 2021
		Reverse	GGTGTCATCATCCAGCGAAC				
5	Beta- Actin	Forward	GCCAACCGTGAGAAGATGAC	20	60ºC	94	Glare *et al*., 2002
		Reverse	AGGCATACAGGGACAGCACA				

S.No.	Steps	Temperature	Time
Step 1	Initial heat activation	95 °C	60 sec
Step 2	Two-step cycling (40 cycles)		
	• Denaturation	95 °C	15 sec
	• Combined annealing/extension	60/63 °C	60 sec
Step 3	Melt curve	95 °C	15 sec
		60 °C	1 min
		95 °C	15 sec

3.2.10 Determination of autophagy induction in LSDV infected cells with different MOIs

To determine whether autophagy induction is guided by the dose of viral infection, MDBK cells were infected with LSDV at 3 different MOIs (0.001, 0.0025, and 0.005) for specific time periods (24, 48, 72, and 96 hpi).

- ✧ MDBK cells grown in a 25-cc flask were subcultured and seeded in a 6-well cell culture plate with a seeding density of 1.5×10^6 cells/well.
- ✧ The cells were infected by LSDV at indicated MOIs and the volume of infection was determined by the following equation:

$$\text{MOI} = (\text{Virus titer} \times 0.7)\ X\ \frac{\text{Volume of virus } (\mu l)}{(\text{Number of cells seeded})} \times \frac{1}{1000}$$

- ✧ The virus suspension was overlaid on the cells for 1.5 h with intermittent gentle rotation. Following virus adsorption, the cells were washed twice and overlaid with complete media.
- ✧ After each predetermined time point *viz.* 24 h, 48 h, 72 h, and 96 h, the cells were harvested and subjected to the detection of autophagy-specific cell protein LC3B II using Western blotting.

3.2.11 Chemical inactivation of LSDV

Binary Ethylineimine (BEI) was used for the inactivation of LSDV as described previously (Hulskotte *et al.,* 1997). Briefly, the following protocol was used:

- ✧ BEI was freshly prepared before the experiment by dissolving 400 mg of 2-bromoethylamine hydrobromide (BEA, SIGMA- Aldrich, China) in 1 ml of 0.2 N NaOH solution to attain a concentration of 0.1 M.
- ✧ The solution was mixed at 37 °C in a shaker for 1 hour to facilitate the conversion of BEA to BEI.
- ✧ The freshly prepared BEI was filter sterilized and 20 µl of the mixture was added to 1 ml of the LSDV suspension to yield a final concentration of 2 mM.
- ✧ The tube was kept at 37 ºC with shaking for 6 hours, followed by transfer to another 2 ml centrifuge tube and kept again at 37 ºC with shaking for a further 24 hours to allow a total contact time of 30 h.
- ✧ The inactivated virus suspension was neutralized by the addition of 1.5 µl of 1M sodium thiosulphate (10% of the volume of the BEI solution used).
- ✧ The inactivated virus suspension was aliquoted and stored at -20 ºC until use.

3.2.11 Validation for the complete inactivation of LSDV

The complete inactivation of LSDV by BEI treatment was confirmed by two approaches:

a) Absence of LSDV-induced CPE in MDBK cells

b) Absence of LSDV genome detection in sequential cell passages

3.2.11.1 *Absence of LSDV-induced CPE in MDBK cells*

- ✧ MDBK cells were seeded in a 6-well cell culture plate at a seeding density of 1.5 x 10^6 cells per well.
- ✧ 25 µl of BEI-inactivated LSDV and live-LSDV (P_7) were inoculated in MDBK cells for 2 h at 37 ºC.
- ✧ Following virus adsorption, the cells were washed and overlaid with complete media.
- ✧ The cells were incubated for 6 days at 37 ºC to detect the presence of LSDV-specific CPE.

- ✧ In the absence of apparent CPE in BEI-inactivated LSDV after 6 days, the cells were freeze-thawed thrice and the lysate was further sonicated (0.5-second sonication at 20% amplitude for 3 cycles with 9 9-second gap between cycles).
- ✧ The lysate was centrifuged at 8000 rpm for 15 min and the supernatant was collected. The supernatant was further used for another round of infection in MDBK cells.
- ✧ The process was repeated twice and the absence of characteristic CPE in the third passage of BEI-inactivated LSDV and the presence of typical cell rounding, degeneration, clumping, and refractile cell in the positive control (live-LSDV) was considered as a marker of complete inactivation of LSDV.

3.2.11.2. *Absence of LSDV genome detection in sequential cell passages*

To further validate that the LSDV is completely inactivated and no traces of live LSDV are present in the BEI-treated virus suspension, the sequential passages of live and BEI-inactivated LSDV in MDBK cells were subjected to the detection of LSDV genome employing SYGR-green-based qPCR.

a). DNA isolation

Total cellular DNA was isolated from the cell lysate as per the instructions of a commercially available kit (Invitrogen, USA, Cat. No- K1820-02) as below:

- ✧ 200 µl of the cell lysate was mixed with 20 µl RNAase A by brief vertexing and incubated at room temperature for 2 minutes.
- ✧ 200 µl genomic lysis/binding buffer was added and the solution was incubated at 55 ºC for 10 minutes to promote protein digestion.
- ✧ 200 µl 96-100% ethanol was added to the sample and the solution was transferred to a fresh spin column.
- ✧ The spin column was centrifuged at 10000×g for 1 minute. The 500 µl wash buffer 1 was added and again centrifuged at 10000×g for 1 minute.
- ✧ After the addition of 500 µl of wash buffer 2 to the spin column, the column was centrifuged at maximum speed for 3 minutes.

✧ 50 µl of the elution buffer was added to the column and the purified DNA was isolated by centrifugation at maximum speed for 1 minute.

b) Real-time PCR for amplification of LSDV gene

The detection of the LSDV RNA polymerase subunit gene (RPO147) was conducted by quantitative real-time PCR with Thunderbird SYBR Green qPCR mix (Puregene, Cat: QPS-201) in StepOnePlus real-time PCR system (Applied Biosystems, CA, USA) as described previously (Gelaye *et al*., 2017). The primers used are detailed in the table 2. Each sample was run in duplicate. Melting curve analysis was employed to confirm the specificity of the amplicon

Table 2: Details of primers used for the amplification of the RPO147 gene of LSDV

Sr. No.	Primer	5'-3' Sequence	Product length (bp)	G+C Content
1	CaPV-Fw	TCCTGGCATTTTAAGTAATGGT	100	38
2	CaPV-Re	GTCAGATATAAACCCGGCAAGTG	100	38

The reactions were set in a 20µl reaction mix in 0.2 ml thin-walled PCR tubes (Axygen, Central Ave Union City, CA USA) as follows:

Components	Volume (µl)
2x PCR master mix	10.0
Forward primer (10 pmol/µl)	0.25
Reverse primer (10 pmol/µl)	0.25
Rox dye	0.40
Template	2.0
Nuclease-free water	7.1
Total:	**20.0 µl**

The details of optimized thermal cycling conditions used for the amplification of the LSDV RPO147 gene are as follows:

S.No.	Steps	Temperature	Time
Step 1	Initial heat activation	95 °C	60 sec
Step 2	Three-step cycling (40 cycles)		
	• Denaturation	95 °C	15 sec
	• Annealing	59 °C	30 sec
	• Extension	72 °C	30 sec
Step 3	Melt curve	95 °C	30 sec
		60 °C	1 min
		85 °C	15 sec

3.2.12 Infection of MDBK cell with BEI-inactivated LSDV

The protocol for the infection of MDBK with BEI-inactivated LSDV is briefly described below:

- ✧ MDBK cells were seeded at a density of 1.5 x 10^6 cells per well in a 6-well cell culture plate.
- ✧ The cells were divided into three groups – i) negative control (mock-infected with media), ii) BEI-inactivated LSDV infected, and iii) positive control (live LSDV infected).
- ✧ Positive control cells were infected with live LSDV (LSDV-WB/IND/19) at MOI = 0.005 and inactivated LSDV group cells were infected with BEI-inactivated LSDV at an equivalent pre-inactivated MOI of 0.005.
- ✧ The cells were incubated for 48 h and 72 h post infection and cells were collected as described earlier.
- ✧ The collected cells were processed for detection of LC3B II protein through Western blot assay.

Results

4 RESULTS

4.1 Detection of autophagy and autophagy flux in response to *in-vitro* LSDV infection

4.1.1 Adaptation of LSDV in homologous cell line and virus titration

To simulate the natural infection, LSDV isolated and passaged in heterologous cell line (Vero cells) were adapted in host homologous cell line MDBK. The MDBK cells showing 70-80% confluency was inoculated with Vero-adapted LSDV and passaged serially. The MDBK cells exhibited no CPE for the initial three passages. In the absence of apparent CPE, consecutive blind passages were given until CPE characteristics to LSDV (cell rounding, clustering, vacuolation, granulation, and the presence of refractile cells) were noted in passage 4 (Figure 1). To increase the virus titer, the virus was further adapted to passage 7 (P_7). The LSDV P_7 was harvested, aliquoted in small batches, and stored at -20 °C. The virus titration was carried out in a 96-well cell culture plate using the Reed and Muench method, and the virus titer was determined as $10^{5.5}TCID_{50}$/ml.

Furthermore, *in-situ* detection of LSDV through an immunofluorescence test demonstrated the cytoplasmic presence of LSDV from 24 hours onwards. At 24 hours post-infection, the number of LSDV-positive cells was meagre (Figure 2A & 2B). The LSDV replication progresses in MDBK cells and by 72 hours post-infection, a large majority of cells were infected by LSDV (Figure 2C & 2D).

4.1.2 Expression of autophagy marker LC3B in response to LSDV infection

The induction of autophagy is characterized by the detection of specific autophagy markers and conversion of LC3B I to LC3B II is considered as the most reliable marker of

autophagy. To detect the effect of LSDV infection on the cellular autophagic machinery, the level of LC3B II was estimated in LSDV-infected MDBK cells through Western blot assay.

The cell lysate collected at pre-determined time points from different groups was subjected to SDS-PAGE, followed by detection of LC3B (14-16 kDa) by Western blotting using anti-LC3B pAb. The bands in the Western blot assay were quantified using densitometry, lane-normalized and normalized against the levels of housekeeping protein β-actin to nullify the variation in sample loading. The data was subjected to suitable statistical analysis.

The results of Western blotting revealed the detection of autophagy marker LC3B across all the groups, *viz.*mock-infected, Rapamycin treated and LSDV infected cells (Figure 3). A basal level of autophagy is evident throughout the Control group, suggesting the high proliferative and metabolic profile of MDBK cells. During the entire experiment, the autophagy marker LC3B showed mild variation in the mock-infected and the LSDV infected cells and were comparable between the groups (Figure 4). A progressive increase in the autophagy was noted in the Rapamycin treated cell post 48 hr. At 96 hr post-treatment, an appreciably higher mean expression of LC3B was noted in the Rapamycin treated cells as compared to the other two groups. Statistical analysis also revealed no significant differences among the mock infected and the LSDV infected cells, suggesting that LSDV is maintaining the basal levels of cellular autophagy either by inhibiting the autophagic induction or by upregulating the lysosomal degradation of autophagic markers.

4.1.3 Influence of LSDV on autophagic flux

The levels of LC3B protein in the cells are subjected to a balance between its formation and its lysosomal degradation in the cell cytoplasm. Therefore, an increase or decrease in the LC3B detection alone is not a conclusive indicator of autophagy induction/inhibition. To this end, differences in the levels of LC3B expression in the presence and absence of lysosomal inhibitor (Bafilomycin A1) were carried out across the groups. The expression of LC3B in cell lysate was carried out through Western blotting and the relative quantification of the LC3 protein levels compared to β-Actin protein levels was determined by densitometry (Figure 5).

Bafilomycin-treated cells in all three groups showed an upregulated expression of LC3B II as compared to those without Bafilomycin treatment, indicating an effective inhibition of the autophagic degradation and accumulation of LC3B in cells (Figure 6). However, LSDV-infected cells post-24-hour infection exhibited a marginal difference in the mean LC3B levels even after the inhibition of lysosomal fusion and degradation by Bafilomycin A1 (Figure 7), implying a probable suppression of autophagosomal degradation. Despite this, no significant variation in the levels of LC3B among the Bafilomycin-treated and untreated cells was noted across the groups.

Collectively, the results of LC3B detection through Western blot assay indicate that *in-vitro* LSDV infection does not alter the basal level of cellular autophagy, likely by maintaining the normal levels of LC3B proteins and by suppression of the lysosomal degradation of autophagosomal contents. Also, the mean expression of LC3B protein levels increases throughout the study in all the groups (Figure 8).

4.1.3 *In-situ* detection of autophagy marker in LSDV-infected cells

Besides the detection of LC3B in cell lysates, LC3B protein was also detected *in-situ* through an immunofluorescence assay. A minimum of ten high-power fields (40x) were observed under the inverted fluorescent microscope and the LC3B positive cells showing bright red fluorescence (DyLight 594) and the total number of cells (blue fluorescence of DAPI) were counted manually. The percentage of the LC3B positive cells was estimated and compared across different groups in the presence and absence of lysosomal inhibitor Bafilomycin A1.

Immunofluorescence assay revealed the presence of LC3B-associated vacuoles in the cytoplasm of cells, localizing in a perinuclear space to encompassing the entire nucleus (Figure 9 & 10). A basal level of autophagy was observed in all the groups throughout the experiment. Interestingly, the mean per cent positivity of LC3B ranged from 17% to 22.8% in the mock-infected cells at different time points. Rapamycin-treated cells demonstrated markedly enhanced expression of LC3B vacuoles as compared to the other groups, particularly in the Bafilomycin A1-treated cells (Figure 11). The level of LC3B expression in mock-infected and LSDV-infected cells was comparable, except for the 24-hour time point. Overall, no significant

difference was noted in the LC3B *in-situ* detection across the mock-infected, rapamycin-treated and LSDV-infected cells at different time points (Figure 12). Also, the immunofluorescence assay exhibited a insignificant difference in the relative fold change expression of LC3B in LSDV-infected MDBK cells with respect to negative control (Figure 13).

4.1.4 Effect of virus titre on cellular autophagy

To assess the effect of LSDV titer on the cellular autophagy machinery, MDBK cells were infected with different MOIs of LSDV (0.001, 0.0025 and 0.005) and the difference in autophagy induction was determined for four-time points (24, 48, 72 and 96 hpi) by Western blotting and calculating the relative expression of the LC3B protein by densitometry.

In all the groups, conversion of LC3B I to II was noted. At 24 hpi, however, a progressive decline in LC3B II detection was noted with an increase in the titer of LSDV used for giving infection. MOI of 0.005 resulted in minimal detection of LC3B II, hinting that higher titers of LSDV are inhibiting the conjugation of LC3B I, although the results were marginally insignificant between MOI = 0.001 and MOI = 0.005 (adjusted $p = 0.0541$) (Figure 14). The results were comparable at later time points (48 h onwards) with no variation in the levels of LC3B following infection with varying MOIs of LSDV (Figure 15).

4.1.5 Expression of ATGs in LSDV-infected cells

The expression levels of the autophagy-specific genes (ATG5, LAMP2, ATG3, and ATG14) were assayed by quantitative real-time PCR (Figure 16 – 18). For each gene, relative fold change expression was determined by the $2^{-\Delta\Delta Ct}$ method and analysed statistically using the two-way mixed model repeated measures ANOVA.

a. Expression of ATG-3 gene

The relative fold change of ATG3 was comparatively more in the rapamycin-treated cells, whereas the expression of the ATG3 gene in mock-infected and LSDV-treated cells was comparable. No significant differences were noted in the ATG3 gene expression within the groups with progression of time. Also, no appreciable variations were observed between the differently treated groups.

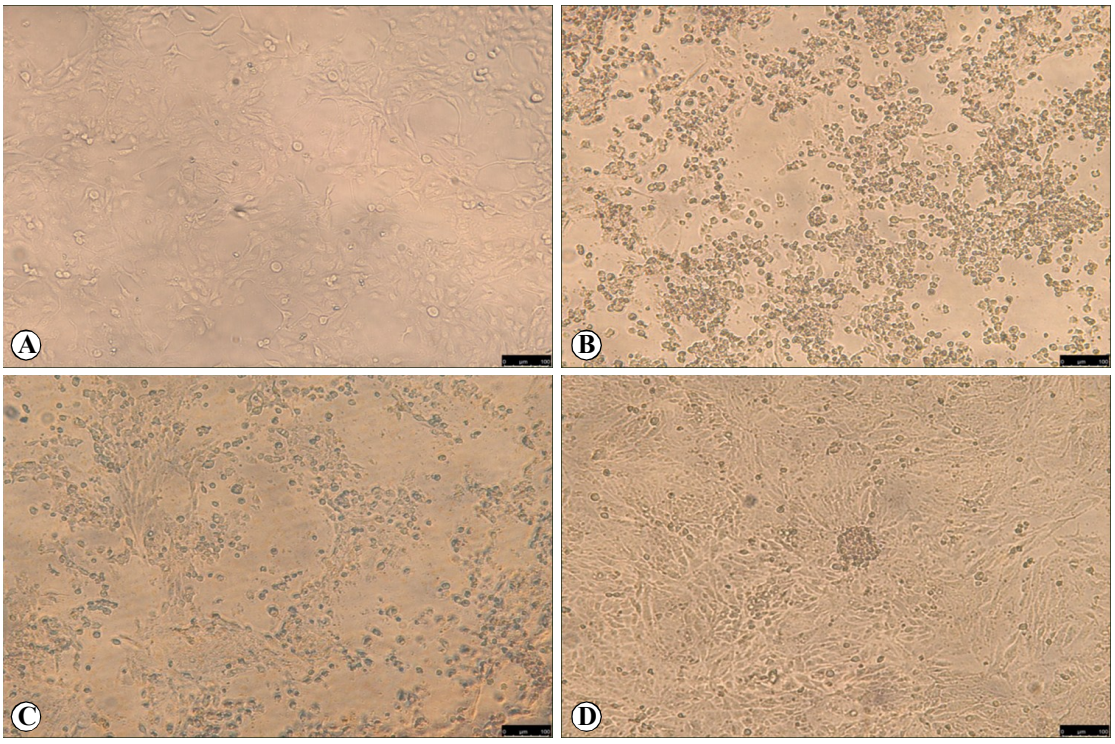

Fig. 1: Morphological changes and cytopathic effects in MDBK cells infected with LSDV. (A) Healthy MDBK cell. MDBK cells infected with (B) 10^{-2} dilution, (C) 10^{-3} dilution and (D) 10^{-4} dilution of LSDV, showing varying levels of degeneration, detachment, cell rounding and clustering

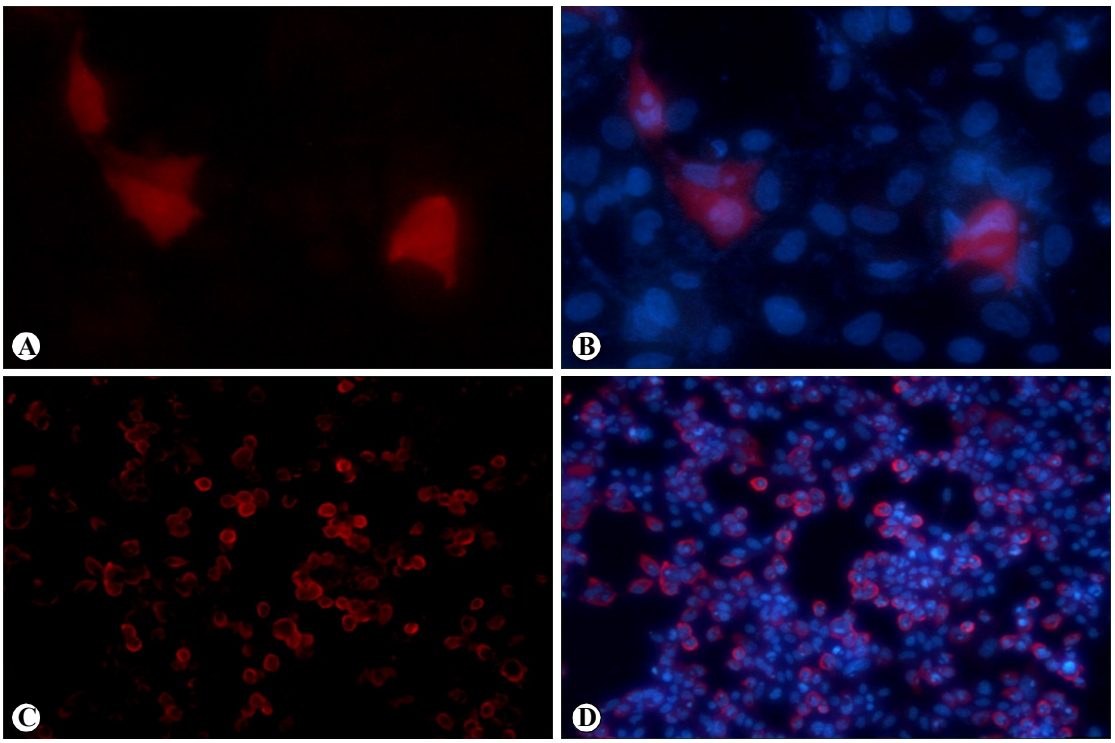

Fig. 2: DyLight 594 labelled cytoplasmic localization of LSDV in the infected cells (A) merged with nuclear stain (DAPI) after 24 hpi, X400 (B). Increased number of LSDV-infected cells (C) merged with nuclear stain (DAPI) at 72 hpi, X100 (D)

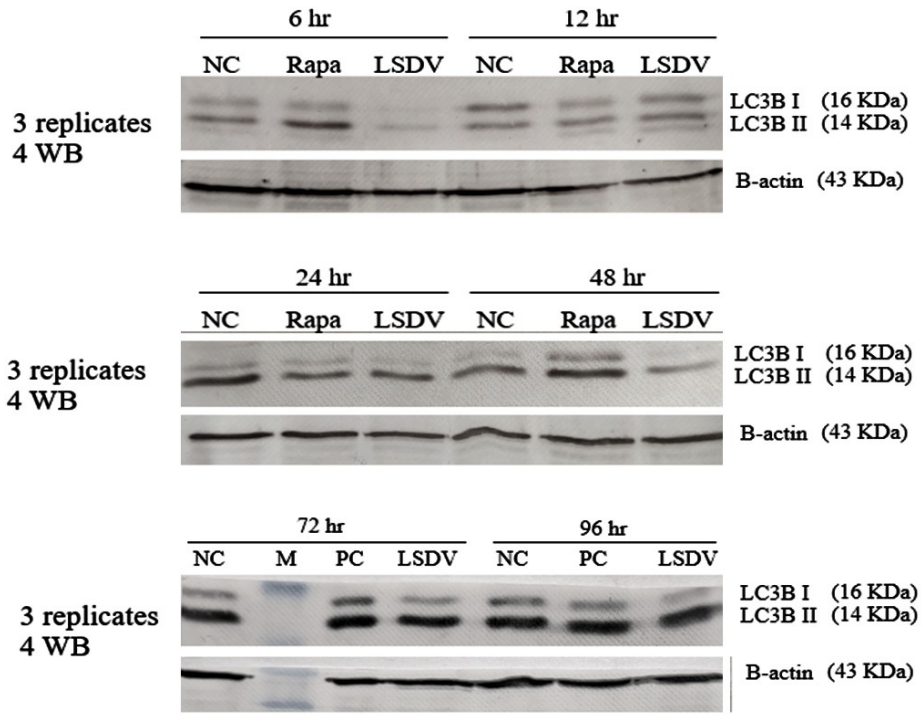

Fig. 3: Detection of autophagy induction by LSDV in MDBK cells. MDBK cells were mock-infected, treated with rapamycin (250nM) and LSDV-infected (MOI = 0.005) and the autophagy marker protein LC3B II was detected through Western blot at 6 h, 12 h, 24 h, 48 h and 96 h post-treatment (A)

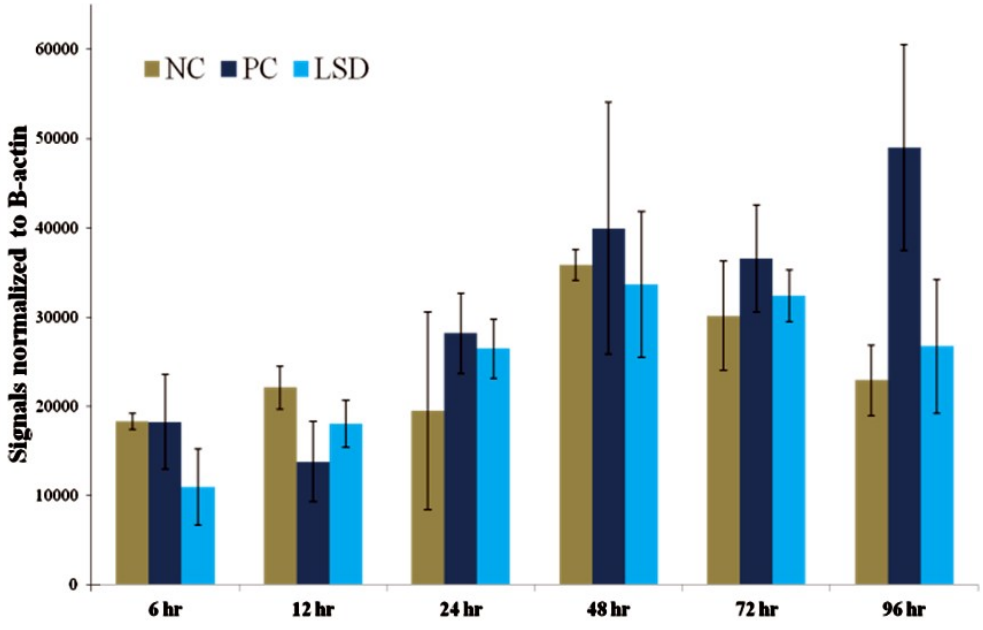

Fig. 4: LC3B II protein expression among mock-infected (NC), rapamycin-treated (PC) and LSDV-infected MDBK cells at different time points

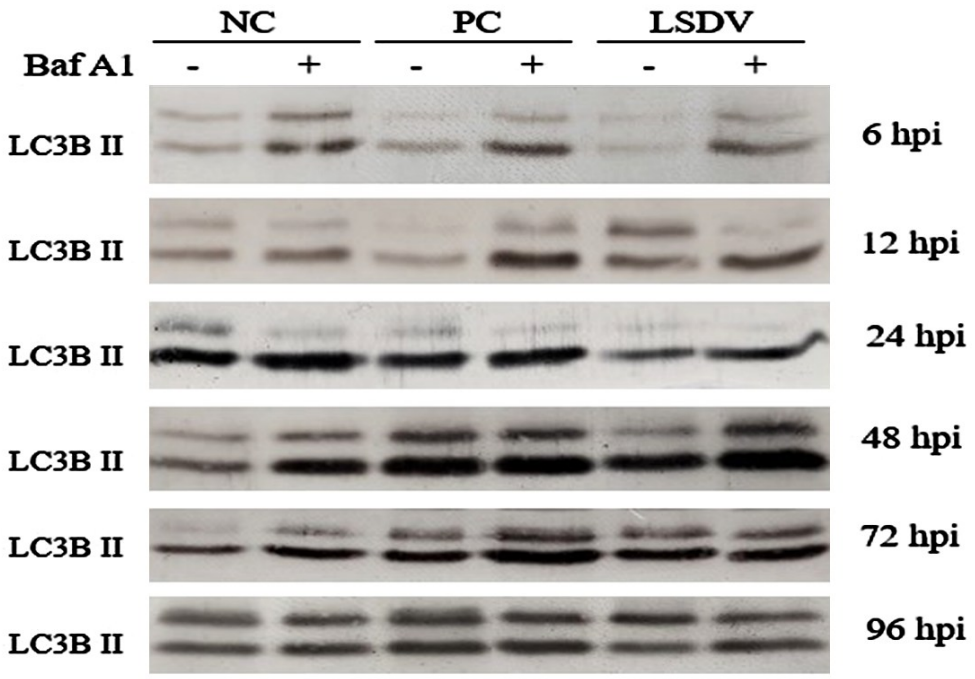

Fig. 5: Detection of LC3B in the mock-infected, Rapamycin treated (250 nM), and LSDV-infected cells in the presence and absence of autophagy inhibitor Bafilomycin A1 (100nM) at different time points through Western blotting using anti-LC3B specific pAb

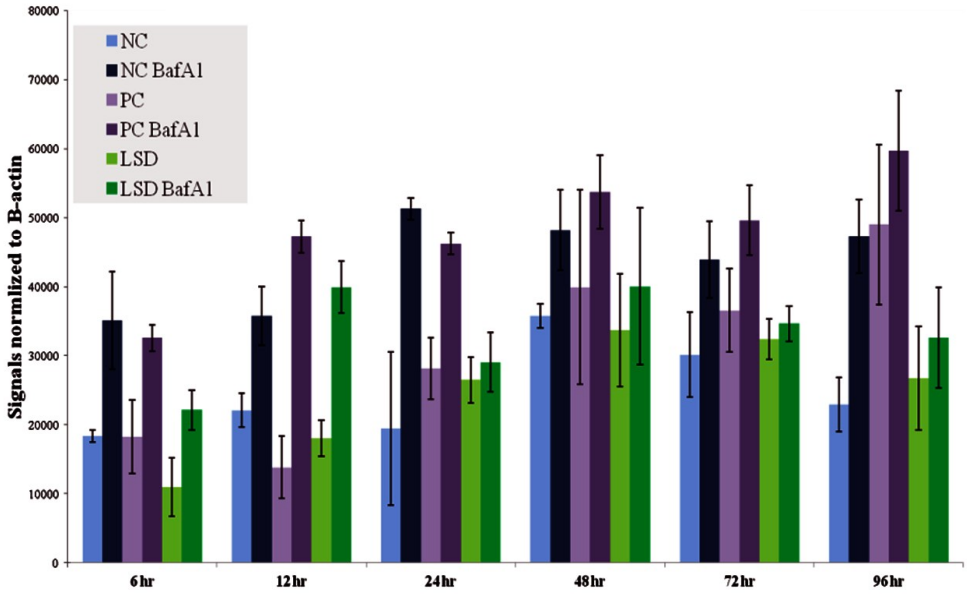

Fig. 6: Graphical presentation of the normalized LC3B II protein in the mock-infected, Rapamycin-treated (250nM), and LSDV-infected (MOI = 0.005) cells in the presence and absence of autophagy inhibitor Bafilomycin A1 (100nM) at different time points

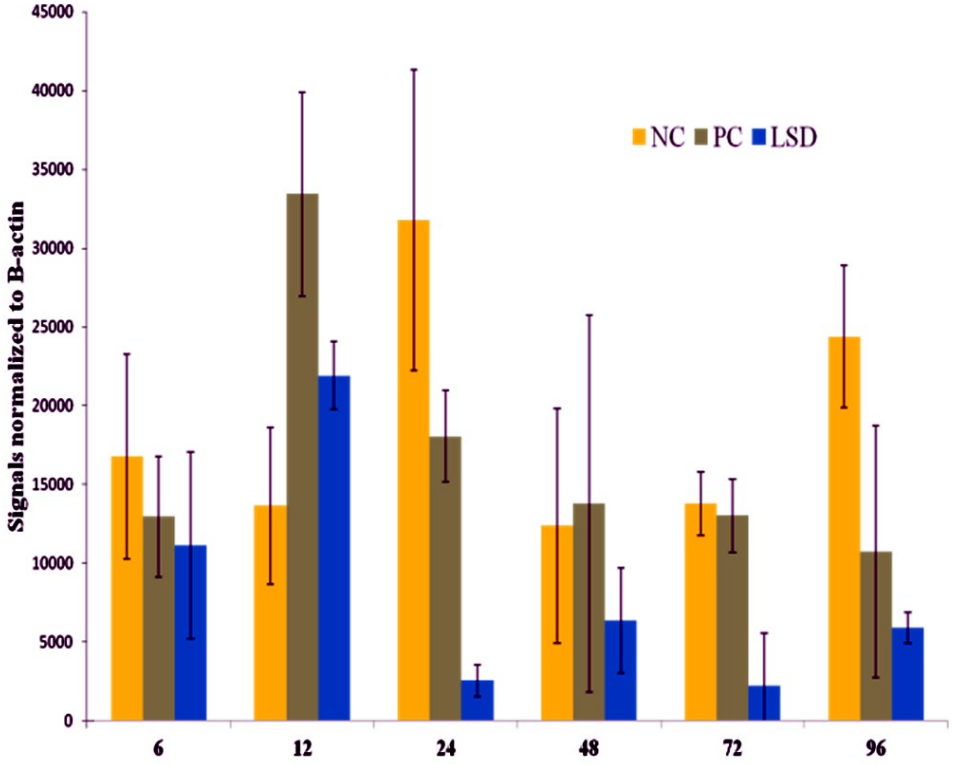

Fig. 7: Graphical representation of the difference in the LC3B II protein expression in the presence and absence of Bafilomycin A1 (100nM) among the different groups at predetermined time points

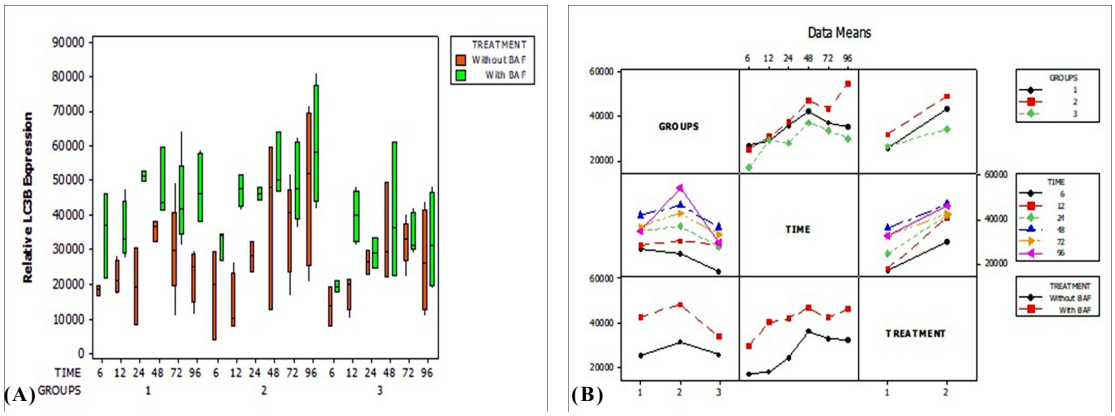

Fig. 8: A) Box- Whisker plot and B) Interaction plot revealing the normalized LC3B II protein in the mock-infected, Rapamycin-treated, and LSDV-infected cells in the presence and absence of autophagy inhibitor Bafilomycin A1 (100nM) at different time points

b. Expression of ATG-5 gene

The normalized expression of ATG5 revealed a near-constant expression in mock-infected and rapamycin-treated cells. Contrary to this, LSDV-infected cells exhibited a sharp rise in ATG5 expression at 12 hr post-infection before reaching the basal levels. A significantly higher expression (adjusted $p = 0.0266$) was noted at 12 hr post-treatment in the LSDV-infected group as compared to the other two groups (Figure 19)

c. Expression of ATG-14 gene

A significantly higher expression of the ATG14 gene was noted in the mock-infected cells at 6 hpi whereas the rapamycin-treated and LSDV-infected cells demonstrated a marked increase in ATG14 gene expression at 24 hpi (Figure 20). The fold change differences were significant between different time points within the groups (adjusted $p = >0.0001$ for all the time points) as well as between different groups (adjusted $p = >0.0001$ between mock and LSDV infected).

d. Expression of LAMP-2 gene

Within the mock-infected group, an appreciable increase in the LAMP2 gene expression was noted at 06-hour post-treatment, however, significantly higher levels were observed at 96-hour post-treatment (adjusted $p = 0.0215$). Contrary to this, LSDV-infected cells maintained the basal levels of LAMP2 up to 72 hours post-infection but revealed a consequential decline in LAMP2 at 96 hours post-infection (Figure 21) as compared to the mock-infected cells (adjusted $p = >0.0001$).

4.2 Cellular autophagy in response to inactivated LSDV

4.2.1 Chemical inactivation of LSDV

The complete inactivation of LSDV P_7 by BEI was confirmed by the absence of characteristic CPE in three sequential passages of inactivated LSDV in the MDBK cells. Contrary to this, equivalent live LSDV produces characteristic CPE and severe degeneration of cells in the subsequent passages. For further confirmation of complete inactivation, healthy MDBK cells, BEI-inactivated LSDV P_3 and LSDV P_{10} were amplified for the LSDV-specific

gene (RNA polymerase subunit gene). The amplification plot and melt curve demonstrated specific PCR amplification in only LSDV P_{10} (figure 22), suggesting the lack of LSDV genome in BEI-inactivated LSDV $P_{3.}$

4.2.2 Effect of LSDV inactivation on cellular autophagy

The cellular autophagic response in terms of LC3B II expression was analyzed in the mock-infected, live LSDV-infected (MOI = 0.005) and BEI-inactivated LSDV (equivalent to pre-inactivated MOI of 0.005) at 48 and 72 hpi. Dunnett's multiple comparisons test revealed a significantly higher (p = 0.0453) LC3B II expression in MDBK cells infected with BEI-inactivated LSDV as compared to the mock-infected cells at 72 hpi (Figure 23). Also, like the previous Western blot assay, the LC3B lipidated form (LC3B II) was comparable between the mock-infected and live LSDV-infected groups, suggesting that live LSDV, and not inactivated LSDV, has the potential to inhibit the autophagy induction.

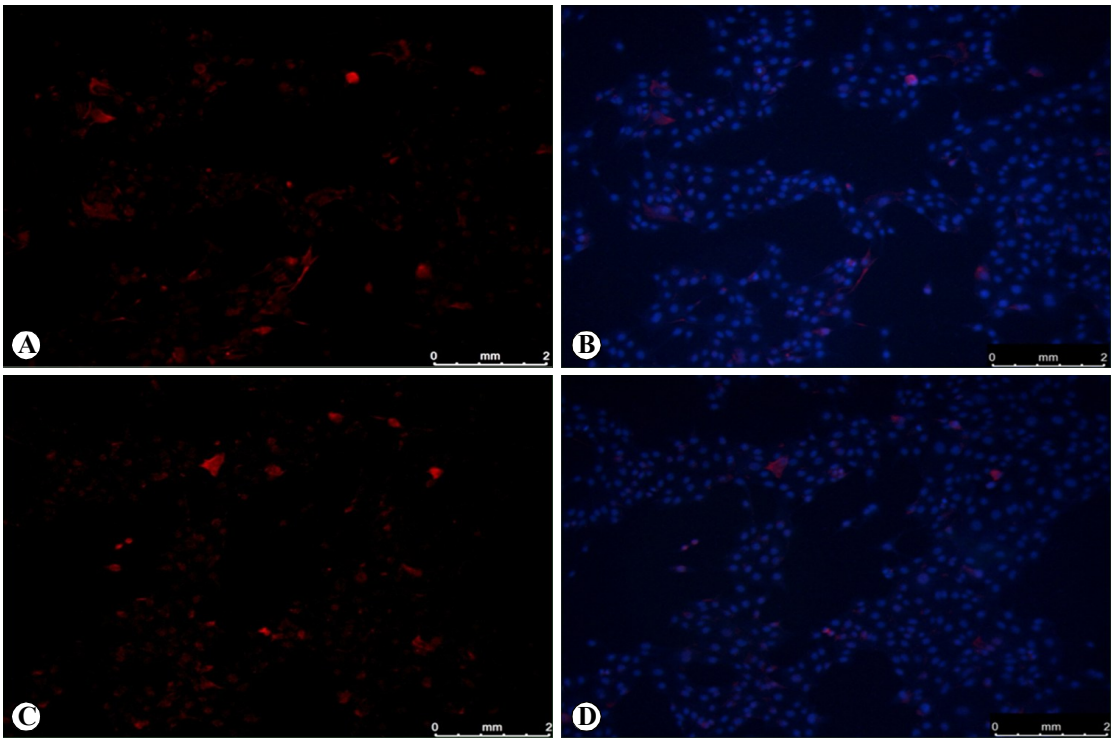

Fig. 9: Immunofluorescenece assay detecting the total LC3B protein in the mock-infected (A & B) and LSDV-infected (C & D) MDBK cells at 12 hpi. FAT with Dylight 594 giving bright red colour to LC3B counterstained with DAPI, X100

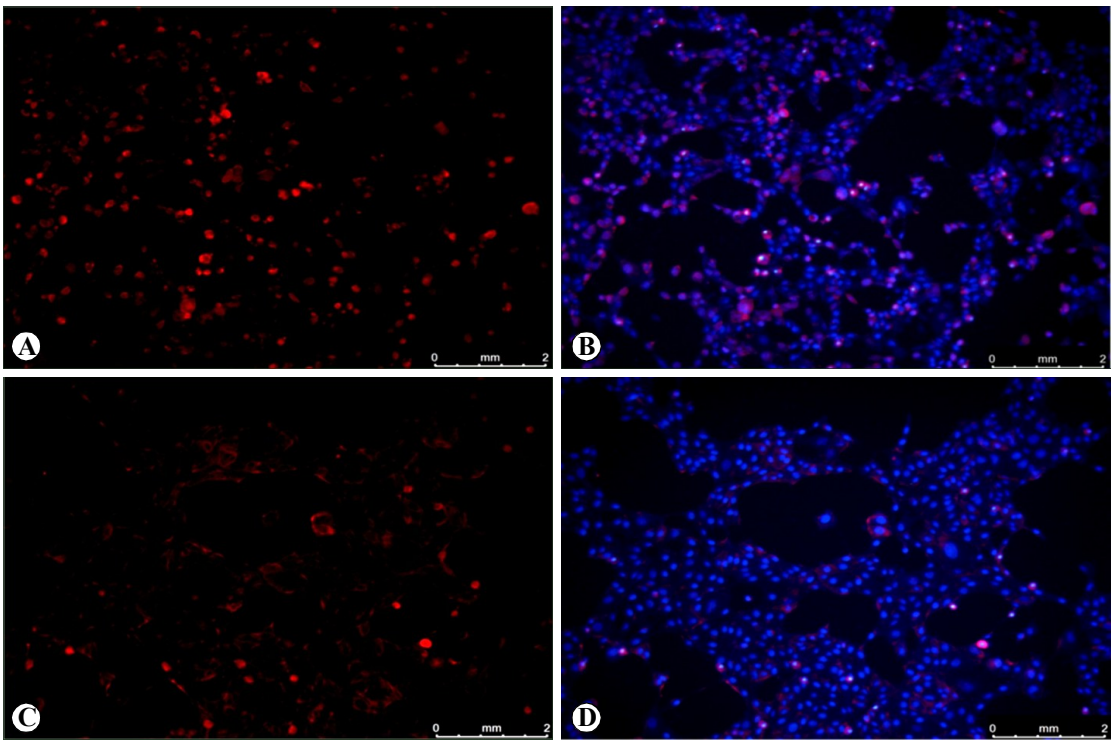

Fig. 10: Immunofluorescenece assay detecting the total LC3B protein in the LSDV-infected (A & B) and mock-infected (C & D) MDBK cells at 24 hpi. FAT with Dylight 594 giving bright red colour to LC3B counterstained with DAPI, X100

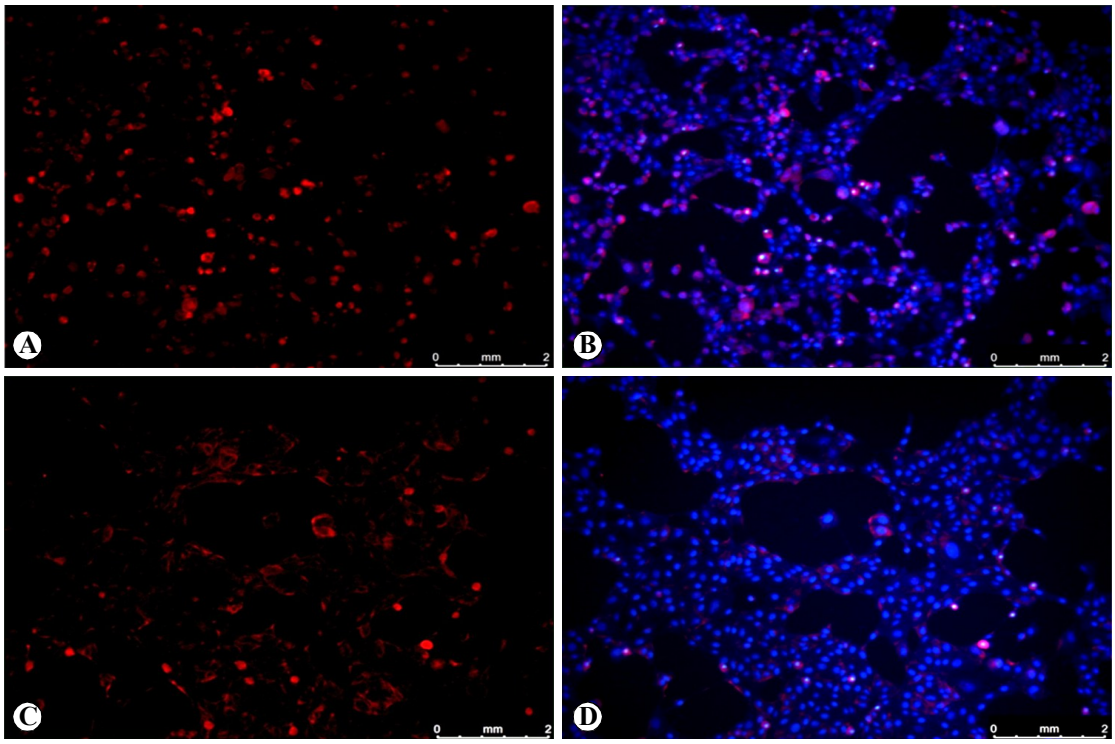

Fig. 11: Immunofluorescenece assay detecting the total LC3B protein in the Rapamycin-treated (A& B) and Bafilomycin A1 treated, in addition to Rapamycin treatment (C & D) MDBK cells 24 hour post treatment. FAT with Dylight 594 giving bright red colour to LC3B counterstained with DAPI, X100

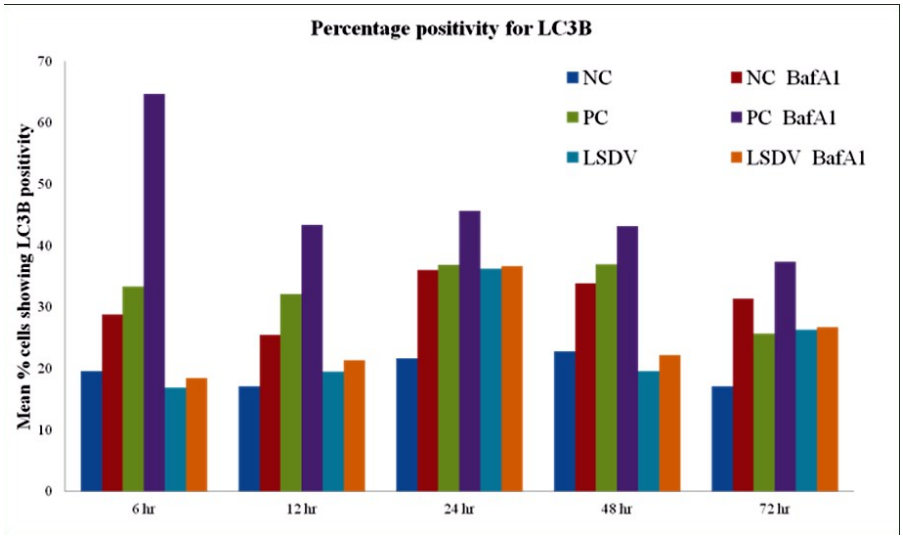

(A)

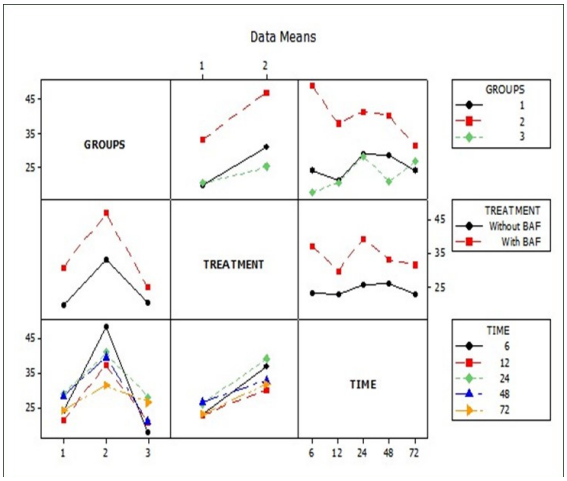

(B)

Fig. 12: A) Bar graph and B) Interaction plot showing the mean percent of cells showing LC3B positivity in immunofluorescence among different groups in the absence and the presence of Bafilomycin A1 (100nM) at predetermined time points of 6 h, 12 h, 24 h, 48 h, and 72 h

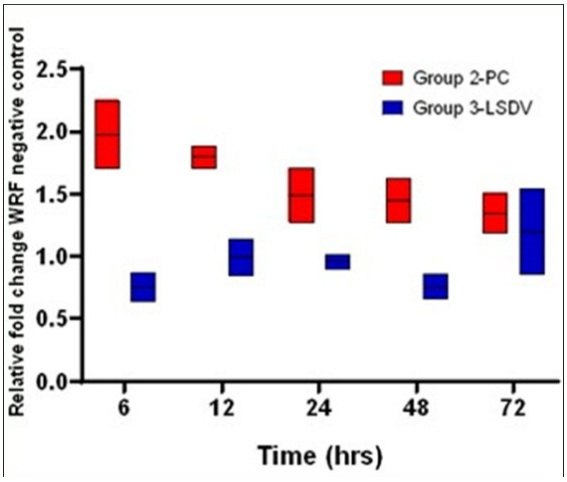

Fig. 13: Relative fold change in the LC3B expression in Rapamycin-treated and LSDV-infected cells with respect to mock-infected negative control

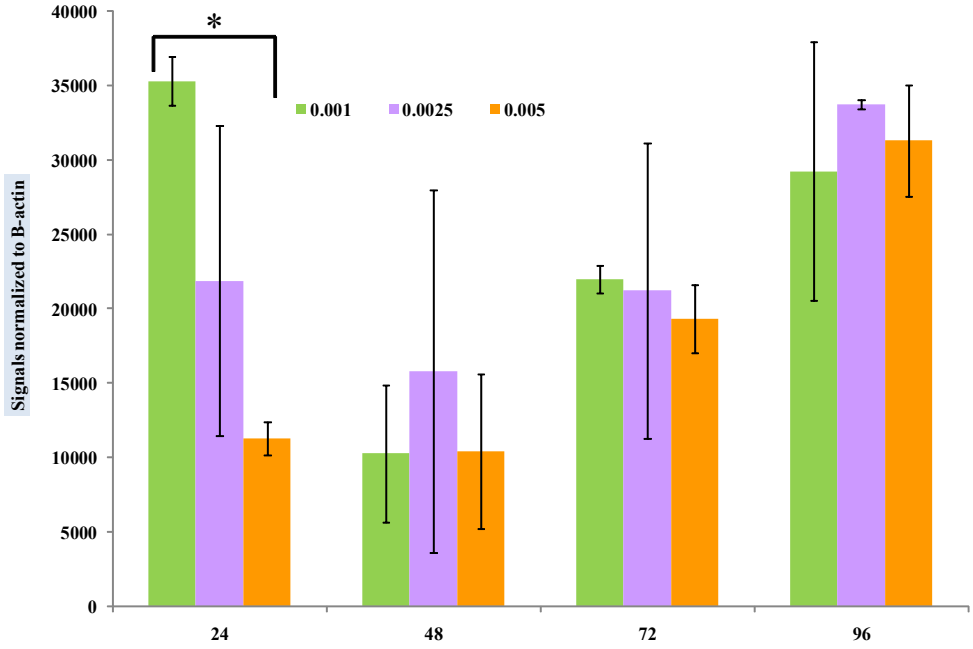

Fig. 14: LC3 II expression in MDBK cells infected with different MOIs of LSDV (0.001, 0.0025 and 0.005) for 24, 48, 72, and 96 hpi. *p = 0.0541

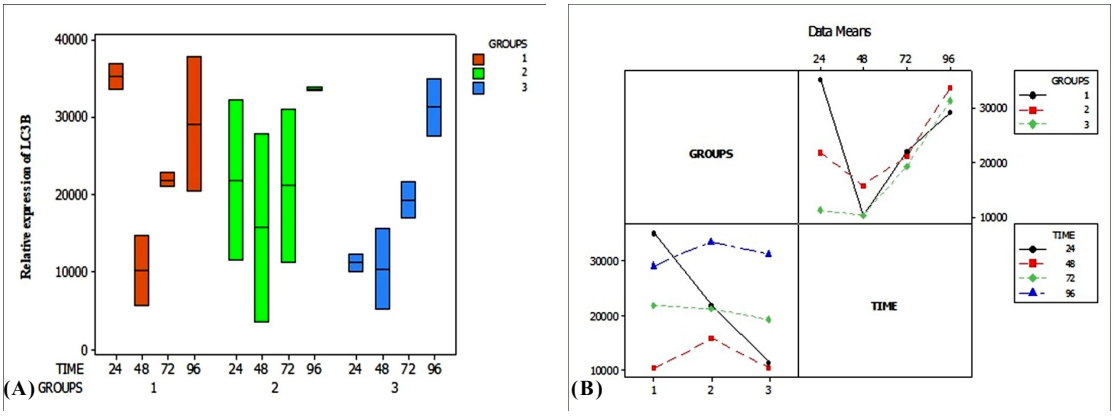

Fig. 15: A) Box- Whisker plot & B) Interaction plot showing LC3 II expression in MDBK cells infected with LSDV with different MOIs (0.001, 0.0025 and 0.005) at 24, 48, 72, and 96 hpi

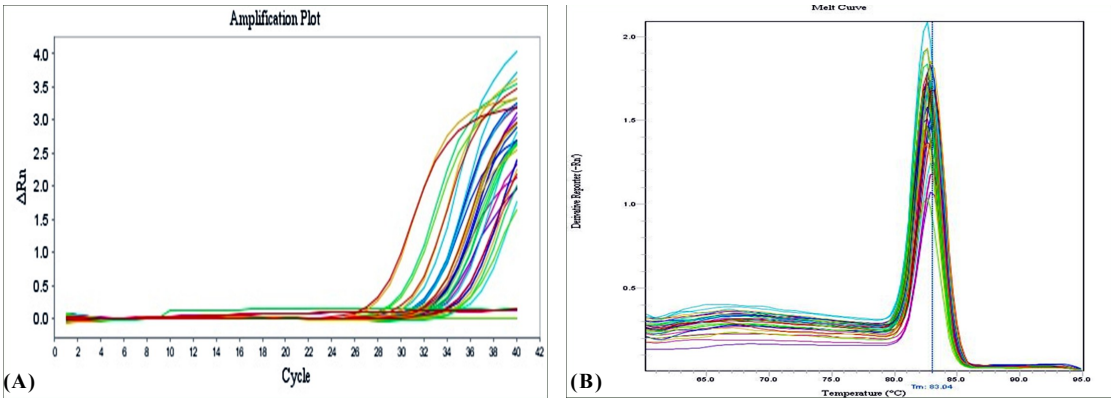

Fig. 16: SYGR-green based RT-qPCR amplification of ATG5 gene in mock-infected, rapamycin-treated and LSD-infected MDBK cell showing A) Amplification plot and B) Melt curve

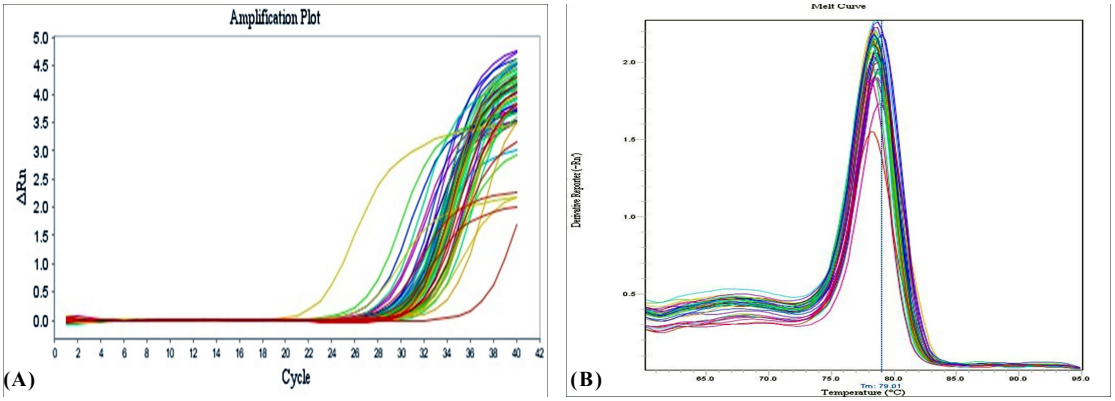

Fig. 17: SYGR-green based RT-qPCR amplification of ATG14 gene in mock-infected, rapamycin-treated and LSD-infected MDBK cell showing A) Amplification plot and B) Melt curve

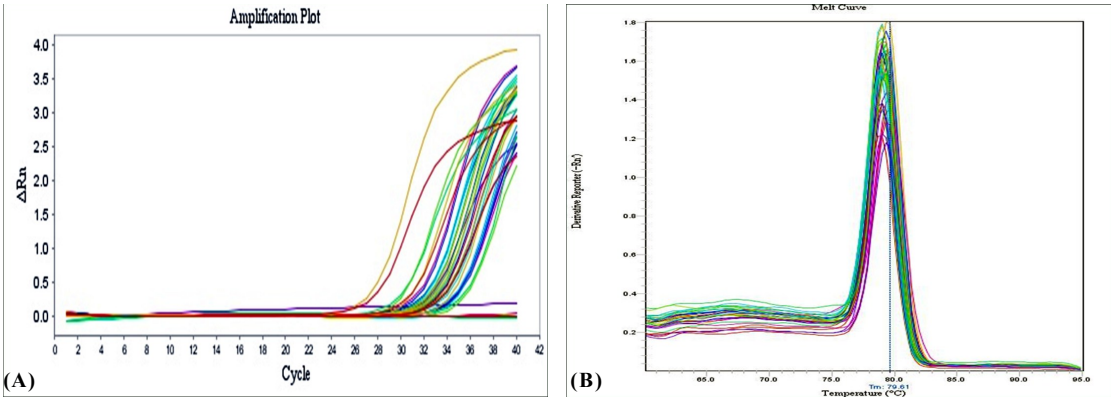

Fig. 18: SYGR-green based RT-qPCR amplification of LAMP2 gene in mock-infected, rapamycin-treated and LSD-infected MDBK cell showing A) Amplification plot and B) Melt curve

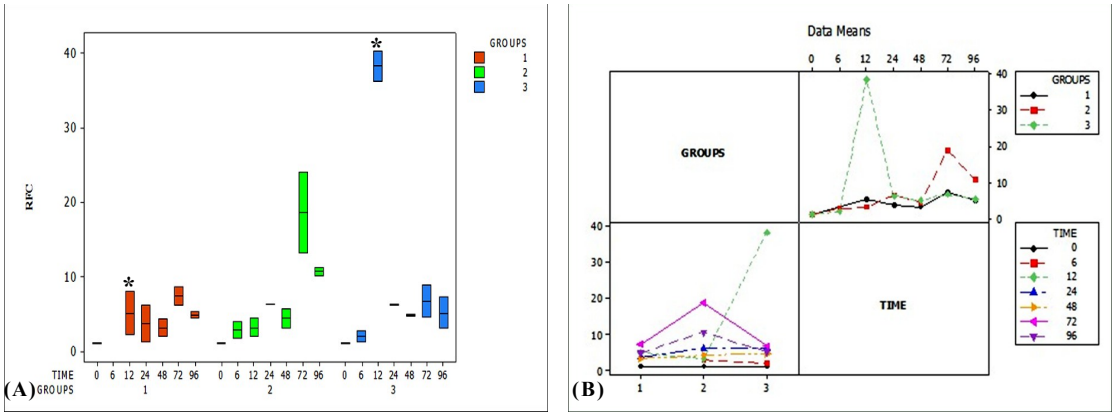

Fig. 19: A) Box- Whisker plot & B) Interaction plot showing the relative fold change of ATG5 gene in the different groups, mock- infected (1), Rapamycin- treated (2), and LSDV- infected (3) for different time points. *- p = 0.0266.

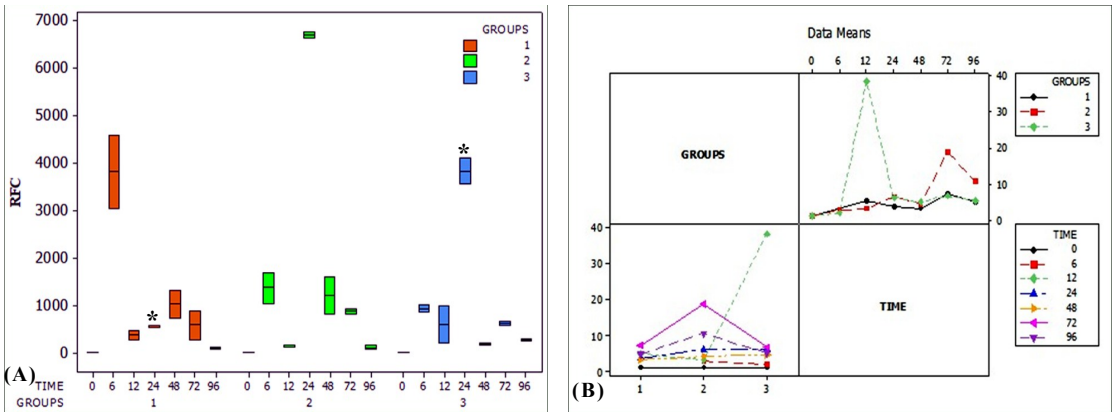

Fig. 20: A) Box- Whisker plot and B) Interaction plot showing the relative fold change of ATG14 gene in the different groups, mock- infected (1), Rapamycin -treated (2), and LSDV- infected (3) for different time points. *p < 0.0001

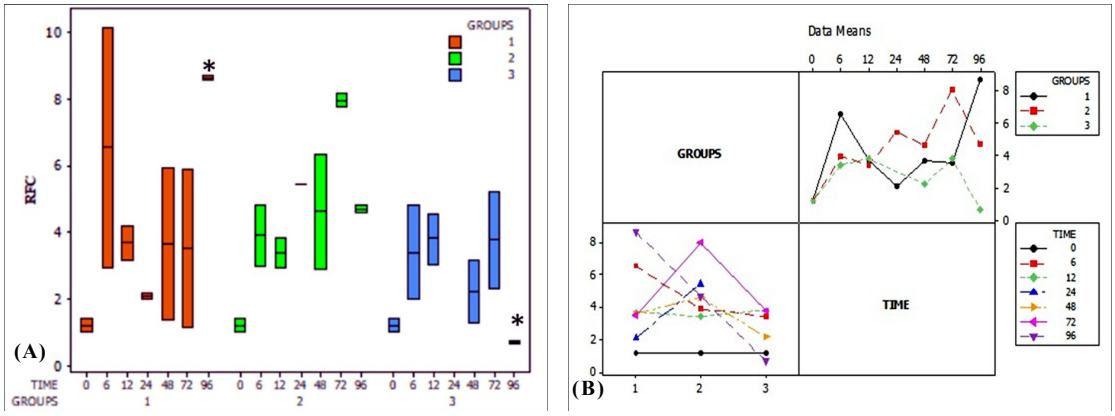

Fig. 21: A) Box-Whisker plot & B) Interaction plot showing the relative fold change of LAMP2 gene in the different groups, mock- infected (1), Rapamycin-treated (2), and LSDV- infected (3) for different time points. *p < 0.0001

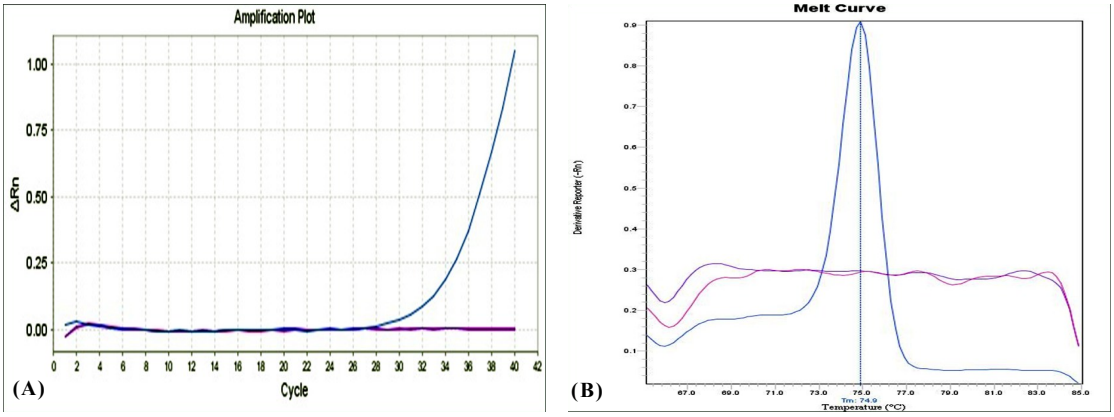

Fig. 22: PCR confirmation of the complete inactivation of LSDV following BEI treatment. (A) Amplification plot showing positive amplification of LSDV in live MDBK adapted LSDV P10 and lack of amplification in mock-infected MDBK and BEI-inactivated P3 of LSDV. (B) Melt curve analysis revealing a single melt curve peak of LSDV positive amplicon

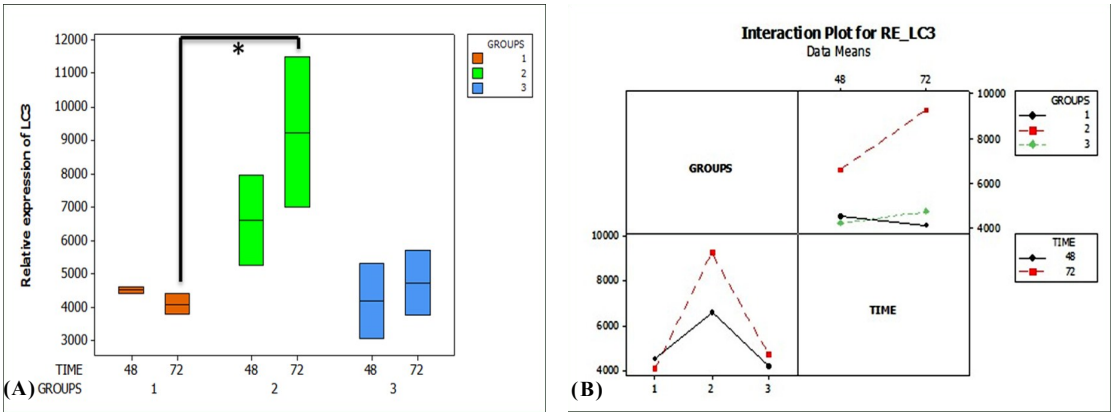

Fig. 23: Box- Whisker plot (A) and interaction plot (B) showing the LC3B II expression in mock-infected (group 1), BEI inactivated LSDV P1 infected (group 2), and live LSDV P10 infected (group 3) MDBK cells at 48 h and 72 h post-infection. *p = 0.0453

Discussion

5 DISCUSSION

The Poxvirus family has caused widespread devastation in humans and animals from time immemorial. With the exception of dogs, the majority of domestic animals can contract diseases spontaneously from viruses belonging to the Poxviridae family. It is distinguished by its extensive and intricate genome, which is made up of a single linear molecule of double-stranded DNA that code for about 200 different proteins. The family contains 8 important genera which are of clinical importance (Quinn *et al*., 2015). The Capripoxvirus genus stands out as particularly detrimental within the Poxviridae family when it comes to impacting domestic ruminants. Starting from the pandemic of smallpox more than 3000 years ago to monkeypox virus outbreaks in 2022, poxviruses continue spreading a scenario of caution and threat to human and animal lives (Tegnell *et al*., 2002; Thornhill *et al*., 2022). A recent point of concern for the global livestock industry is a series of Lumpy skin disease outbreaks in Southeast Asian countries from 2019 onwards, surpassing over 1 lakh cattle mortality in India (Kumar and Tripathi, 2022). An estimated INR 18337.76 crores (USD 2217.26 million) were lost in India as a result of the LSD outbreak in cows (Singh *et al*., 2023). Persistent poxvirus outbreaks prompt apprehension regarding viral transmission and pathogenesis, necessitating comprehensive studies for a better understanding of host-pathogen interaction.

LSDV is a crucial member of the Capripoxvirus genus along with the goatpox virus and sheeppox virus. LSDV exhibits a nucleotide sequence homology with GTPV and SPPV that surpasses 97% (Gershon *et al*., 1989). LSDV possesses severe economic ramifications by impacting cattle hides, reproduction, and the quality of milk, leading to significant financial losses. Approximately 2.4 million animals were impacted as of October 21, 2022, with over 110,000 animal deaths recorded in India alone (Mathivanan *et al*., 2023).

Continuing research efforts are directed towards creating advanced vaccines and diagnostic tools to better combat lumpy skin disease. Despite the widespread acceptance of prevention-based strategies in virus control, it remains critical to thoroughly examine the disease process triggered by the virus. Also, vaccines against LSDV trigger short-term protection (6 months to 1 year) and require repeated booster doses. More importantly, LSDV replicates efficiently in cell cytoplasm despite an armour of anti-viral innate immune responses. This further necessitates the need to understand the host-pathogen interaction at the molecular level for devising better and long-lasting prophylactic/therapeutic interventions.

Among the various innate cellular immune responses, autophagy plays an important role in curbing the progression of viral infections by mediating the lysosome-mediated cytoplasmic degradation. Despite a plethora of autophagic studies in viral infections (Deretic, 2009), the information on the role of autophagy in LSDV infection remains largely unknown. To this end, the present study was aimed at delineating the role of autophagy in the molecular pathogenesis of LSDV in the cell culture system.

LSDV exhibits a limited spectrum of permissibility in cell culture. Historically, its cultivation has predominantly relied on primary cells derived from ruminants, including lamb testis cells, fetal bovine muscle and skin cells (Binepal *et al*., 2001). Cell lines such as BHK-21 cells (Davies, 1982), Vero cells (Ayelet *et al*., 2013), MDBK cells (Awad *et al*., 2010), ovine testis cell line (OA3.Ts) (Babiuk *et al*., 2007) have been used for the isolation and propagation of LSDV. To simulate the natural infection as closely as possible, a homologous cell line of bovine origin, MDBK cells, was used for the present study. The LSDV adapted well in the MDBK cells and started showing characteristic CPE from P_4 and attained a titer of $10^{5.5}TCID_{50}$/ml in just seven passages in MDBK. The growth characteristics of LSDV in MDBK cells have been reported previously (Fay *et al*., 2020). The adaptation of LSDV in MDBK cells and the cytopathic effects observed in the present study were very similar to those reported in the previous studies (Fay *et al*., 2020; Naveen *et al.,* 2021).

To evaluate the effect of LSDV replication on cellular autophagy, we determined the levels of protein LC3B II and total LC3B through Western blot assay and immunofluorescence,

respectively, in mock-infected, rapamycin-treated, and LSDV-infected MDBK cells. Because the amount of LC3-II represents the number of autophagosomes and autophagy-related structures, LC3 is now the most extensively utilized autophagosome marker (Yoshii *et al*., 2017). Our Western blot assay revealed a marked conversion of LC3B I to II in Rapamycin-treated cells, indicating the strong induction of autophagy in response to an inciting stimulus. More importantly, no significant differences were observed in the levels of LC3B II among the mock-infected and the LSDV-infected MDBK cells. Also, at several time points, the level of LC3B II in LSDV treated cells is even lower than the mock-infected cells. These findings suggest that LSDV is somehow allowing basal autophagy and is inhibiting the induction of cellular autophagy machinery to facilitate its replication. Another *in-vitro* study by Tan and co-workers (2023) in Bovine Embryonic Fibroblasts (BEF) revealed induction of autophagy by LSDV at 96 hpi. However, no LSDV-mediated autophagy was observed in BEI at earlier time points. A slight contrast in the result at 96 hpi in the present and previous study (Tan *et al*., 2023) could be attributed to differences in the cell lines. Varied autophagic responses in different cell lines have been reported when subjected to similar stimuli or conditions (Prins *et al*., 2021). Another contrasting factor is the normalization of Western blot data. The present study expressed the levels of LC3B II protein in relation to housekeeping protein β-Actin whereas Tan and co-workers used a ratio of LC3B II and LC3B I. The ratio of LC3B II/I is prone to erroneous interpretations as LC3B I is more prone to degradation and LC3B II tends to be more sensitive to immunodetection (Mizushima and Yoshimori, 2007).

The endogenous level of LC3B is subject to degradation during autophagy, and thus, estimating LC3B alone is not a marker of cellular autophagy (Tanida *et al*, 2005). For the estimation of cellular autophagic response, the determination of autophagic flux or lysosomal turnover is estimated. The present study assessed the lysosomal turnover by estimating the LC3B levels in the presence and absence of lysosomal inhibitor Bafilomycin A1. We found apparent differences in the LC3B II levels in the mock-infected and the rapamycin-treated cells, however, the differences in the LSDV-infected groups were marginal. Though we could not find any statistically significant differences between the mock-infected and the LSDV-infected MDBK cells with and without Bafilomycin A1, our results gave an indication that LSDV is inhibiting lysosomal degradation.

Previous *in-vitro* and *in-vivo* studies have demonstrated that the interaction between the poxviruses and cellular autophagy is quite complex and varies remarkably. During mousepox-causing Ectromelia virus infection, the expression of Beclin 1 is upregulated, while Beclin 2 expression is downregulated (Martyniszyn *et al*., 2013; Martyniszyn *et al.,* 2011). The Molluscum contagiosum virus harnesses the viral FLIP protein to regulate autophagy (Kaiser *et al*., 2009). According to Zhang *et al*. (2006), autophagy is not necessary for the replication and maturation of the Vaccinia virus, and its replication kinetics are unaffected by cellular ATG5, ATG7, and Beclin1 levels. Further evidence of the vaccinia virus-mediated abnormal LC3 lipidation and total suppression of autophagosome formation was provided by Mologhney and colleagues (Moloughney *et al*., 2011). The vaccinia virus also blocks autophagic flux by modifying the autophagic reporter protein p62's nuclear shunting (Krause *et al*., 2021). Another member of the poxvirus family, Orf virus suppresses the signalling pathway of mTOR *in-vivo* to enhance autophagy (Huang *et al*., 2022). In light of these findings, the present study indicates that LSDV may be inhibiting not only the induction of autophagy, but also the lysosomal degradation in infected cells.

To further validate our findings, the *in-situ* detection of LC3B in MDBK cells was performed using immunofluorescence. Cells showing a distinct bright-red color of Alexa Fluor 594 were considered as positive for LC3B and the results were expressed as per cent positivity. The results of immunofluorescence corroborate with our Western blot assay with no significant difference in the level of total LC3B between the mock-infected and the LSDV-infected cells up to 96 h of infection, implying the inhibition of autophagy induction/autophagosome formation by LSDV. However, the immunofluorescence assay performed in the present study has a limitation. In the immunofluoresence assay, we were able to detect total LC3B protein instead of the lipidated LC3B II. Contrary to Western blot assay, where two separate bands for LC3B I (16 KDa) and LC3B II (14 KDa) can be differentiated and the lipidated form (PE-conjugated LC3B II) could be used for analysis, the lipidation of LC3B I to II in immunofluorescence is characterized by punctae formation, which could be distinctly visualized by the use of a confocal microscope (Runwal *et al*., 2019). In the absence of a confocal microscope, the cytoplasmic accumulation of LC3B I, which is actually not a marker of

autophagosome formation, has also contributed towards the immunofluorescence signal generation. This could be the most probable reason for a reasonably high per cent positivity of LC3B in all the groups during IFT assay. To nullify this effect, the results of rapamycin-treated and LSDV-infected groups were expressed as the fold change relative to the mock-infected group.

Previous studies have used different MOIs of LSDV for *in-vitro* infection, with MOI = 0.01 being the most common (Fay *et al*., 2020; Tran *et al*., 2023). The use of MOI = 0.01 led to the degeneration and detachment of MDBK cells at 96 hpi, and to this end, we employed an MOI = 0.005 for the autophagic study. To study the effect of varying MOIs of LSDV on cellular autophagy, we used MOI = 0.005, 0.0025, and 0.001. At 24 hpi, we observed an apparent decline in LC3B II formation in higher MOI (0.005) as compared to the lowest MOI (0.001), nonetheless, the difference was slightly inconsequential ($p = 0.0541$). To the best of our knowledge, the effect of LSDV dose on cellular autophagy has not been reported previously, but we believe that the incorporation of a higher MOI or a log fold increment in MOI would provide a better insight into the effect of LSDV dose on autophagy inhibition and could be a subject matter of further studies.

Despite the generation of new information, the possible mechanisms of LSDV-induced inhibition of autophagy induction and lysosomal turnover remain unclear to us. To address this, we amplified three autophagy-related genes (ATG3, ATG5, and ATG14) involved in the initiation and progression of autophagosome formation and one gene (LAMP2) attributed to lysosomal turnover. A significantly higher level of ATG5 and ATG14 were detected in the LSDV-infected cells at 12 and 24 hpi, respectively, as compared to the mock-infected cells. Both ATG5 and ATG14 are required for the lipidation of LC3B and upregulated gene expressions are expected to increase the autophagy. Contrary to this, no increase in the LC3B II was noted at the protein level suggesting that LSDV might be adopting multiple strategies to counter cellular innate autophagic response. Furthermore, a significant drop in the LAMP2 transcription in LSDV-infected cells in the later stages of infection (96 hpi) could probably be accounted for the partial inhibition of autophagic flux. The information on the transcription of autophagy-related genes in LSDV is nearly non-existent. In vaccinia virus infection, aberrant LC3 lipidation

which is independent of ATG5 has been reported (Moloughney *et al.,* 2011).

We further analyzed whether replication of LSDV is required to inhibit the lipidation of LC3B or whether the attachment and entry are sufficient to induce the inhibitory effect. For complete inactivation of LSDV without alkylation of viral proteins, BEI was used at a final concentration of 2 mM for 30 h. Matsiela and co-workers (2022) have also inactivated LSDV using the same concentration of BEI for 36 h for the preparation of LSDV inactivated vaccine. Though other methods of LSDV inactivation, such as UV exposure, have also been reported (Fay *et al.,* 2022). BEI inactivation of the vaccinia virus using varying concentrations and exposure time has been described previously (Hulskotte *et al.,* 1997).

The results of the LSDV inactivation study reveal a significantly higher level of LC3B II ($p = 0.0453$) in the BEI-inactivated LSDV (equivalent to the pre-inactivated MOI = 0.005) as compared to the mock-infected cells, whereas, the live LSDV at MOI of 0.005 showed comparable LC3B II levels. Our results demonstrated that despite the preservation of the entry-associated viral proteins, inactivated LSDV loses its potential to inhibit autophagy and incite an upregulated LC3B I to II conversion. These findings suggest that effective inhibition of cellular autophagy response by LSDV requires replication and translation of viral proteins other than/in addition to those present in the viral lateral bodies. Even though it is evident that the LSDV is inhibiting the autophagy as well as the lysosomal degradation, the mechanism regarding the process and, the influence of autophagic machinery in virus replication are yet to be elucidated, which stand as the future perspectives of the study.

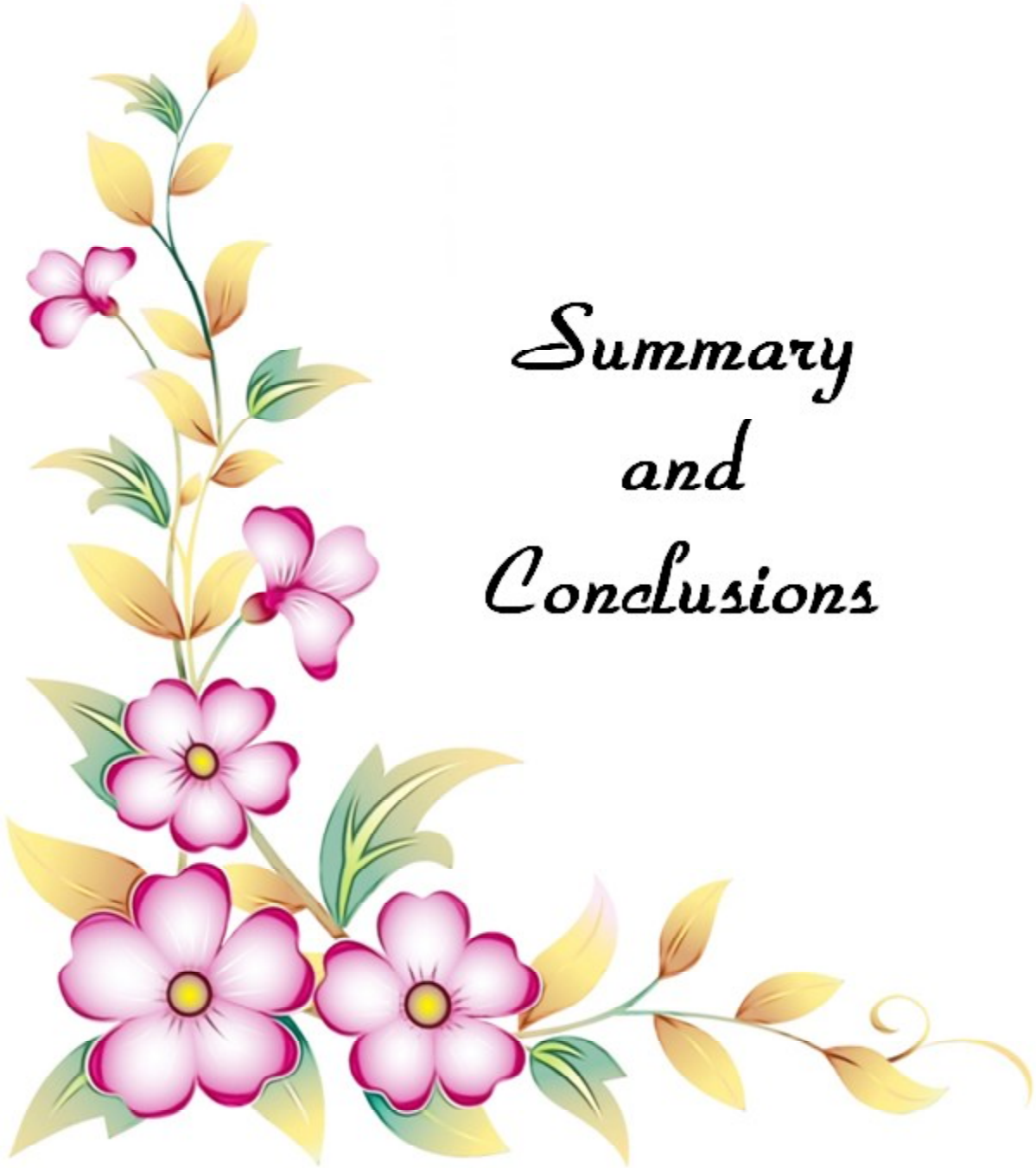

Summary and Conclusions

6 SUMMARY AND CONCLUSIONS

Lumpy Skin Disease (LSD) is an infectious, nodular disease of mainly cattle and buffalo caused by the LSD virus of the *Capripoxvirus* genus and the Poxviridae family. The disease is associated with severe economic losses and can readily cross national and international boundaries, and thus has been classified as an OIE notifiable disease for cattle. Considering the socio-economic impact of LSD on the global livestock economy, it is pertinent to understand the host-pathogen interaction comprehensively.

Poxviruses replicate in the cytoplasm of infected cells and to do so efficiently, they produce a plethora of proteins to counteract the host's innate immune response. One critical non-specific anti-viral innate cellular response is autophagy which regulates the lysosome-mediated elimination of intracellular pathogens. Although limited information on the modulation of the autophagic pathway in poxvirus has been reported, the cellular autophagic response in *Capripoxviruses*, LSDV in particular, remains largely unexplored. Addressing this knowledge gap, the present study was envisioned to understand of the role of autophagy in the molecular pathogenesis of the LSD in the cell culture system.

MDBK cells were mock-infected (negative control), treated with autophagy inducer rapamycin (250nM; positive control), and infected with LSDV (MOI = 0.005). Cells were analyzed at predetermined time points viz. 6 h, 12 h, 24 h, 48 h, 72 h, and 96 h post-treatment/ infection for the presence of lapidated LC3B II through Western blot and immunofluorescence. Autophagy flux (lysosomal turnover) was determined by treating cells with the autophagy inhibitor Bafilomycin A1 (100nM) for two hours prior to each time point. The relative

transcription of ATG3, ATG5, ATG14 and LAMP2 genes was also estimated through two-step RT-qPCR (SYBR green-based chemistry).

Our Western blot results suggest that LSDV is inhibiting the induction of cellular autophagic response and is preventing the accumulation of lipidated LC3B II in the cells through some unknown mechanisms. We also noted, although marginally insignificant, that LSDV is suppressing the lysosomal degradation in infected cells, particularly from 24 hpi onwards. These findings were further corroborated by the mean per cent positivity of LC3B across different groups in our immunofluorescence assay. Also, significantly higher expression of ATG5, ATG14 and LAMP2 was perceived in the LSDV-infected cells as compared to the mock-infected cells at 12, 24 and 96 hpi.

To assess the effect of initial LSDV titer on the cellular autophagy machinery, MDBK cells were infected with MOIs of 0.001, 0.0025 and 0.005 and the difference in autophagy induction was determined by measuring LC3BII levels at 24, 48, 72 and 96 hpi. At the earliest time point of 24 hpi, drastically lower levels of LC3B were observed in MOI of 0.005, hinting that higher titers of LSDV are inhibiting the PE conjugation of LC3B I. It is important to note that the results were marginally insignificant between MOI = 0.001 and MOI = 0.005 (adjusted $p = 0.0541$).

Furthermore, the influence of inactivated LSDV on host cell autophagy was studied. The LSDV was inactivated chemically using BEI (2 mM) and the virus inactivation was confirmed through cell culture (absence of CPE in sequential passages) and RT-qPCR. An inactivated virus with an equivalent dose of pre-inactivated 0.005 MOI was used for infecting the MDBK cells along with the live LSDV and negative control. Our results indicated that inactivated LSDV failed to contain the autophagic response in the MDBK cells and induced a significantly higher level of LC3B II as compared to the negative control group.

Overall, the present study provided new insights into the host-pathogen interaction of LSDV with the following conclusive remarks:

- *In vitro* infection of LSDV in MDBK cells inhibits the induction of autophagic response

- LSDV causes apparent but inconsequential inhibition of cellular autophagosomal degradation.
- The cellular autophagic response is independent of the initial LSDV titre.
- Significant fold change of the autophagy genes, ATG5, ATG14, and LAMP2 occurred at 12, 24 and 96 hpi, respectively.
- BEI-inactivated LSDV resulted in higher expression of LC3 II reflecting that live virus is required for suppression of autophagy induction.


Mini Abstract

7 MINI ABSTRACT

Lumpy Skin Disease (LSD) is an OIE notifiable cattle disease of global socio-economic concern with poorly understood molecular pathogenesis and host-pathogen interaction. The LSDV-mediated suppression of cellular innate immune responses, with special reference to autophagy, has not been explored yet. To this end, the present study was envisaged to understand the cellular autophagic response during the LSDV infection in MDBK cells. MDBK cells were infected with LSDV (MOI = 0.005) along with mock infection (Negative Control) and treatment with rapamycin (Positive Control). The cells were either collected or fixed at 6 h, 12 h, 24 h, 48 h, 72 h, and 96 h post-infection/treatment for Western blotting and immunofluorescence (IFT) assays, respectively. Also, cells were preserved at predetermined time points for relative quantification of autophagy-related genes through RT-qPCR. The LSDV infection was also carried out at varying low multiplicities of infections (MOIs = 0.001, 0.0025 and 0.005) and with binary ethylenimine (BEI) inactivated LSDV. The results of the Western blot and IFT assay revealed comparable levels of LC3B II among Negative Control and LSDV-infected MDBK cells. Also, lower differences in the LC3B II levels were noted in the presence and absence of lysosomal inhibitor Bafilomycin A1 in the LSDV-infected MDBK cells. Higher MOIs of LSDV (0.005 as compared to 0.001) tend to inhibit the autophagic response more strongly during the early phase of infection (24 h). Also, BEI-inactivated LSDV failed to suppress the cellular autophagic response, highlighting the importance of viral replication in modulating autophagy. ATG 5, ATG14, and LAMP2 transcription were significantly higher in LSDV-infected cells at 12, 24, and 96 hpi. Conclusively, the results of the present study bring valuable insights into LSDV-mediated autophagy in cell culture systems suggesting inhibition of autophagy induction and lysosomal degradation by LSDV.

लघु सारांश

8 लघु सारांश

लम्पी त्वचा रोग (लम्पी स्किन डिजीज) मुख्यतयः गायों में होने वाली एक विषाणुजनक रोग है जो वैश्विक अर्थव्यवस्था पर अत्यधिक दबाव के कारण पशु स्वास्थ्य विश्व संगठन द्वारा सूचित रोगों की सूची में दर्ज है। उपलब्ध साहित्य के अनुसार लम्पी त्वचा रोग की आणविक रोगजनन और मेजबान–रोगज़नक अंतःक्रिया को अभी ठीक ढंग से समझा नहीं गया है। लम्पी स्किन डिजीज विषाणु (एलएसडीवी) द्वारा कोशिकाओं की रोग–प्रतिरोधक क्षमताओं पर, खासकर स्वायत्तजीवी (ऑटोफैगी) के विशेष संदर्भ में, प्रभाव को समझना अभी बाकी है। इस उद्देश्य से, एमडीबीके कोशिकाओं में एलएसडीवी संक्रमण के दौरान सेलुलर ऑटोफैगी प्रतिक्रिया को समझने के लिए वर्तमान अध्ययन की परिकल्पना की गई। एमडीबीके कोशिकाओं को नकली संक्रमण (नकारात्मक नियंत्रण), एलएसडीवी से संक्रमित (एमओआई =0.005) और रैपामाइसिन से अनावृत किया गया। संक्रमण के 6, 12, 24, 48, 72 एवं 96 घंटों के पश्चात कोशिकाओं के नमूने वेस्टर्न ब्लॉटिंग एवं इम्मुनोफ्लुओरेसेन्स (आईएफटी) के लिए एकत्रित किये गए। इसके अलावा, ऑटोफैगी–संबंधित जीन के सापेक्ष मात्रा निर्धारण के लिए आरटी–क्यूपीसीआर का इस्तेंमाल किया गया। एलएसडीवी संक्रमण की अलग–अलग कम बहुलता (एमओआई 0.001, 0.0025 और 0.005) और बाइनरी एथिलीनिमाइन (बीईआई) निष्क्रिय एलएसडीवी के साथ किया गया। वेस्टर्न ब्लॉट और आईएफटी परख के परिणामों से नकारात्मक नियंत्रण और एलएसडीवी–संक्रमित एमडीबीके कोशिकाओं के बीच एलसी3बी II के तुलनीय स्तर का पता चला। इसके अलावा, एलएसडीवी–संक्रमित एमडीबीके कोशिकाओं में लाइसोसोमल अवरोधक बाफिलोमाइसिन ए1 की उपस्थिति और अनुपस्थिति में एलसी3बी II स्तरों में कम अंतर देखा गया। एलएसडीवी के उच्च एमओआई (0.001 की तुलना में 0.005) संक्रमण के प्रारंभिक चरण (24 घंटे) के दौरान ऑटोफैजिक प्रतिक्रिया में कमी देखी गयी। इसके अलावा, बीईआई–निष्क्रिय एलएसडीवी सेलुलर ऑटोफैजिक प्रतिक्रिया को दबाने में विफल रहा, जिससे ऑटोफैगी को संशोधित करने में वायरल प्रतिकृति के महत्व का पता चलता है। एलएसडीवी–संक्रमित कोशिकाओं में संक्रमण के 12, 24 और 96 पश्चात एटीजी5, एटीजी14 और एलएएमपी2 प्रतिलेखन स्तर में क्रमशः अंतर पाया गया। निर्यायक रूप से, वर्तमान अध्ययन के नतीजों एलएसडीवी–मध्यस्थ ऑटोफैगी में मूल्यवान अंतर्दृष्टि लाते हैं और कोशिका संवर्धन प्रणाली में एलएसडीवी द्वारा ऑटोफैगी प्रेरण और लाइसोसोमल क्षरण को रोकने का सुझाव देते हैं।

References

9 REFERENCES

Abera, Z., Degefu, H., Gari, G. and Ayana, Z. 2015. Review on epidemiology and economic importance of lumpy skin disease. Int. J. Basic Appl. Virol. **4**: 8-21.

Abutarbush, S.M. 2015. Hematological and serum biochemical findings in clinical cases of cattle naturally infected with lumpy skin disease. J. Infect. Dev. Ctries. **9**(03): 283-288.

Abutarbush, S.M. 2017. Lumpy skin disease (knopvelsiekte, pseudo-urticaria, neethling virus disease, exanthema nodularis bovis). In: Emerging and Re-emerging Infectious Diseases of Livestock. Cham, Springer. 309-326.

Abutarbush, S.M., Ababneh, M.M., Al Zoubi, I.G., Al Sheyab, O.M., Al Zoubi, M.G., Alekish, M.O. and Al Gharabat, R.J. 2015. Lumpy Skin Disease in Jordan: Disease emergence, clinical signs, complications and preliminary associated economic losses. Transbound. Emerg. Dis. **62**(5): 549-554.

Abutarbush, S.M., Hananeh, W.M., Ramadan, W., Al Sheyab, O.M., Alnajjar, A.R., Al Zoubi, I.G., Knowles, N.J., Bachanek Bankowska, K. and Tuppurainen, E.S.M. 2016. Adverse reactions to field vaccination against lumpy skin disease in Jordan. Transbound. Emerg. Dis. **63**(2): 213-219.

Agianniotaki, E.I., Tasioudi, K.E., Chaintoutis, S.C., Iliadou, P., Mangana-Vougiouka, O., Kirtzalidou, A., Alexandropoulos, T., Sachpatzidis, A., Plevraki, E., Dovas, C.I. and Chondrokouki, E. 2017. Lumpy skin disease outbreaks in Greece during 2015–16, implementation of emergency immunization and genetic differentiation between field isolates and vaccine virus strains. Vet. Microbiol. **201**:78-84.

Ahmad, L., Mostowy, S. and Sancho-Shimizu, V. 2018. Autophagy-virus interplay: from cell biology to human disease. Front. Cell Dev. Biol. **6**:155.

Ahmed, A.M. and Dessouki, A.A. 2013. Abattoir-based survey and histopathological findings of lumpy skin disease in cattle at Ismailia abattoir. Int. J. Biosci. Biochem. Bioinforma. **3**(4): 372.

Ali, A.A., Esmat, M., Attia, H., Selim, A. and Abdel-Hamid, Y.M. 1990. Clinical and pathological studies of lumpy skin disease in Egypt. Vet. Rec. **127**(22): 549-550.

Ali, B.H. and Obeid, H.M. 1977. Investigation of the first outbreaks of lumpy skin disease in Sudan. Br. Vet. J. **133**(2): 184-189.

Alirezaei, M., Flynn, C.T., Garcia, S.D., Kimura, T. and Whitton, J.L., 2021. A food-responsive switch modulates TFEB and autophagy and determines susceptibility to coxsackievirus infection and pancreatitis. Autophagy. **17**(2): 402-419.

Al Salihi, K.A. and Hassan, I.Q.2015. Lumpy skin disease in Iraq: a study of the disease emergence. Transbound. Emerg. Dis. **62**(5): 457-462.

Annandale, C.H., Holm, D.E., Ebersohn, K. and Venter, E.H. 2014. Seminal transmission of lumpy skin disease virus in heifers. Transbound. Emerg. Dis. **61**(5): 443-448.

Awad W.S., Ibrahim A.K., Mahran K., Fararh K.M. & Moniem M.I.A, 2010, 'Evaluation of different diagnostic methods for diagnosis of lumpy skin disease in cows. Trop. Anim. Health Prod. **42**. 777–783.

Ayelet, G., Abate, Y., Sisay, T., Nigussie, H., Gelaye, E., Jemberie, S. and Asmare, K. 2013. Lumpy skin disease, preliminary vaccine efficacy assessment and overview on outbreak impact in dairy cattle at Debre Zeit, central Ethiopia. Antiviral Res. **98(2)**: 261-265.

Babiuk, S., Parkyn G., Copps J., Larence J. E., Sabara M. I., Bowden T. R., Boyle D. B. and Kitching R. P., 2007. Evaluation of an ovine testes cell line (OA3.Ts) for use in the propagation and detection of capripox virus and development of immunostaining technique for viral plaque visualization. J. Vet. Diagn. Invest. **19(**5**)**: 486–491.

Babiuk, S., Bowden, T.R., Boyle, D.B., Wallace, D.B. and Kitching, R.P. 2008. Capripox viruses: an emerging worldwide threat to sheep, goats, and cattle. Transbound. Emerg. Dis. **55**(7): 263-272.

Babiuk, S., Bowden, T.R., Parkyn, G., Dalman, B., Manning, L., Neufeld, J., Embury Hyatt, C., Copps, J. and Boyle, D.B.2008. Quantification of lumpy skin disease virus following experimental infection in cattle. Transbound. Emerg. Dis. **55**(7): 299-307.

Bader, C.A., Shandala, T., Ng, Y.S., Johnson, I.R.D. and Brooks, D.A.2015. Atg9 is required for intraluminal vesicles in amphisomes and autolysosomes. Biol. Open **4**(11): 1345-1355.

Baldacchino, F., Muenworn, V., Desquesnes, M., Desoli, F., Charoenviriyaphap, T. and Duvallet, G.2013. Transmission of pathogens by Stomoxys flies (Diptera, Muscidae): a review. Parasite. **20**.

Balinsky, C.A., Delhon, G.U.S.T.A.V.O., Smoliga, G., Prarat, M.E.L.A.N.I.E., French, R.A., Geary, S.J., Rock, D.L. and Rodriguez, L.L. 2008. Rapid preclinical detection of sheeppox virus by a real-time PCR assay. J. Clin. Microbiol. **46**(2): 438-442.

Beard, P.M. 2016. Lumpy skin disease: a direct threat to Europe. Vet. Rec. **178**(22): 557.

Bhanuprakash, V., Indrani, B.K., Hosamani, M. and Singh, R.K., 2006. The current status of sheep pox disease. Comp. Immunol. Microbiol. Infect. Dis. **29**(1): 27-60.

Binepal, Y.S., Ongadi, F.A. and Chepkwony, J.C., 2001. Alternative cell lines for the propagation of lumpy skin disease virus. Onderstepoort. J. Vet. Res. **68**: 151-153

Body, M., Singh, K.P., Hussain, M.H., Al-Rawahi, A., Al-Maawali, M., Al-Lamki, K. and Al-Habsy, S.2012. Clinico-histopathological findings and PCR-based diagnosis of lumpy skin disease in the Sultanate of Oman. Pak. Vet. J. **32**(2): 206-210.

Bowden, T.R., Babiuk, S.L., Parkyn, G.R., Copps, J.S. and Boyle, D.B., 2008. Capripox virus tissue tropism and shedding: A quantitative study in experimentally infected sheep and goats. Virology. **371**(2): 380-393.

Burdin, M.L. 1959. The use of histopathological examinations of skin material for the diagnosis of lumpy skin disease in Kenya. Bull. Epizootic Dis. of Africa **7**:21-26.

Campbell, P., Morris, H. and Schapira, A. 2018. Chaperone-mediated autophagy as a therapeutic target for Parkinson's disease. Expert Opin. Ther. Targets. **22**(10): 823-832.

Carn, V.M. and Kitching, R.P.1995. An investigation of possible routes of transmission of lumpy skin disease virus (Neethling). Epidemiol. Infect. **114**(1): 219-226.

Carn, V.M., Kitching, R.P., Hammond, J.M. and Chand, P.1994. Use of a recombinant antigen in an indirect ELISA for detecting bovine antibody to capripox virus. J. Virol. Methods **49**(3): 285-294.

Casal, J., Allepuz, A., Miteva, A., Pite, L., Tabakovsky, B., Terzievski, D., Alexandrov, T. and Beltrįn Alcrudo, D. 2018. The economic cost of lumpy skin disease outbreaks in three Balkan countries: Albania, Bulgaria, and the Former Yugoslav Republic of Macedonia (2016 2017). Transbound. Emerg. Dis. **65**(6): 1680-1688.

Cheng, C.Y., Tseng, H.H., Chiu, H.C., Chang, C. D., Nielsen, B.L. and Liu, H.J., 2019. Bovine ephemeral fever virus triggers autophagy enhancing virus replication via upregulation of the Src/JNK/AP1 and PI3K/Akt/NF-źB pathways and suppression of the PI3K/Akt/mTOR pathway. Vet. Res. **50**: 1-15.

Chihota, C.M., Rennie, L.F., Kitching, R.P. and Mellor, P.S. 2001. Mechanical transmission of lumpy skin disease virus by *Aedes aegypti* (Diptera: Culicidae). Epidemiol. Infect. **126**(2): 317-321.

Chihota, C.M., Rennie, L.F., Kitching, R.P. and Mellor, P.S. 2003. Attempted mechanical transmission of lumpy skin disease virus by biting insects. Med. Vet. Entomol.**17**(3): 294-300.

Coetzer, J.A.W. and Tuppurainen, E. S. M. 2004. Lumpy skin disease, In: Infectious diseases of livestock, edited by Coetzer, J. A. W. and Tustin, R.C. Cape Town: Oxford University Press Southern Africa. **2**: 1268-1276.

Constable, P.D., Hinchcliff, K.W., Done, S.H. and Grünberg, W. 2016. Veterinary medicine: a textbook of the diseases of cattle, horses, sheep, pigs, and goats. (485-498). Elsevier Health Sciences.

Cooper, K.F. 2018. Till death do us part: the marriage of autophagy and apoptosis. Oxid. Med. Cell. Longev. **7**(11): 454-464.

Cottam, E.M., Maier, H.J., Manifava, M., Vaux, L.C., Chandra-Schoenfelder, P., Gerner, W., Britton, P., Ktistakis, N.T. and Wileman, T. 2011. Corona virus nsp6 proteins generate autophagosomes from the endoplasmic reticulum via an omegasome intermediate. Autophagy. **7**(11): 1335-1347.

Cuervo, A.M., 2004. Autophagy: in sickness and in health. Trends in Cell Biology, **14**(2): 70-77.

Das, M., Chowdhury, M.S.R., Akter, S., Mondal, A.K., Uddin, M.J., Rahman, M.M. and Rahman, M.M. 2021. An updated review on lumpy skin disease: Perspective of Southeast Asian countries. J. Adv. Biotechnol. Exp. Ther. **4**(3): 322-333.

Daskalaki, I., Gkikas, I. and Tavernarakis, N. 2018. Hypoxia and selective autophagy in cancer development and therapy. Front. Cell Dev. Biol.**6:** 104.

Davies, F. G. 1982. Observations on the epidemiology of lumpy skin disease in Kenya. J. Hyg. (Lond). **88(**1**)**: 95-102.

Davies, F.G. 1991. Lumpy skin disease of cattle: a growing problem in Africa and the Near East. Large Anim. Rev. **68**(3): 37-42.

Davies, F.G. 1991. Lumpy skin disease, an African Capri pox virus disease of cattle. Br. Vet. J. **147**(6): 489-503.

Deretic, V. 2009. Multiple regulatory and effector roles of autophagy in immunity. Curr. Opin. Immunol. **21**(1): 53-62.

Diesel, A.M. 1949. The epizootiology of lumpy skin disease in South Africa. Proc. 14th Int. Vet. Congr. Lond. **2**: 492-500.

Dorn, B.R., Dunn Jr, W.A. and Progulske Fox, A. 2002. Bacterial interactions with the autophagic pathway. Cell Microbiol. **4**(1): 1-10.

Dreux, M., Gastaminza, P., Wieland, S.F. and Chisari, F.V.2009. The autophagy machinery is required to initiate hepatitis C virus replication. Proc. Natl. Acad. Sci. **106**(33): 14046-14051.

Egger, D., Wolk, B., Gosert, R., Bianchi, L., Blum, H.E., Moradpour, D. and Bienz, K. 2002. Expression of hepatitis C virus proteins induces distinct membrane alterations including a candidate viral replication complex. J. Virol. **76**(12): 5974-5984.

El-Kenawy, A.A. and El-Tholoth, M.S. 2010. Sequence analysis of attachment gene of lumpy skin disease and sheep poxviruses. Virol. Sin. **25**(6): 409-416.

El-Nahas, E.M., El-Habbaa, A.S., El-Bagoury, G.F. and Radwan, M.E. 2011. Isolation and identification of lumpy skin disease virus from naturally infected buffaloes at Kaluobia, Egypt. Glob. Vet. **7**(3): 234-237.

El-Neweshy, M.S., El-Shemey, T.M. and Youssef, S.A. 2013. Pathologic and immunohistochemical findings of natural lumpy skin disease in Egyptian cattle. Pak. Vet. J. **33**(1): 60-64.

Fan, X., Han, S., Yan, D., Gao, Y., Wei, Y., Liu, X., Liao, Y., Guo, H. and Sun, S. 2018. Foot-and-mouth disease virus infection suppresses autophagy and NF-źB antiviral responses via degradation of ATG5-ATG12 by 3Cpro. Cell Death Dis. **8**(1): 2561-2561.

Fay, P.C., Cook, C.G., Wijesiriwardana, N., Tore, G., Comtet, L., Carpentier, A., Shih, B., Freimanis, G., Haga, I.R. and Beard, P.M., 2020. Madin-Darby bovine kidney (MDBK) cells are a suitable cell line for the propagation and study of the bovine poxvirus lumpy skin disease virus. J.virol. Methods. **285**: 113943.

Fay, P.C., Wijesiriwardana, N., Munyanduki, H., Sanz-Bernardo, B., Lewis, I., Haga, I.R., Moffat, K., van Vliet, A.H., Hope, J., Graham, S.P. and Beard, P.M., 2022. The immune response to lumpy skin disease virus in cattle is influenced by inoculation route. Front. Immunol. **13**: 6947.

Fang, D., Xie, H., Hu, T., Shan, H. and Li, M., 2021. Binding features and functions of ATG3. Front. Cell Develop. Biol. **9**. p.685625.

Fu, Q., Shi, H., Ren, Y., Guo, F., Ni, W., Qiao, J., Wang, P., Zhang, H. and Chen, C. 2014. Bovine viral diarrhea virus infection induces autophagy in MDBK cells. J. Microbiol. **52**(7): 619-625.

Fujikake, N., Shin, M. and Shimizu, S. 2018. Association between autophagy and neurodegenerative diseases. Front. Neurosci. **12:** 255.

Füllgrabe, J., Ghislat, G., Cho, D.H. and Rubinsztein, D.C. 2016. Transcriptional regulation of mammalian autophagy at a glance. J. Cell Sci. **129**(16): 3059-3066.

Gari, G., Abie, G., Gizaw, D., Wubete, A., Kidane, M., Asgedom, H., Bayissa, B., Ayelet, G., Oura, C.A., Roger, F. and Tuppurainen, E.S. 2015. Evaluation of the safety, immunogenicity, and efficacy of three capripoxvirus vaccine strains against lumpy skin disease virus. Vaccine. **33**(28): 3256-3261.

Gari, G., Bonnet, P., Roger, F. and Waret-Szkuta, A. 2011. Epidemiological aspects and financial impact of lumpy skin disease in Ethiopia. Prev. Vet. Med. **102**(4): 274-283.

Gari, G., Waret-Szkuta, A., Grosbois, V., Jacquiet, P. and Roger, F. 2010. Risk factors associated with observed clinical lumpy skin disease in Ethiopia. Epidemiol. Infect. **138**(11): 1657-1666.

Gelaye, E., Mach, L., Kolodziejek, J., Grabherr, R., Loitsch, A., Achenbach, J.E., Nowotny, N., Diallo, A. and Lamien, C.E., 2017. A novel HRM assay for the simultaneous detection and differentiation of eight poxviruses of medical and veterinary importance. Sci. Rep. **7**(1): 42892.

Gershon, P. D., Ansell, D. M., and Black, D. N. (1989a). A comparison of the genome organization of capripoxvirus with that of the orthopoxviruses. J. Virol. **63**. 4703–4708.

Glare, E.M., Divjak, M., Bailey, M.J. and Walters, E.H., 2002. ā-Actin and GAPDH housekeeping gene expression in asthmatic airways is variable and not suitable for normalising mRNA levels. Thorax. **57**(9): 765-770.

Glick, D., Barth, S. and Macleod, K.F. 2010. Autophagy: cellular and molecular mechanisms. J. Pathol. **221**(1): 3-12.

Greth, A., Calvez, D., Vassart, M. and Lefčvre, P.C., 1992. Serological survey for bovine bacterial and viral pathogens in captive Arabian oryx (*Oryx leucoryx*). International Office of Epizootics. **11**(4): 1163-1168.

Gubbins, S., Carpenter, S., Baylis, M., Wood, J.L. and Mellor, P.S. 2008. Assessing the risk of bluetongue to UK livestock: uncertainty and sensitivity analyses of a temperature-dependent model for the basic reproduction number. J. Res. Soc. Interface. **5**(20): 363-371.

Heine, H.G., Stevens, M.P., Foord, A. J. and Boyle, D.B. 1999. A capripox virus detection PCR and antibody ELISA based on the major antigen P32, the homolog of the vaccinia virus H3L gene. J. Immunol. Methods. **227**(1-2): 187-196.

Herb, M., Gluschko, A. and Schramm, M. 2020, May. LC3-associated phagocytosis-The highway to hell for phagocytosed microbes. Semin. Cell Dev. **101**: 68-76.

Hsu, P. and Shi, Y. 2017. Regulation of autophagy by mitochondrial phospholipids in health and diseases. Biochim. Biophys. Acta - Mol. Cell Biol. Lipids. **1862**(1): 114-129.

https://en.m.wikipedia.org/wiki/Lumpy_skin_disease_outbreak_in_India, Lumpy skin disease outbreak in India, visited on 2nd January 2023.

Huang, Y., Gong, K., Chen, J., Deng, H., Weng, K., Wu, H., Li, K., Xiao, B., Luo, S. and Hao, W., 2022. Preclinical efficacy and involvement of mTOR signaling in the mechanism of orf virus against nasopharyngeal carcinoma cells. Life Sciences. **291**: 120297.

Hulskotte, E.G., Dings, M.E., Norley, S.G. and Osterhaus, A.D., 1997. Chemical inactivation of recombinant vaccinia viruses and the effects on antigenicity and immunogenicity of recombinant simian immunodeficiency virus envelope glycoproteins. Vaccine. **15**(17-18). pp: 1839-1845.

Ince, O.B., Ēakir, S. and Dereli, M.A. 2016. Risk analysis of lumpy skin disease in Turkey. Indian J. Anim. Res. **50**(6): 1013-1017.

Irons, P.C., Tuppurainen, E.S.M. and Venter, E.H. 2005. Excretion of lumpy skin disease virus in bull semen. Theriogenology. **63**(5): 1290-1297.

Itakura, E.; Kishi-Itakura, C.; Mizushima, N., 2012. The hairpin-type tail-anchored SNARE syntaxin 17 targets to autophagosomes for fusion with endosomes/lysosomes. Cell. **151:** 1256–1269.

Jiang, H., White, E.J., Gomez-Manzano, C. and Fueyo-Margareto, J. 2008. Adenovirus's last trick: you say lysis, we say autophagy. Autophagy. **4**(1): 118-120.

Joy, S., Thirunavukkarasu, L., Agrawal, P., Singh, A., Sagar, B.K., Manjithaya, R. and Surolia, N. 2018. Basal and starvation-induced autophagy mediates parasite survival during intraerythrocytic stages of *Plasmodium falciparum*. Cell Death Discov. **4**(1): 1-13.

Kahana Sutin, E., Klement, E., Lensky, I. and Gottlieb, Y. 2017. A high relative abundance of the stable fly *Stomoxys calcitrans* is associated with lumpy skin disease outbreaks in Israeli dairy farms. Med. Vet. Entomol. **31**(2): 150-160.

Kaiser, W.J., Upton, J.W. and Mocarski, E.S., 2013. Viral modulation of programmed necrosis. Current opinion in virology. **3**(3): 296-306.

Karthik, L., Kumar, G., Keswani, T., Bhattacharyya, A., Chandar, S.S. and Bhaskara Rao, K.V. 2014. Protease inhibitors from marine actinobacteria as a potential source of the antimalarial compound. PLOS One. **9**(3): 90972.

Käsermann, F., Wyss, K. and Kempf, C., 2001. Virus inactivation and protein modifications by ethyleneimines. Antiviral research. **52**(1): 33-41.

Kaur, J. and Debnath, J.2015. Autophagy at the crossroads of catabolism and anabolism.Nat. Rev. Mol. Cell Biol. **16**(8): 461-472.

Ke, P.Y. and Chen, S.S.L. 2011. Activation of the unfolded protein response and autophagy after hepatitis C virus infection suppresses innate antiviral immunity *in vitro*. J. Clin.**121**(1): 37-56.

Khandia, R., Dadar, M., Munjal, A., Dhama, K., Karthik, K., Tiwari, R., Yatoo, M.I., Iqbal, H.M., Singh, K.P., Joshi, S.K. and Chaicumpa, W. 2019. A comprehensive review of autophagy and its various roles in infectious, non-infectious, and lifestyle diseases: current knowledge and prospects for disease prevention, novel drug design, and therapy. Cells **8**(7): 674.

King, A.M., Adams, M.J., Carstens, E.B. and Lefkowitz, E.J. 2012. Virus taxonomy: classification and nomenclature of viruses. **7**: 1327-1327.

Kiovį, I.B., Salin, B., Schaeffer, J., Bhatia, S., Manon, S. and Camougrand, N. 2007. Selective and non-selective autophagic degradation of mitochondria in yeast. Autophagy. **3**(4): 329-336.

Klionsky, D.; Agholme, L.; Agnello, M.; Agostinis, P.; Aguirre-ghiso, J.A.; Ahn, H.J.; Ait-mohamed, O.; Brown, E.J.; Brumell, J.H.; Brunetti-pierri, N.; *et al.,* 2016. Guidelines for the use and interpretation of assays for monitoring autophagy. Autophagy **8**: 445–544.

Krause, M., Yakimovich, A., Kriston-Vizi, J., Huttunen, M. and Mercer, J., 2021. Vaccinia virus subverts xenophagy through phosphorylation and nuclear targeting of p62. Biorxiv: 2021-04.

Kudchodkar, S.B. and Levine, B. 2009. Viruses and autophagy. Rev. Med. Virol. **19**(6): 359-378.

Kumar, N., Chander, Y., Kumar, R., Khandelwal, N., Riyesh, T., Chaudhary, K., Shanmugasundaram, K., Kumar, S., Kumar, A., Gupta, M.K. and Pal, Y., 2021. Isolation and characterization of lumpy skin disease virus from cattle in India. PLOS One. **16**(1): 0241022.

Kumar, N. and Tripathi, B.N., 2022. A serious skin virus epidemic sweeping through the Indian subcontinent is a threat to the livelihood of farmers. Virulence. **13**(1): 1943-1944.

Kunz, J.B., Schwarz, H. and Mayer, A. 2004. Determination of four sequential stages during microautophagy *in vitro*. J. Org. Chem. **279**(11): 9987-9996.

Kyei, G.B., Dinkins, C., Davis, A.S., Roberts, E., Singh, S.B., Dong, C., Wu, L., Kominami, E., Ueno, T., Yamamoto, A. and Federico, M. 2009. The autophagy pathway intersects with HIV-1 biosynthesis and regulates viral yields in macrophages. J. Cell Biol. **186**(2): 255-268.

Laemmli, U.K., 1970. Cleavage of structural proteins during the assembly of the head of bacteriophage T4. Nature. **227**(5259): 680-685.

Lamien, C.E., Le Goff, C., Silber, R., Wallace, D.B., Gulyaz, V., Tuppurainen, E., Madani, H., Caufour, P., Adam, T., El Harrak, M. and Luckins, A.G., 2011. Use of the Capripox virus homolog of Vaccinia virus 30 kDa RNA polymerase subunit

(RPO30) gene as a novel diagnostic and genotyping target: Development of a classical PCR method to differentiate Goatpox virus from Sheeppox virus. Vet. Microbiol. **149**(1-2): 30-39.

Lamien, C.E., Lelenta, M., Goger, W., Silber, R., Tuppurainen, E., Matijevic, M., Luckins, A.G. and Diallo, A. 2011. Real-time PCR method for simultaneous detection, quantitation, and differentiation of capripox viruses. J. Virol. Methods. **171**(1): 134-140.

Lan, Y., Wang, G., Song, D., He, W., Zhang, D., Huang, H., Bi, J., Gao, F. and Zhao, K. 2016. Role of autophagy in cellular response to infection with Orf virus Jilin isolate. Vet. Microbiol. **193:** 22-27.

Lee, M.S. 2018. Overview of the mini-reviews on autophagy. Mol. Cells. **41**(1): 1-2.

Lee, W.S., Sung, M.S., Lee, E. G., Yoo, H.G., Cheon, Y.H., Chae, H.J. and Yoo, W.H. 2015. A pathogenic role for ER stress induced autophagy and ER chaperone GRP78/BiP in T lymphocyte Systemic Lupus Erythematosus. J. Leukoc. Biol. **97**(2): 425-433.

Lee, Y.A., Noon, L.A., Akat, K.M., Ybanez, M.D., Lee, T.F., Berres, M.L., Fujiwara, N., Goossens, N., Chou, H.I., Parvin-Nejad, F.P. and Khambu, B. 2018. Autophagy is a gatekeeper of hepatic differentiation and carcinogenesis by controlling the degradation of Yap. Nat. Commun. **9**(1): 1-12.

Lee, Y.R., Lei, H.Y., Liu, M.T., Wang, J.R., Chen, S.H., Jiang-Shieh, Y.F., Lin, Y.S., Yeh, T.M., Liu, C.C. and Liu, H.S. 2008. Autophagic machinery activated by the dengue virus enhances virus replication. Virology. **374**(2): 240-248.

Levine, B. and Klionsky, D.J., 2004. Development by self-digestion: molecular mechanisms and biological functions of autophagy. Developmental Cell. **6**(4): 463-477.

Li, C., Fu, X., Lin, Q., Liu, L., Liang, H., Huang, Z. and Li, N. 2017. Autophagy promoted infectious kidney and spleen necrosis virus replication and decreased infectious virus yields in the CPB cell line. Fish Shellfish Immunol. **60:** 25-32.

Li, S.J., Sun, S.J., Gao, J. and Sun, F.B.2016. Wogonin induces Beclin-1/PI3K and reactive oxygen species-mediated autophagy in human pancreatic cancer cells. Oncol. Lett. **12**(6): 5059-5067.

Li, W.W., Li, J. and Bao, J.K. 2012. Microautophagy: lesser-known self-eating. Cell. Mol. Life Sci. **69**(7): 1125-1136.

Liu, R., Cui, J., Sun, Y., Xu, W., Wang, Z., Wu, M., Dong, H., Yang, C., Hong, S., Yin, S. and Wang, H., 2021. Autophagy deficiency promotes M1 macrophage polarization to exacerbate acute liver injury via ATG5 repression during aging. Cell Death Discov. **7**(1). 397.

Lubinga, J.C., Clift, S.J., Tuppurainen, E.S., Stoltsz, W.H., Babiuk, S., Coetzer, J.A. and Venter, E.H.2014. Demonstration of lumpy skin disease virus infection in *Amblyomma hebraeum* and *Rhipicephalus appendiculatus* ticks using immunohistochemistry. Tick Borne Dis**. 5**(2): 113-120.

Lubinga, J.C., Tuppurainen, E.S.M., Mahlare, R., Coetzer, J.A.W., Stoltsz, W.H. and Venter, E.H. 2015. Evidence of transstadial and mechanical transmission of lumpy skin disease virus by *Amblyomma hebraeum***.** Ticks. Transbound. Emerg. Dis. **62**(2): 174-182.

Lubinga, J.C., Tuppurainen, E.S.M., Stoltsz, W.H., Ebersohn, K., Coetzer, J.A.W. and Venter, E.H. 2013. Detection of lumpy skin disease virus in the saliva of ticks fed on lumpy skin disease virus-infected cattle. Exp. Appl. Acarol. **61**(1): 129-138.

Magori-Cohen, R., Louzoun, Y., Herziger, Y., Oron, E., Arazi, A., Tuppurainen, E., Shpigel, N.Y. and Klement, E. 2012. Mathematical modeling and evaluation of the different routes of transmission of lumpy skin disease virus. Vet. Res**. 43**(1): 1-13.

Maier, H.J. and Britton, P. 2012. Involvement of autophagy in corona virus replication. Viruses. **4**(12): 3440-3451.

Majdoul, S., Cosette, J., Seye, A.K., Bernard, E., Frin, S., Holic, N., Chazal, N., Briant, L., Espert, L., Galy, A. and Fenard, D. 2017. Peptides derived from evolutionarily conserved domains in Beclin-1 and Beclin-2 enhance the entry of lentiviral vectors into human cells. J. Biol. Chem. **292**(45): 18672-18681.

Majeski, A.E. and Dice, J.F. 2004. Mechanisms of chaperone-mediated autophagy. Int. J. Biochem. **36**(12): 2435-2444.

Mari, M., Griffith, J., Rieter, E., Krishnappa, L., Klionsky, D.J. and Reggiori, F. 2010. An Atg9-containing compartment that functions in the early steps of autophagosome biogenesis. J. Cell Biol. **190**(6): 1005-1022.

Martyniszyn, L., Szulc, L., Boratyńska, A. and Niemia³towski, M.G., 2011. Beclin 1 is involved in regulation of apoptosis and autophagy during replication of ectromelia virus in permissive L929 cells. Archivum immunologiae et therapiae experimentalis. **59**: 463-471.

Martyniszyn, L., Szulc-Dabrowska, L., Boratynska-Jasinska, A., Badowska-Kozakiewicz, A.M. and Niemialtowski, M.G. 2013. *In vivo* induction of autophagy in splenocytes of C57BL/6 and BALB/c mice infected with ectromelia orthopox virus. Pol. J. Vet. Sci. **16**(1).

Mathivanan, E., Raju, K. and Murugan, R., 2023. Outbreak of Lumpy skin disease in India 2022-an emerging threat to livestock & livelihoods. Global Biosecurity 5.

Matsiela, M.S., Naicker, L., Dibakwane, V.S., Ntombela, N., Khoza, T. and Mokoena, N., 2022. Improved safety profile of inactivated Neethling strain of the Lumpy Skin Disease Vaccine. Vaccine: X. **12**: 100209.

Mauthe, M., Langereis, M., Jung, J., Zhou, X., Jones, A., Omta, W., Tooze, S. A., Stork, B., Paludan, S. R., Ahola, T. and Egan, D. 2016. A siRNA screen for ATG protein depletion reveals the extent of the unconventional functions of the autophagy proteome in virus replication. J. Cell Biol. **214**(5): 619-635.

Menasherow, S., Rubinstein-Giuni, M., Kovtunenko, A., Eyngor, Y., Fridgut, O., Rotenberg, D., Khinich, Y. and Stram, Y. 2014. Development of an assay to differentiate between virulent and vaccine strains of lumpy skin disease virus (LSDV). J. Virol. Methods. **199:** 95-101.

Meng, C., Zhou, Z., Jiang, K., Yu, S., Jia, L., Wu, Y., Liu, Y., Meng, S. and Ding, C. 2012. Newcastle disease virus triggers autophagy in U251 glioma cells to enhance virus replication. Arch. Virol. **157**(6): 1011-1018.

Mercer, T.J., Gubas, A. and Tooze, S.A. 2018. A molecular perspective of mammalian autophagosome biogenesis. J. Biol. Chem. **293**(15): 5386-5395.

Metaxakis, A., Ploumi, C. and Tavernarakis, N. 2018. Autophagy in age-associated neurodegeneration. Cells. **7**(5): 37.

Mizushima, N. 2007. Autophagy: process and function. Genes Dev. **21**(22): 2861-2873.

Mizushima, N. and Komatsu, M. 2011. Autophagy: renovation of cells and tissues. Cell. **147**(4): 728-741.

Mizushima, N., Levine, B., Cuervo, A.M. and Klionsky, D.J. 2008. Autophagy fights disease through cellular self-digestion. Nature. **451**(7182): 1069-1075.

Mizushima, N., Yoshimori, T., 2007. How to interpret LC3 immunoblotting. Autophagy. **3**: 542–545.

Mizushima, N., Yoshimori, T. and Levine, B. 2010. Methods in mammalian autophagy research. Cell. **140**: 313–326.

Moloughney, J.G., Monken, C.E., Tao, H., Zhang, H., Thomas, J.D., Lattime, E.C. and Jin, S.V., 2011. Vaccinia virus leads to ATG12–ATG3 conjugation and deficiency in autophagosome formation. Autophagy. **7**(12): 1434-1447.

Morris, J.P.A. 1930. Pseudo-urticaria. Northern Rhodesia. Dept. Anim. Health Ann. Rept. 12.

Moy, R.H., Gold, B., Molleston, J.M., Schad, V., Yanger, K., Salzano, M.V., Yagi, Y., Fitzgerald, K.A., Stanger, B.Z., Soldan, S.S. and Cherry, S. 2014. Antiviral autophagy restricts Rift Valley fever virus infection and is conserved from flies to mammals. Immunity. **40**(1): 51-65.

Mulatu, E. and Feyisa, A. 2018. Review: Lumpy Skin Disease. J. Vet. Sci. Tech. **9**(535): 1-8

Nagar, R. 2017. Autophagy: A brief overview in perspective of dermatology. Indian J. Dermatol. Venereol. Leprol. **83**(3): 17-34.

Nakamoto, M., Moy, R.H., Xu, J., Bambina, S., Yasunaga, A., Shelly, S.S., Gold, B. and Cherry, S. 2012. Virus recognition by Toll-7 activates antiviral autophagy in Drosophila. Immunity. **36**(4): 658-667.

Neamat-Allah, A.N. 2015. Immunological, hematological, biochemical, and histopathological studies on cows naturally infected with lumpy skin disease. Vet World. **8**(9): 1131.

Needs, S., Kaas, S., Horne, T., Alonzi, D. and Allman, S. 2016. Stimulation of autophagy by salicylamide derivatives-implications for viral infection. In: Proceedings of the Frankfurt Conference on Ubiquitin and Autophagy "Quality Control in Life Processes", Frankfurt am Main, Germany. **13**(4): 128-135

Nimmerjahn, F., Milosevic, S., Behrends, U., Jaffee, E.M., Pardoll, D.M., Bornkamm, G.W. and Mautner, J. 2003. Major histocompatibility complex class II restricted presentation of a cytosolic antigen by autophagy.Eur. J. Immunol. **33**(5): 1250-1259.

O'Donnell, V., Pacheco, J.M., LaRocco, M., Burrage, T., Jackson, W., Rodriguez, L.L., Borca, M.V. and Baxt, B. 2011. Foot-and-mouth disease virus utilizes an autophagic pathway during viral replication. J. Virol. **410**(1): 142-150.

Orlova, E.S., Shcherbakov, A.V., Diev, V. I. and Zakharov, V.M. 2006. Differentiation of capripox virus species and strains by polymerase chain reaction. Mol. Biol. **40**(1): 139-145.

Orvedahl, A., MacPherson, S., Sumpter Jr, R., Tallóczy, Z., Zou, Z. and Levine, B. 2010. Autophagy protects against Sindbis virus infection of the central nervous system. Cell Host Microbe. **7**(2): 115-127.

Owczarczyk, A.B., Schaller, M.A., Reed, M., Rasky, A.J., Lombard, D.B. and Lukacs, N.W. 2015. Sirtuin 1 regulates dendritic cell activation and autophagy during respiratory syncytial virus–induced immune responses. J. Immunol. **195**(4): 1637-1646.

Oxford, K.L., Eberhardt, M.K., Yang, K.W., Strelow, L., Kelly, S., Zhou, S.S. and Barry, P.A. 2008. Protein coding content of the ULb2 region of wild-type rhesus cytomegalovirus. J. Virol. **373**(1): 181-188.

Paolini, A., Omairi, S., Mitchell, R., Vaughan, D., Matsakas, A., Vaiyapuri, S., Ricketts, T., Rubinsztein, D.C. and Patel, K. 2018. Attenuation of autophagy impacts muscle fiber development, starvation-induced stress, and fiber regeneration following acute injury. Sci. Rep. **8**(1): 1-12.

Paul, P. and Münz, C. 2016. Autophagy and mammalian viruses: roles in immune response, viral replication, and beyond. Adv. Virus Res. **95:** 149-195.

Pleet, M.L., Branscome, H., DeMarino, C., Pinto, D.O., Zadeh, M.A., Rodriguez, M., Sariyer, I.K., El-Hage, N. and Kashanchi, F. 2018. Autophagy, EVs, and infections: a perfect question for a perfect time. Front. Microbiol. **8:** 362.

Prins, M.M., van Roest, M., Vermeulen, J.L., Tjabringa, G.S., van de Graaf, S.F., Koelink, P.J. and Wildenberg, M.E., 2021. Applicability of different cell line-derived dendritic cell-like cells in autophagy research. J. Immunol. Methods. **497**. pp:113106.

Pukac, L.A., Carter, J.E., Morrison, K.S. and Karnovsky, M.J., 1997. Enhancement of diaminobenzidine colorimetric signal in immunoblotting. Biotechniques. **23**(3): 385-388.

Quinn, P.J., Markey, B.K., Leonard, F.C., FitzPatrick, E.S. and Fanning, S. 2015. Concise review of veterinary microbiology. 2nd ed. Wiley:142.

Reggiori, F., Monastyrska, I., Verheije, M.H., Calǵ, T., Ulasli, M., Bianchi, S., Bernasconi, R., De Haan, C.A. and Molinari, M.2010. Corona viruses hijack the LC3-I-positive endosomes, ER-derived vesicles exporting short-lived ERAD regulators, for replication. Cell Host Microbe. **7**(6): 500-508.

Reed, L.J. and Muench, H., 1938. A simple method of estimating fifty per cent endpoints. Am. J. Epidemiol. **27**(3):493-497.

Rossiter, P.B. and Al Hammadi, N. 2009. Living with transboundary animal diseases (TADs). Trop. Anim. Health Prod. **41**(7): 999-1004.

Rossman, J.S. and Lamb, R.A. 2009. Autophagy, apoptosis, and the influenza virus M2 protein. Cell Host Microbe. **6**(4): 299-300.

Roy, A.C., Chang, G., Roy, S., Ma, N., Gao, Q. and Shen, X., 2021. ć d Glutamyl meso diaminopimelic acid induces autophagy in bovine hepatocytes during nucleotide binding oligomerization domain 1 mediated inflammation. J. Cell. Physiol. **236**(7): 5212-5234.

Runwal, G., Stamatakou, E., Siddiqi, F.H., Puri, C., Zhu, Y. and Rubinsztein, D.C., 2019. LC3-positive structures are prominent in autophagy-deficient cells. Scientific reports. **9**(1): 10147.

Sajid, A., Chaudhary, Z.I., Sadique, U., Maqbol, A., Anjum, A.A., Qureshi, M.S., Hassan, Z.U., Idress, M. and Shahid, M. 2012. Prevalence of goatpox disease in Punjab province of Pakistan. J. Anim. Poult. Sci. **22**(2): 28-32.

Salib, F.A. and Osman, A.H. 2011. Incidence of lumpy skin disease among Egyptian cattle in Giza Governorate, Egypt. Vet World. **4**(4): 345- 364.

Schmid, D., Pypaert, M. and Münz, C. 2007. Antigen-loading compartments for major histocompatibility complex class II molecules continuously receive input from autophagosomes. Immunity. **26**(1): 79-92.

Schmotz, C., Ušurlu, H., Vilen, S., Shrestha, S., Fagerlund, R. and Saksela, K., 2019. MC159 of molluscum contagiosum virus suppresses autophagy by recruiting cellular SH3BP4 via an SH3 domain-mediated interaction. J. Virol. **93**(10): 10-1128.

Ževik, M. and Došan, M. 2017. Epidemiological and molecular studies on lumpy skin disease outbreaks in Turkey during 2014–2015. Transbound. Emerg. Dis. **64**(4): 1268-1279.

Ževik, M., Avci, O., Došan, M. and Żnce, Ö.B.2016. Serum biochemistry of lumpy skin disease virus-infected cattle. Biomed. Res. Int. **7**: 25-29

Sharma, V., Verma, S., Seranova, E., Sarkar, S. and Kumar, D. 2018. Selective autophagy and xenophagy in infection and disease. Front. Cell Dev. Biol. **6:** 147.

Shelly, S., Lukinova, N., Bambina, S., Berman, A. and Cherry, S. 2009. Autophagy is an essential component of Drosophila immunity against the vesicular stomatitis virus. Immunity. **30**(4): 588-598.

Shintani, T. and Klionsky, D.J. 2004. Autophagy in health and disease: a double-edged sword. Science. **306**(5698): 990-995.

Shoji-Kawata, S., Sumpter, R., Leveno, M., Campbell, G.R., Zou, Z., Kinch, L., Wilkins, A.D., Sun, Q., Pallauf, K., MacDuff, D. and Huerta, C. 2013. Identification of a candidate therapeutic autophagy-inducing peptide. Nature. **494**(7436): 201-206.

Shrivastava, S., Raychoudhuri, A., Steele, R., Ray, R. and Ray, R.B. 2011. Knockdown of autophagy enhances the innate immune response in hepatitis C virus–infected hepatocytes. Hepatology. **53**(2): 406-414.

Singh, A., Kour, G., Dhillon, S.S. and Brar, P.S., 2023. Impact of Lumpy Skin Disease in India: Socio-behavioural Analysis, Epidemiology and Economics.

Sir, D., Chen, W.L., Choi, J., Wakita, T., Yen, T.B. and Ou, J.H.J. 2008. Induction of incomplete autophagic response by Hepatitis C virus via the unfolded protein response. Hepatology **48**(4): 1054-1061.

Smith, G.L., Vanderplasschen, A. and Law, M. 2002. The formation and function of extracellular enveloped vaccinia virus. J. Gen. Virol. **83**(12): 2915-2931.

Sprygin, A., Babin, Y., Pestova, Y., Kononova, S., Wallace, D.B., Van Schalkwyk, A., Byadovskaya, O., Diev, V., Lozovoy, D. and Kononov, A. 2018. Analysis and insights into recombination signals in lumpy skin disease virus recovered in the field. PLOS One. **13**(12): 0207480.

Stubbs, S., Oura, C.A., Henstock, M., Bowden, T.R., King, D.P. and Tuppurainen, E.S. 2012. Validation of a high-throughput real-time polymerase chain reaction assay for the detection of Capripoxviral DNA. J. Virol. Methods. **179**(2): 419-422.

Su, Z., Wang, T., Zhu, H., Zhang, P., Han, R., Liu, Y., Ni, P., Shen, H., Xu, W. and Xu, H. 2015. HMGB1 modulates Lewis cell autophagy and promotes cell survival via RAGE-HMGB1-Erk1/2 positive feedback during nutrient depletion. Immunobiology. **220**(5): 539-544.

Sudhakar, S.B., Mishra, N., Kalaiyarasu, S., Jhade, S.K., Hemadri, D., Sood, R., Bal, G.C., Nayak, M.K., Pradhan, S.K. and Singh, V.P. 2020. Lumpy skin disease (LSD)

outbreaks in cattle in Odisha state, India in August 2019: Epidemiological features and molecular studies. Transbound. Emerg. Dis. **67**(6): 2408-2422.

Tan, J., Liu, Y., Li, W., Zhang, Y., Chen, G., Fang, Y., He, X. and Jing, Z., 2023. Lumpy Skin Disease Virus Infection Activates Autophagy and Endoplasmic Reticulum Stress-Related Cell Apoptosis in Primary Bovine Embryonic Fibroblast Cells. Microorganisms. **11**(8):1883.

Tang, S.W., Ducroux, A., Jeang, K.T. and Neuveut, C. 2012. Impact of cellular autophagy on viruses: Insights from Hepatitis B virus and human retroviruses. J. Biomed. Sci. **19**(1): 1-11.

Tang, Y., Jacobi, A., Vater, C., Zou, L., Zou, X. and Stiehler, M. 2015. Icariin promotes angiogenic differentiation and prevents oxidative stress induced autophagy in endothelial progenitor cells. Stem Cells Dev. **33**(6): 1863-1877.

Tanida, I., Minematsu-Ikeguchi, N., Ueno, T. and Kominami, E., 2005. Lysosomal turnover, but not a cellular level, of endogenous LC3 is a marker for autophagy. Autophagy. **1**(2): 84-91.

Taylor, M. P. and Kirkegaard, K. 2007. Modification of cellular autophagy protein LC3 by poliovirus. J. Virol. **81**(22): 12543-12553.

Tegnell, A., Wahren, B. and Elgh, F., 2002. Smallpox—eradicated, but a growing terror threat. Clinical microbiology and infection. **8**(8): 504-509.

Thomas, A. M. and Maré, C. V. E. 1945. Knopvelsiekte. J. South Afr. Vet. Assoc. **16**(1): 36-43.

Thornhill, J.P., Barkati, S., Walmsley, S., Rockstroh, J., Antinori, A., Harrison, L.B., Palich, R., Nori, A., Reeves, I., Habibi, M.S. and Apea, V., 2022. Monkeypox virus infection in humans across 16 countries—April–June 2022. N. Engl. J. of Med. **387**(8): 679-691.

Tran, A.T., Truong, A.D., Nguyen, D.T.K., Nguyen, H.T., Nguyen, T.T., Tran, H.T.T. and Dang, H.V., 2023. Biological properties and diverse cytokine profiles followed by in vitro and in vivo infections with LSDV strain isolated in first outbreaks in Vietnam. Vet. Res. Commun: 1-12.

Tulman, E.R., Afonso, C.L., Lu, Z., Zsak, L., Sur, J.H., Sandybaev, N.T., Kerembekova, U.Z., Zaitsev, V.L., Kutish, G.F. and Rock, D.L. 2002. The genomes of sheeppox and goatpox viruses. J. Virol. **76**(12): 6054-6061.

Tuppurainen, E., Alexandrov, T. and Beltrįn-Alcrudo, D. 2017. Lumpy skin disease: A field manual for veterinarians. FAO. Anim. Prod. Health Man. **20:** 1-60.

Tuppurainen, E.S., Babiuk, S. and Klement, E. 2018. Lumpy skin disease. Cham, Springer International Publishing. 47-51.

Tuppurainen, E.S., Lubinga, J.C., Stoltsz, W.H., Troskie, M., Carpenter, S.T., Coetzer, J.A., Venter, E.H. and Oura, C.A. 2013. Evidence of vertical transmission of lumpy skin disease virus in *Rhipicephalus decoloratus* ticks. Ticks Tick Borne Dis. **4**(4): 329-333.

Tuppurainen, E.S., Stoltsz, W.H., Troskie, M., Wallace, D.B., Oura, C.A.L., Mellor, P.S., Coetzer, J.A. and Venter, E.H. 2011. A potential role for ixodid (hard) tick vectors in the transmission of lumpy skin disease virus in cattle. Transbound. Emerg. Dis. **58**(2): 93-104.

Tuppurainen, E.S., Venter, E.H. and Coetzer, J.A.W. 2005. The detection of lumpy skin disease virus in samples of experimentally infected cattle using different diagnostic techniques. Onderstepoort J. Vet. **72**(2): 153-164.

Tuppurainen, E.S., Venter, E.H., Coetzer, J.A. and Bell-Sakyi, L., 2015. Lumpy skin disease: attempted propagation in tick cell lines and presence of viral DNA in field ticks collected from naturally-infected cattle. Ticks Tick Borne Dis. **6**(2): 134-140.

Tuppurainen, E.S.M. and Oura, C.A.L. 2012. Lumpy skin disease: an emerging threat to Europe, the Middle East, and Asia. Transbound. Emerg. Dis. **59**(1): 40-48.

Tuppurainen, E.S.M., Venter, E.H., Shisler, J.L., Gari, G., Mekonnen, G.A., Juleff, N., Lyons, N.A., De Clercq, K., Upton, C., Bowden, T.R. and Babiuk, S. 2017. Capripox virus diseases: current status and opportunities for control. Transbound. Emerg. Dis. **64**(3): 729-745.

Turan, N., Yilmaz, A., Tekelioglu, B.K. and Yilmaz, H. 2017. Lumpy skin disease: Global and Turkish perspectives. Poult. Sci. **1**(1).

Ueno, T. and Komatsu, M. 2017. Autophagy in the liver: functions in health and disease.Nat. Rev. Gastroenterol. Hepatol. **14**(3): 170-184.

Von Backstrom, U. 1945. Ngamiland cattle disease: preliminary report on a new disease, the etiological agent being probably of an infectious nature. J. South Afr. Vet. Assoc. **16**(1): 29-35.

Vorster, H. and Mapham, H. 2008. Pathology of lumpy skin disease. Livest. Health Prod. Rev. **1:**16-21.

Wainwright, S., El Idrissi, A., Mattioli, R., Tibbo, M., Njeumi, F., & Raizman, E., 2013. Emergence of lumpy skin disease in the Eastern Mediterranean Basin countries. FAO Empres Watch **29**: 1–6.

Wang, Y., Duan, Y., Han, C., Yao, S., Qi, X., Gao, Y., Maier, H.J., Britton, P., Chen, L., Zhang, L. and Gao, L. 2017. Infectious bursal disease virus subverts autophagic vacuoles to promote viral maturation and release. Virol. J. **91**(5): 01883-16.

Weiss, K.E. 1968. Lumpy skin disease virus. **23**: 111-131

Wong, J., Zhang, J., Si, X., Gao, G., Mao, I., McManus, B.M. and Luo, H. 2008. Autophagosome supports coxsackievirus B3 replication in host cells. Virol. J. **82**(18): 9143-9153.

Xu, J., Li, Z., Liu, Y., Zhang, X., Niu, F., Zheng, H., Wang, L., Kang, L., Wang, K. and Xu, B., 2021. Danon disease: a case report and literature review. Diagnostic Pathol. **16**(1): 39.

Yang, Z. and Klionsky, D.J. 2010. Mammalian autophagy: core molecular machinery and signaling regulation. Curr. Opin. **22**(2): 124-131.

Yang, Z., Goronzy, J.J. and Weyand, C.M. 2015. Autophagy in autoimmune disease. J. Mol. Med. **93**(7): 707-717.

Yang, Z., Zhong, L., Zhong, S., Xian, R. and Yuan, B. 2015. Hypoxia induces microglia autophagy and neural inflammation injury in the focal cerebral ischemia model. Exp. Mol. Pathol. **98**(2): 219-224.

Yang, Z.J., Chee, C.E., Huang, S. and Sinicrope, F.A. 2011. The role of autophagy in cancer: therapeutic implications. Mol. Cancer. Ther. **10**(9): 1533-1541.

Yeruham, I., Nir, O., Braverman, Y., Davidson, M., Grinstein, H., Haymovitch, M. and Zamir, O. 1995. Spread of lumpy skin disease in Israeli dairy herds. Vet. Rec. **137**: 91-93.

Yoshii, S.R. and Mizushima, N., 2017. Monitoring and measuring autophagy. Int. J. Mol. Sci. **18**(9).1865.

Yu, L., McPhee, C.K., Zheng, L., Mardones, G.A., Rong, Y., Peng, J., Mi, N., Zhao, Y., Liu, Z., Wan, F. and Hailey, D.W.2010. Termination of autophagy and reformation of lysosomes regulated by mTOR. Nature. **465**(7300): 942-946.

Yun, C.W. and Lee, S.H.2018. The roles of autophagy in cancer. Int. J. Mol. Sci. **19**(11): 3466.

Zaffagnini, G. and Martens, S. 2016. Mechanisms of selective autophagy. J. Mol. Biol. **428**(9): 1714-1724.

Zhang, H., Monken, C.E., Lenard, J., Mizushima, N., Lattime, E.C. and Jin, S., 2006. Cellular autophagy machinery is not required for vaccinia virus replication and maturation. Autophagy. **2**(2): 91-95.

Zheng, M., Liu, Q., Jin, N., Guo, J., Huang, X., Li, H., Zhu, W. and Xiong, Y. 2007. A duplex PCR assay for simultaneous detection and differentiation of Capripox virus and Orf virus. Mol. Cell. Probes. **21**(4): 276-281.

Zhou, D. and Spector, S.A. 2008. Human immunodeficiency virus type-1 infection inhibits autophagy. AIDS (London, England). **22**(6): 695.

Zhou, Z., Jiang, X., Liu, D., Fan, Z., Hu, X., Yan, J., Wang, M. and Gao, G.F. 2009.

Autophagy is involved in influenza A virus replication. Autophagy. **5**(3): 321-328.

Zhou, Y., Ren, Y., Cong, Y., Mu, Y., Yin, R. and Ding, Z., 2017. Autophagy induced by bovine viral diarrhea virus infection counteracts apoptosis and innate immune activation. Arch. Virol.**162**: 3103-3118.

Appendix

APPENDIX

1. SOLUTIONS USED FOR SDS-PAGE

10X Tris-glycine SDS gel running buffer

25 mM Tris base	30.0 g
192 mM glycine	144.0 g
SDS (0.1%)	10.0 g
Double Distilled Water (DDW)	upto 1000 ml

Acrylamide solution (40% w/v)

Acrylamide	29.2 g
N, N'- methylene bisacrylamide	0.8 g
DDW	upto 100 ml

The solution filtered through a nitrocellulose filter (0.45µm pore size). Filtered solution was stored in dark bottles at 4ºC.

Ammonium Persulfate (10%w/v)

Ammonium Persulfate	100mg
DDW	1 ml

1.5 M Tris-Buffer (ph 8.8)

Tris base	18.17 g
DDW	upto 100 ml
Adjust ph to 8.8 with HCl	

0.5 M Tris-Buffer (ph 6.8)

Tris base	6.05 g
DDW	upto 100 ml
Adjust ph to 6.8 with HCl	

Resolving gel (15%), 15 ml

40% Acrylamide Bis-Acrylamide	5.7 ml
DDW	3.3 ml
1.5 M Tris HCl (ph 8.8)	6.0 ml
10% Ammonium Persulfate	100.0 µl
TEMED	12.5 µl

Stacking gel (5%), 5 ml

40% Acrylamide Bis-Acrylamide	0.62 ml
DDW	3.36 ml
0.5 M Tris HCl (ph 6.8)	1.0 ml
10% Ammonium Persulfate	25.0 µl
TEMED	2.5 µl

5X Loading dye (500 µl)

5X Laemmli buffer	400 µl
β mercaptoethanol	100 µl

2. SOLUTIONS FOR WESTERN BLOTTING

1X Transfer buffer

10X Tris-Glycine buffer	50 ml
Absolute methanol	100 ml
DDW	upto 500 ml

10X TBST

Tris base	24.0 g
Sodium chloride	88.0 g
DDW	upto 1.0 L
Tween-20	1.0 ml

DAB Solution (For 1ml)

DAB Powder	0.5 mg
0.1 M Imidazole	1.0 ml
Cobalt Chloride	12.5 µl
3% Hydrogen Peroxide	0.75 µl

3. SOLUTIONS FOR IMMUNOFLUORESCENCE

10% Neutral Buffered Formaline

37-40% Formaldehyde	200 ml
Sodium phosphate monobasic	8.0 g
Anhydrous disodium phosphate	13.0 g
DDW	upto 2.0 L

Tyramide working solution

Tyramide	3.0 µl
1X TBST	300.0 µL
3% H_2O_2	1.5 µL

Atofluorescnce quenching solution

Reagent A	100.0 µL
Reagent B	100.0 µL
Reagent C	100.0 µL

4. REAGENTS FOR CELL CULTURE

Growth Medium

Leibovitz's L-15 media supplemented with 10% (v/v) fetal bovine serum.

Maintenance Medium

Leibovitz's L-15 media supplemented with 2% (v/v) fetal bovine serum.

VITAE

Name	:	**Dr Syam Sugunan**
Father's name	:	Shri Sugunanandan T.
Mother's name	:	Smt. Jalajamany T.
Date of birth	:	14. 10. 1996
Permanent Address	:	Kattungal House Vandanam P. O. Alappuzha District, Kerala- 688005
Phone	:	9562929070
E- mail	:	syamshilpa1359@gmail.com

Educational qualifications

Degree	Board/university	Year of passing	OGPA
B.V.Sc. & AH	COVAS Pookode (KVASU)	2021	7.95
M.V.Sc.	ICAR-IVRI, Izatnagar, U. P.	2023	8.30

Membership :

1. Kerala State Veterinary Council
2. Indian Veterinary Association, Kerala Chapters

Awards/ Fellowships

1. Junior Research Fellowship (J. R. F.) of ICAR for Masters
2. A. S. R. B. NET (ICAR-NET 2023) qualified for Assistant Professor

Symposium/conferences attended :

1. International Conference on Veterinary Pathology, Hyderabad
2. Society of Toxicologic Pathologists(STP) India conference, Gandhinagar, Gujarat